論文 / 著書情報
Article / Book Information

題目(和文)	
Title(English)	Development of a Trocar Insertion Device for Laparoscopic Surgery
著者(和文)	SUN JUNPENG
Author(English)	Junpeng Sun
出典(和文)	学位:博士(工学), 学位授与機関:東京工業大学, 報告番号:甲第11187号, 授与年月日:2019年3月26日, 学位の種別:課程博士, 審査員:只野 耕太郎,小俣 透,初澤 毅,中村 健太郎,石田 忠
Citation(English)	Degree:Doctor (Engineering), Conferring organization: Tokyo Institute of Technology, Report number:甲第11187号, Conferred date:2019/3/26, Degree Type:Course doctor, Examiner:,,,,
学位種別(和文)	博士論文
Type(English)	Doctoral Thesis

Tokyo Institute of Technology

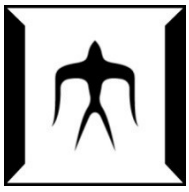

2019 doctoral thesis

Development of a Trocar Insertion Device for Laparoscopic Surgery

Life Engineering Course, Doctoral Program

SUN JUNPENG

Adviser: Kotaro Tadano

Contents

Chapter 1. Introduction

1.1 Trocar Insertion

1.1.1 Laparoscopic Surgery

Laparoscopic surgery is a kind of operation performed in the abdomen or pelvis using small incisions (usually 0.5-1.5cm) with the aid of a camera. The laparoscope aids diagnosis or therapeutic interventions with a few small cuts in the abdomen. There are a number of advantages to patients with laparoscopic surgery versus an open procedure. These include reduced pain due to smaller incision and hemorrhaging and shorter recovery time. [1]

Now, almost elective abdominopelvic surgeries can be performed laparoscopically. For instance, gastrointestinal surgery, gynecological surgery, urological surgery and diagnostic laparoscopic surgery. [2]

The procedure of laparoscopic surgery follows:

a. **Anesthesia**: general anesthesia (most common), spinal anesthesia with/without epidural anesthesia may be used in some cases.
b. **Access to the peritoneal cavity**: Surgeons make a small cut on the outside of the body (usually near the navel for abdominal surgery) and a trocar (thin tube)/veress needle is inserted into the incision.

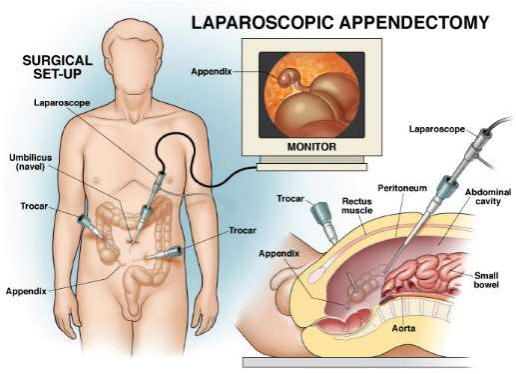

Fig.1-1. Laparoscopic surgery [3]

Fig.1-2. Laparoscopic surgery [3]

c. **Creating a pneumopritoneum**: For certain procedures, carbon dioxide gas is injected into the abdomen. This creates an open space to get a better view of patients' organs.

d. **Creation of other port sites**: More cuts and trocar insertions are made for other medical tools

e. **Taking the operation**: The camera on the laparoscope allows surgeons to view inside of patient's body on a video screen in the operating room.

f. **Evacuation of pneumoperitoneum and Closure of the port sites**: When the operation is finished, surgeons remove instruments and stich the incisions closed. [2, 4]

Advantages of laparoscopic surgery include:

- Less postoperative pain, which leads to:
  - Early mobilization – decreased risk of developing deep vein thrombosis, pulmonary embolism, or pneumonia
  - Minimal use of analgesics
  - Shorter hospital stay
- Shorter duration of postoperative ileus
- Better cosmetic outcome (smaller scars)
- Less intra-abdominal adhesion formation

Disadvantages of laparoscopic surgery mainly include:

- The surgical field is converted to two-dimensional images on a monitor
- Technically more challenging than laparotomy
- Difficulty in controlling intra-operative hemorrhage
- Laparoscopy-specific complications [4]

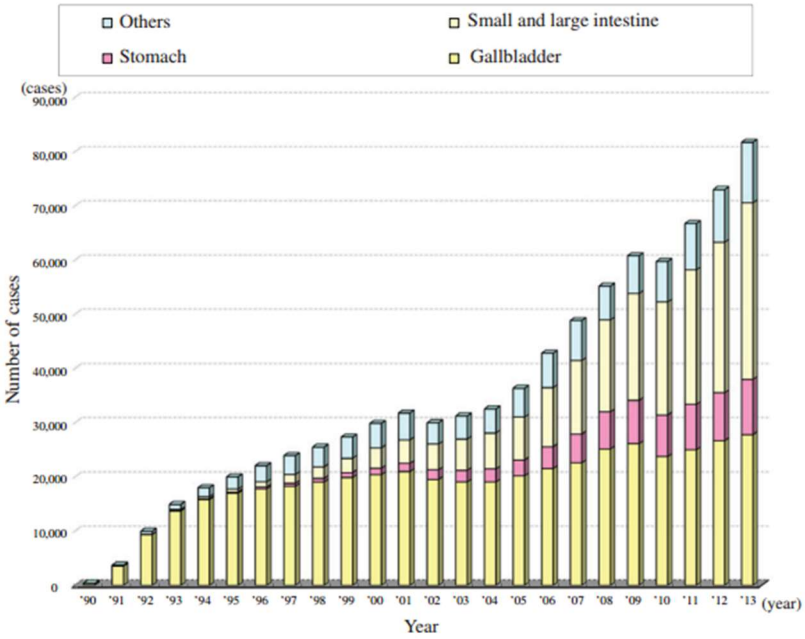

Fig.1-3 Annual number of laparoscopic procedures for abdominal disease [5]

In recent years, number of patients who underwent endoscopic operations increased in most domains. From 1990 to 2013, a total of 1,640,646 patients underwent endoscopic operations in Japan. Of these patients, 846,745 underwent endoscopic abdominal surgery, 410,989 underwent endoscopic surgery for obstetrics and gynecologic problems, 236,792 underwent endoscopic thoracic surgery and 77,285 underwent endoscopic urological surgery. Taking the abdominal surgery for an example, number of laparoscopic abdominal surgeries has increased considerably since 1990. In total, 846,745 patients underwent this surgery through the end of 2013 as shown in Fig 1-3. [5]

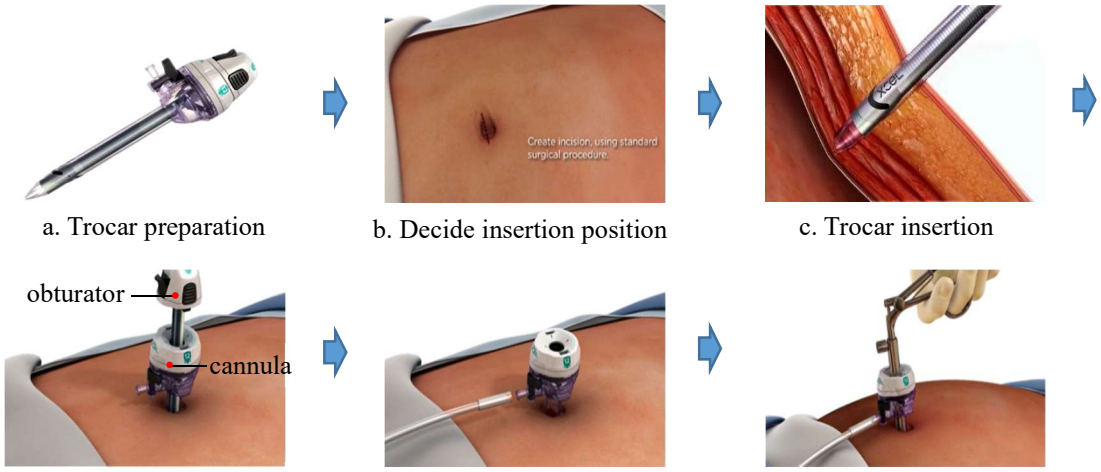

a. Trocar preparation
b. Decide insertion position
c. Trocar insertion
d. Draw out the obturator
e. Inject carbon dioxide
f. Insert medical tools through cannula

Fig.1-4. Procedure of trocar insertion [6]

1.1.2 Trocar Insertion

Usually, Trocar insertion is a necessary step in laparoscopic surgery. Trocar is a long sharp tool and it consists of two parts, an obturator (which may be a metal or plastic sharpened or non-bladed tip) and a cannula (basically a hollow tube), as shown in Fig.1-4. After insertion, the cannula allows other medical tools to insert into abdomen. The procedure of primary trocar insertion shows in Fig.1-4. [6]

A laparoscopic surgery involves use of multiple trocars. The primary trocar is used to create a pneumoperitoneum and place a cannula through which a laparoscope is inserted to view internal structures. Later trocars aid in insertion of other instruments such as biopsy forceps, etc.

There are many kinds of trocar products or similar medical tools in market. They can be roughly classified into three kinds by diameter. As shown in Fig.1-5, the thinnest kind is Veress Needle, whose diameter is approximately 2 mm. It can be only used to create a pneumoperitoneum. Slightly thicker kind is 5 mm trocar, whose cannula enables certain amount of thin medical tools to access. However, usual laparoscopies are too thick to access. The commonest kind is 12 mm trocar. It enables nearly all laparoscopic surgical tools to access. [7]

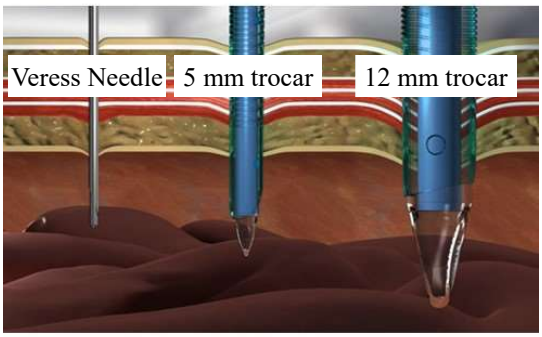

Fig.1-5. Three kinds classified by diameter [8]

In addition, trocars also can be classified into some kinds by type of tips. As shown in Fig.1-6, 2mm Veress Needle has two kinds of tips, with sheath and without sheath. And 5 or 12 mm trocars have two types, bladed tip and bladeless tip. Bladed tip trocars also consist of retractile ones and non-retractile ones. As introduced above, the primary trocar insertion need to place a cannula which is possible to access laparoscopy, usually 12 mm trocar are used in the primary insertion.

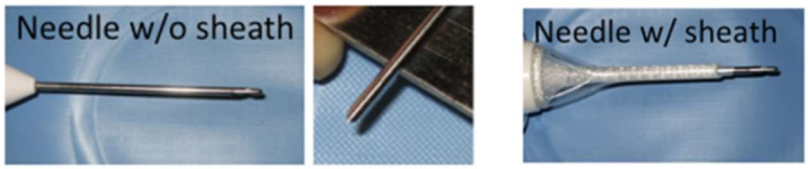

Veress Needle

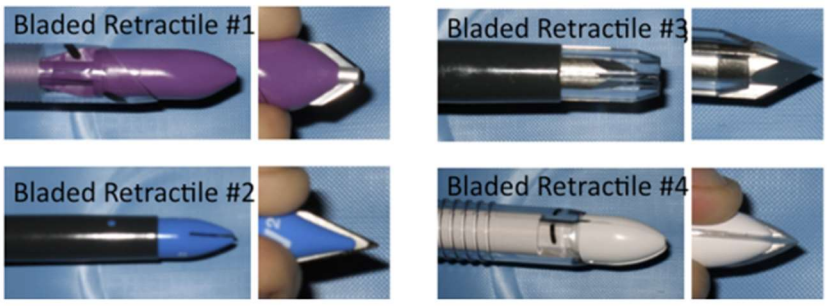

Bladed tip trocar (retractile)

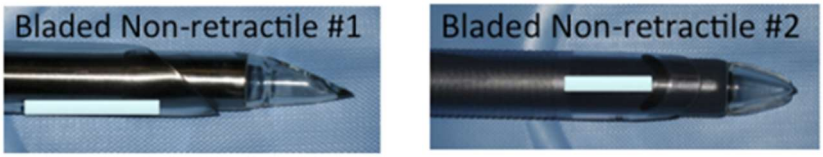

Bladed tip trocar (non-retractile)

Fig.1-6. Kinds of trocars classified by tip types [9]

Bladeless tip trocar [10, 11]

Fig.1-6. Kinds of trocars classified by tip types [9]

1.1.3 Problems during Trocar Insertion

In the procedure of trocar insertion, there are some problems as introduced following.

A) Overshooting causes injuries, especially during the primary trocar insertion.

According to relevant researches [14], improperly inserted trocar or needles cause mechanical injury to underlying tissues or organs, as shown in Fig.1-7. Approximately 75,000 inadvertent injuries of organs or arteries inside abdomen occur annually in the U.S. alone. Besides, with the growing problem of obesity, the skin-to-target distance is increasingly variable, and important anatomical landmarks are more difficult to recognize. This would result in slower procedure times and the requirement of greater operative skill. [15]

Current techniques for accessing specific regions of the body with needles and trocars typically involve blind guidance, where the physician or nurse relies entirely on tactile feedback, experience, superficial anatomical landmarks and fluid return through the instrument. The operator must sense when the needle or trocar enters the target space and discontinue advancement. However, existing needles and trocars systems often do not provide sufficient feedback to the physician to indicate correct position. [16]

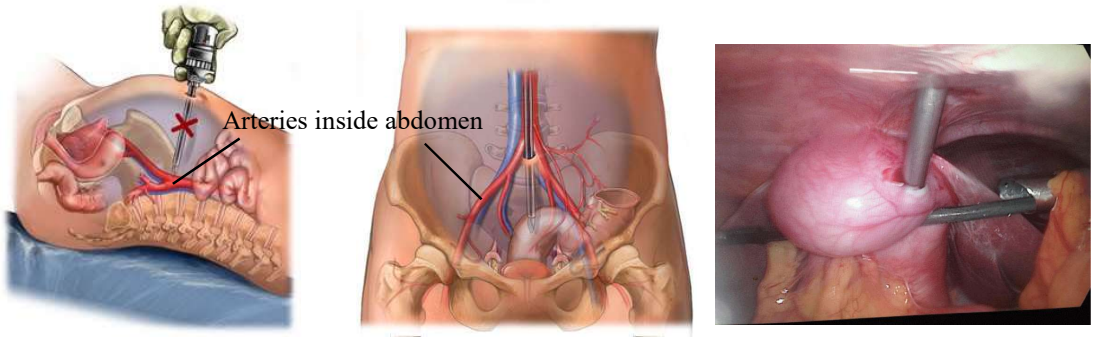

Fig.1-7. Overshooting during trocar insertion causes injuries [12, 13]

Fig.1-8. Two surgeons insert a trocar [19]

Fig.1-9. Lift up the abdominal wall and insert a trocar by oneself [20]

Current device like Veress Needles and some trocars attempt to address these problems with spring-loaded blade sheathes or retractable blades, which are mentioned above. In both cases, these intended safety features do not always prevent damage to underlying organs. [17] Accordingly, the FDA (US Food and Drug Administration) published a report in 2003 regarding laparoscopic procedures to state that most complications occur at initial trocar insertion and stressed the need for medical device companies to improve their products. [18]

B) Troublesome Operation

Usually, two surgeons must cooperate with each other to finish the trocar insertion. One lifts up the abdominal wall to make it stable, and the other one inserts the trocar into the abdomen, as shown in Fig.1-8. Actually, some operators also insert the trocar by himself or herself, as shown in Fig. 1-9. However, it depends on the insertion location and requires certain experience. [19,20] Besides, it has been reported that operation of trocar insertion requires large force, which is difficult for some female surgeons. [21]

C) Patient's individuality and trocar's diversity grow the difficulty to achieve safe trocar insertion

Usually, umbilicus is regarded as a reference to estimate the location of the aortic bifurcation. It can help to avoid injuring arteries in trocar insertion. [22] However, as shown in Fig.1-10, position of umbilicus relative to the aortic bifurcation is negatively correlated with body mass. [23] The individual obesity makes it difficult to estimate correctly.

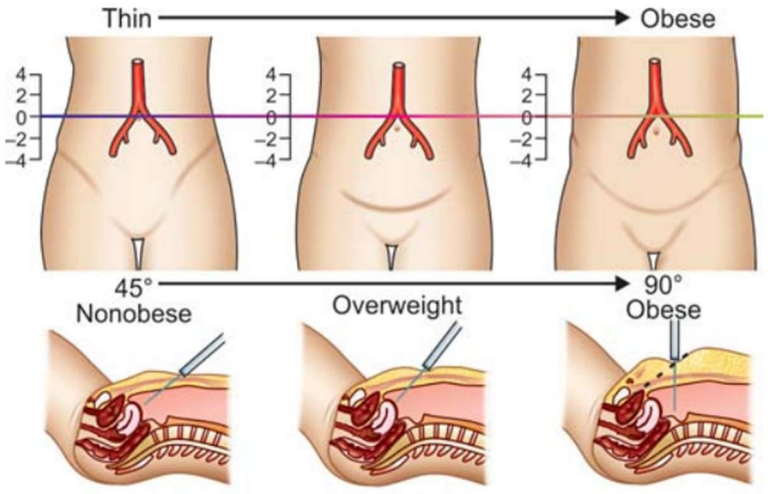

Fig.1-10. Influence of obesity on location of trocar insertion [23]

Not only that, there is not a definite value of insertion force. It depends on many factors, such as patient's obesity, age, trocar types, etc. [24, 25] Thus, trocar insertion is not so easy for novices.

1.2 Related research

As mentioned above, dangers and inconveniences exactly exist during trocar insertion, especially the primary one because it is done before pneumoperitoneum. Therefore, many researches have been done to improve this procedure. These researches can be briefly classified into two branches. One branch is to improve trocars or to develop new type trocars to achieve safe insertion. The other one is to train operators, to make them sophisticated.

1.2.1 Improvement of Trocars

Some improvements and relevant researches were conducted. The commonest trocar products, which is improved, is the retractile trocar (in Fig.1-6) and the optical trocar (in Fig.1-11). As shown in Fig.1-6, the sharp edge retreats to avoid overshooting upon the abdominal wall is penetrated out. And the optical trocar allows the laparoscopy to be placed inside [26], as shown in Fig.1-11. In this way, surgeons can

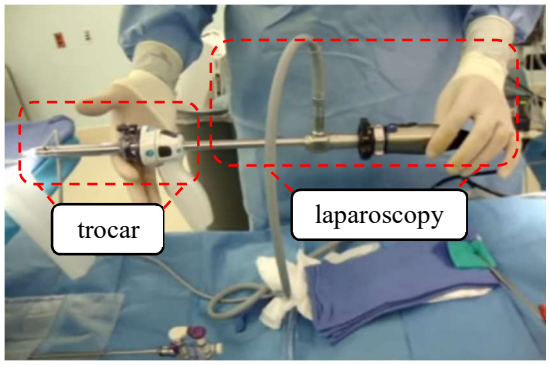

Fig.1-11. Place the laparoscopy inside the optical trocar [26]

Fig.1-12. Understand the insertion depth by seeing monitor [27]

understand the inserting depth by seeing the monitor to achieve safe insertion [27] as shown in Fig.1-12.

In addition to the medical tools mentioned above, a variety of guidance and sensing-based systems have been developed to improve targeted placement of needles and trocars [28-37]. Examples include ultrasound and active sensing systems on the tips of the trocar (or needles). For instance, Joho Yun,et al proposed a micro-electrical impedance spectroscopy-on-a-needle [38] for depth profiling of biotissue to prevent and immediately recognize iatrogenic injury during trocars or Veress Needle insertion, as shown in Fig.1-13.

Besides, there are some researchers, who consider the electrical sensor is a burdensome or an unreliable way. They think it is a better way to achieve safe insertion by ingenious mechanical design. The most representative in this branch is the

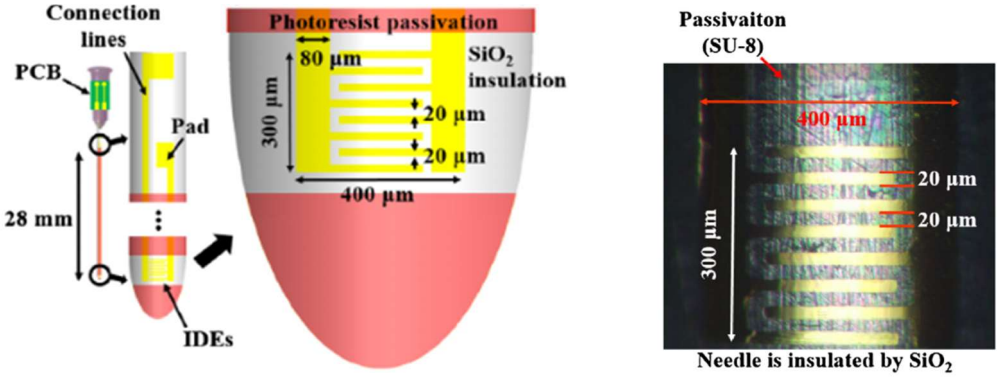

Fig.1-13. A micro-electrical impedance spectroscopy-on-a-needle [38]

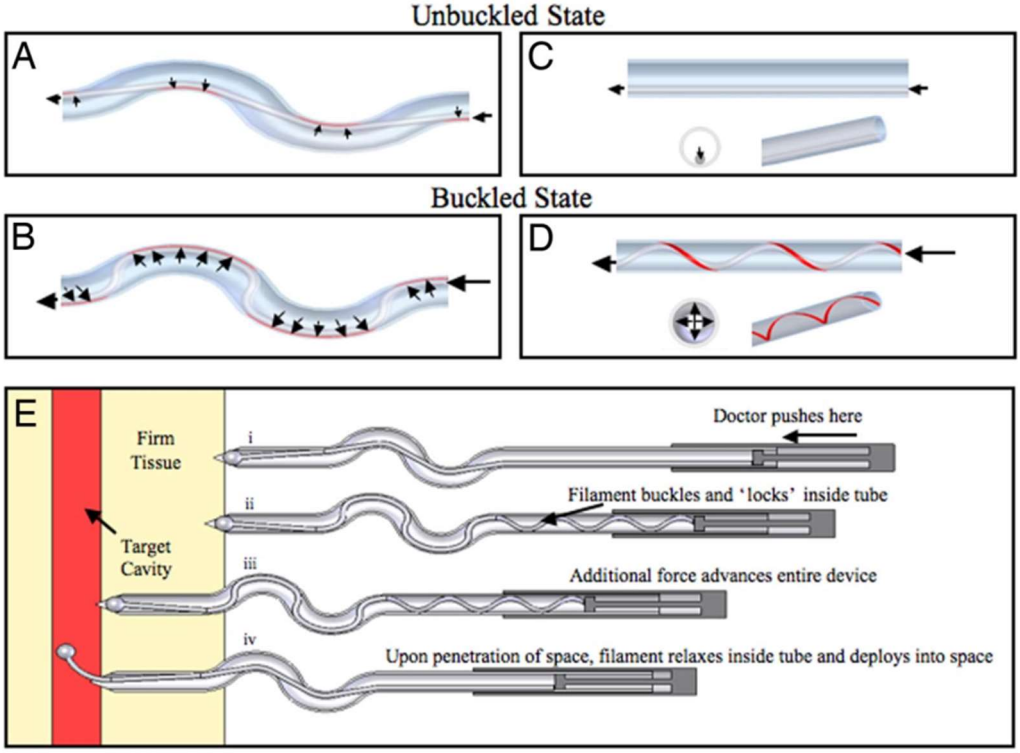

Fig.1-14. A mechanical clutch-based needle-insertion device [39]

mechanical clutch-based needle-insertion device [39], which was developed by Erik k and Jeffery M from MIT. By ingenious mechanical design, as shown in Fig.1-14, it effectively reduced the risk of damaging organs or arteries caused by overshooting. But just because it completely subvert the original design of the usual trocar products in the market, it is hard to spread widely in medical applications.

And following the opinion of pure mechanical design, Yancheng Wang, et al researched on the trocar tip design to minimize the insertion force [40], as shown in Fig.1-15. They clarified that the longer the bevel length of the trocar, the less force

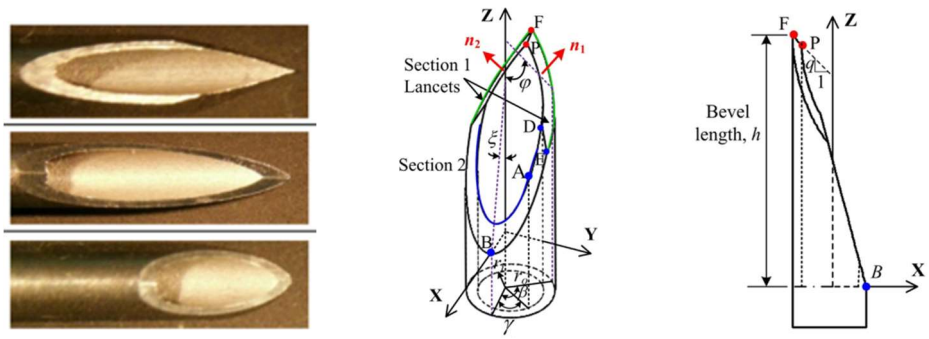

Fig.1-15. Research on the relationship between the tip shape and insertion firce [40]

trocar insertion requires. Their research on the relationship between the tip shape and the insertion force offers a valuable reference to trocar insertion force analysis.

1.2.2 Training system for Trocar Insertion

As mentioned above, the other branch is to develop training systems for operators. It simulates the trocar insertion situation (force and torque change) to make operators sophisticated [41-54]. In Japan, Sakaguchi, et al from Nagoya Technology University developed a training system [55, 56] as shown in Fig.1-16. Force sensors and actuators are assembled in this system to simulate the operative insertion. According to the experiment in this research, the operators trained by this system can achieve better insertion effect than operators without its trained.

There are also similar researches overseas. For instance, A. Chowriappa, et al from New York State University proposed a predictive model for haptic assistance in robot assisted trocar insertion [57, 58]. It utilized a master-slave robot system to operate

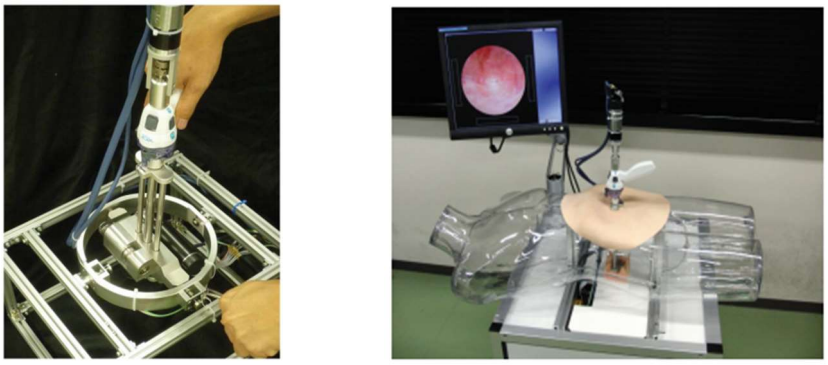

Fig.1-16. Virtual Reality real-time trocar insertion training system [55,56]

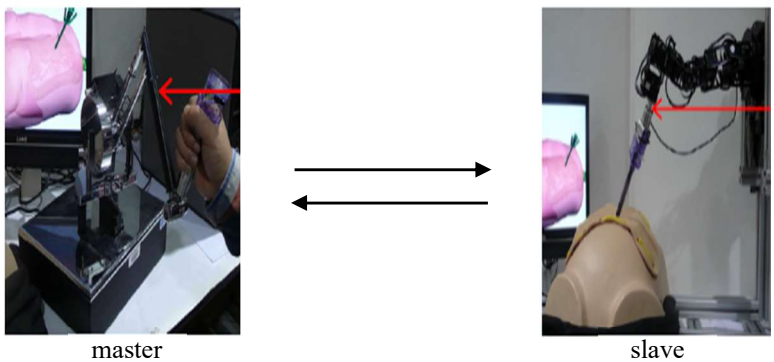

Fig.1-17. Master-Slave robot assisted trocar insertion training [57,58]

trocar insertion, as shown in Fig.1-17. And in software aspect, this system adopted a predictive model to optimize the insertion. It could effectively avoid misoperations during insertion.

1.2.3 Research on Insertion Force

In addition to the two branches mentioned above, to avoid overshooting, there are a great many researches on needle insertion force analysis [59-68] as shown in Fig.1-18. Even though the needle is thinner than trocar and their applied field is different, they are both the research that a long thin rigid tool inserts into soft biotissue. Therefore, these researches can be regarded as references.

Mohsen Mahvsh and Pierre E studied the mechanics of dynamic needle insertion into a biological material [69]. Even though it is not about trocar insertion, it clarified the principle when a sharp tool inserts biotissue. This offers fundaments for explanation of the trocar insertion force trend.

A.M.Okamura, et al also proposed the force modeling when needle inserts into

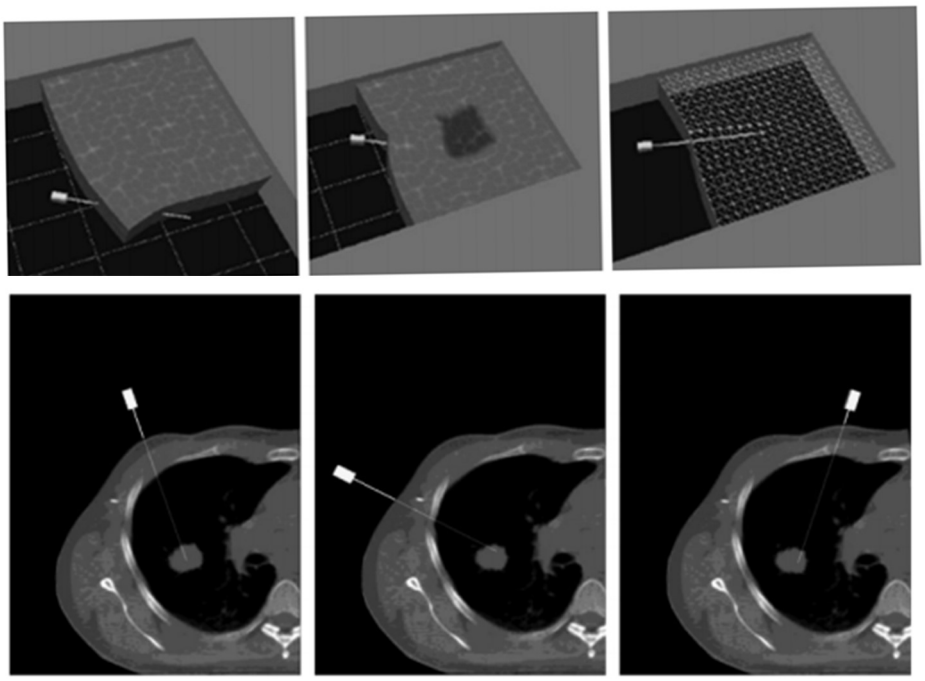

Fig.1-18. Interactive virtual needle insertion and lung nodule biopsy [62]

soft biotissue. They divided the insertion force into several parts, which are capsual stiffness, friction and cutting. [70]

1.3 Purpose of this research

Related researches introduced above have contributed to the achievement of safe trocar insertion. However, they also have their own defects respectively. Safety of insertion is the prerequisite, they all improved the safety of insertion at a certain level. But the easiness of operation and universal applicability of every method cannot be ignored.

Fig.1-19. shows advantages and disadvantages of every research mentioned above. Specifically, even though the optical trocar can avoid overshooting effectively and is widely adopted, it still requires two surgeons to operate. Besides, it is necessary to study the recognition of images at every phase during insertion. Methods that taping electric sensor on trocar tips and the new pure mechanical trocar do not grow the complexity of operation, however, they are difficult to widely spread at short time. And the trocar insertion training systems do not eliminate the necessity of studying or training.

Therefore, as shown in Fig.1-19, a trocar insertion device is desired which has both high easiness of operation and universal applicability. The purpose of this research is to develop a trocar insertion device that can satisfy requirements as following:

- Safety: It can detect the penetration-out correctly and stop inserting to avoid overshooting immediately and automatically
- Universal applicability: This device must be accessible for majority of trocar products.
- Easiness of operation: This device must be easy to use. Even novices are able to operate without training. Besides, if it can enable one surgeon to operate without others' help, it will be well appreciated.

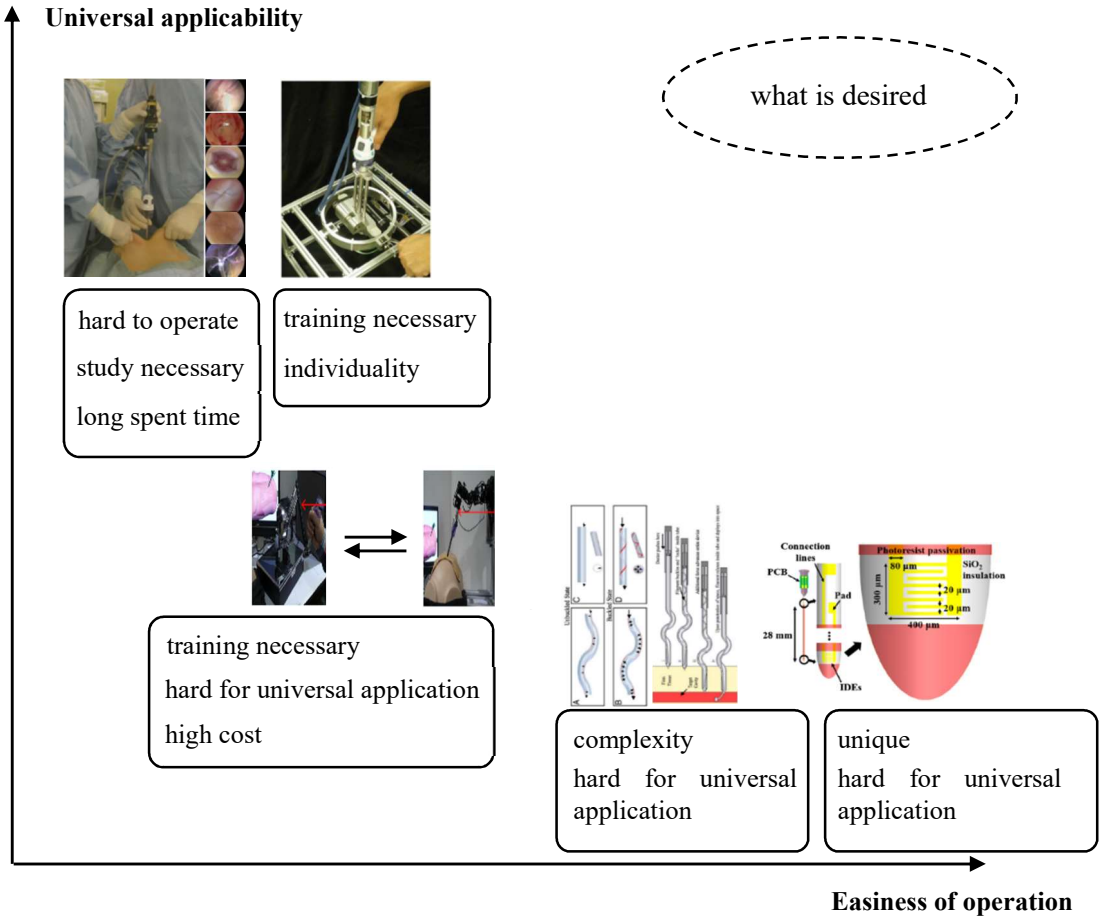

Fig.1-19. Positioning of related researches mentioned above

1.4 Structure of this thesis

The structure of this research is shown in Fig.1-20. There are four chapters as following:

In the 2nd chapter, a trocar insertion force measurement platform is built. Using porcine abdominal wall, trocar insertion force is measured in different experimental conditions (different types of trocar, different insertion methods). And according to measurements, relationship between the insertion force trend and the abdominal multilayers structure is studied. It offers a fundament for the safe insertion control. In addition, in this chapter, the influence of many factors (insertion speed, insertion methods and trocar types) on insertion force and abdominal deformation is also discussed.

In the 3rd chapter, based on the measurement in the 2nd chapter, the trocar insertion device is designed. This device integrated functions of lifting up abdominal wall and trocar insertion, which enables one surgeon to finish the insertion by himself or herself. Then the control method of actuators and the whole insertion device system are introduced. Finally, *Exvivo* experiment with porcine abdominal wall is conducted to verify every actuator's control and insertion force sensing. Besides, the sterilization and universal applicability for majority trocar products are also considered in an improved version.

In the 4rd chapter, based on the clarification of insertion force trend in 2nd chapter, an automatic stop (auto-stop) algorithm is applied in this device. Upon the penetrate-out is detected, it automatically discontinues inserting to avoid overshooting. *Exvivo* experiment with porcine abdominal wall is conducted to verify its effectiveness. Besides that, comparing with human insertion, using this device can short the exposure length of trocar and spent time of operation.

Finally, in 5rd chapter, conclusions of this research are listed.

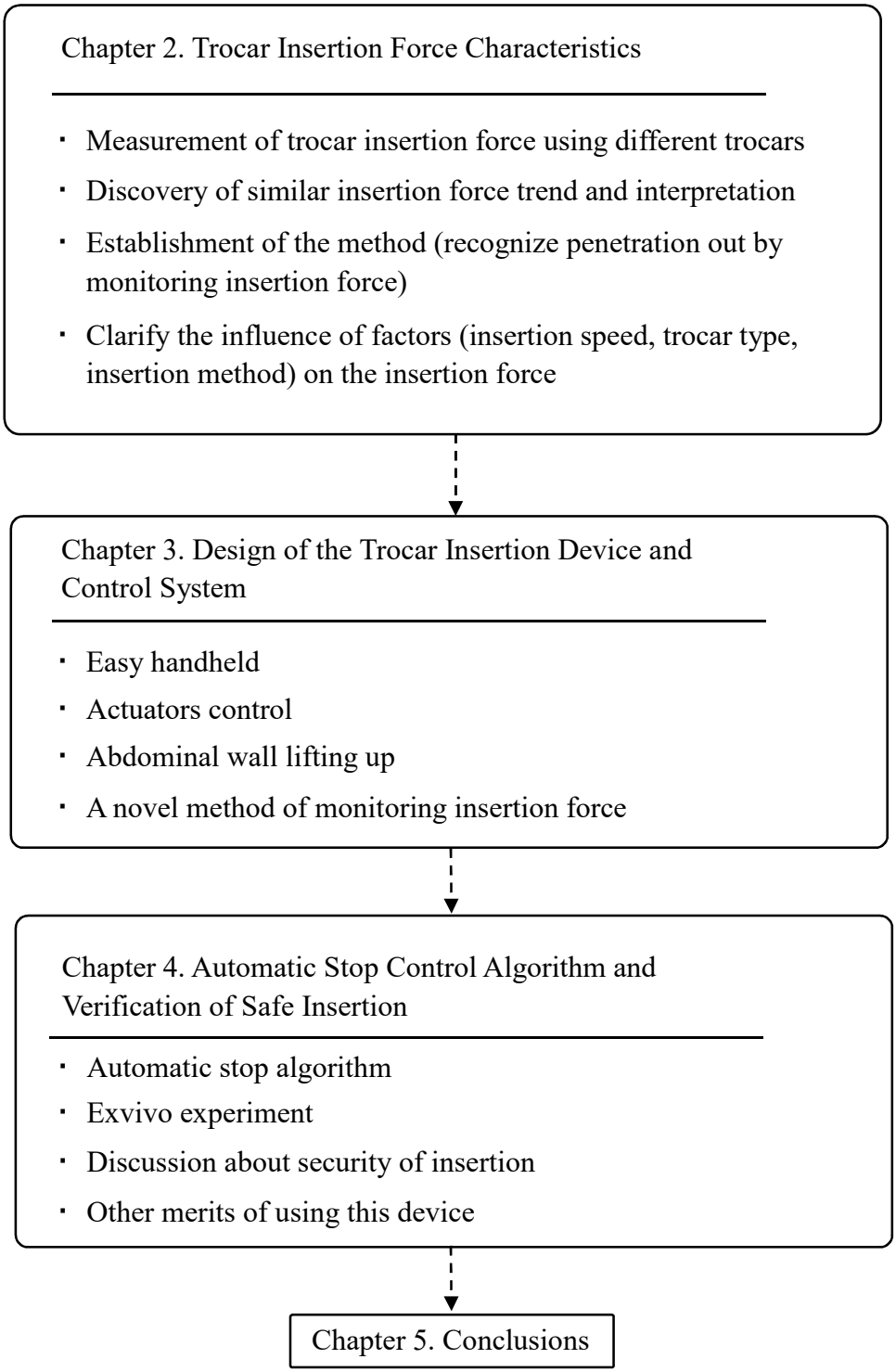

Fig.1-20. Structure of this thesis

Chapter 2. Trocar Insertion Force Characteristics

In order to select appropriate actuators for trocar insertion device design later, it is necessary to roughly know how much the insertion force is. Not only that, but also clarifying insertion force characteristics can supply a useful evidence to recognize the abdominal penetration out by monitoring insertion force when the automatic stop algorithm is designed to avoid overshooting. Thus, this chapter interprets the insertion force in details.

2.1 Measurement of trocar insertion force

2.1.1 Experimental apparatus

To measure the insertion force, a trocar insertion measurement platform is built as shown in Fig.2-1. It has two DOFs, which drives the trocar to insert downward and rotate. There are two motor combinations, which consists of motor, gearhead and encoder. By a ball screw (No.4 component in Fig.2-1), whose lead is 2 mm, one motor combination drives the trocar to move vertically downward. And the other one drives the trocar to rotate. Besides that, a single-axis force sensor (No.7 component in Fig.2-1) is installed above the trocar to measure the insertion force. Components and basic

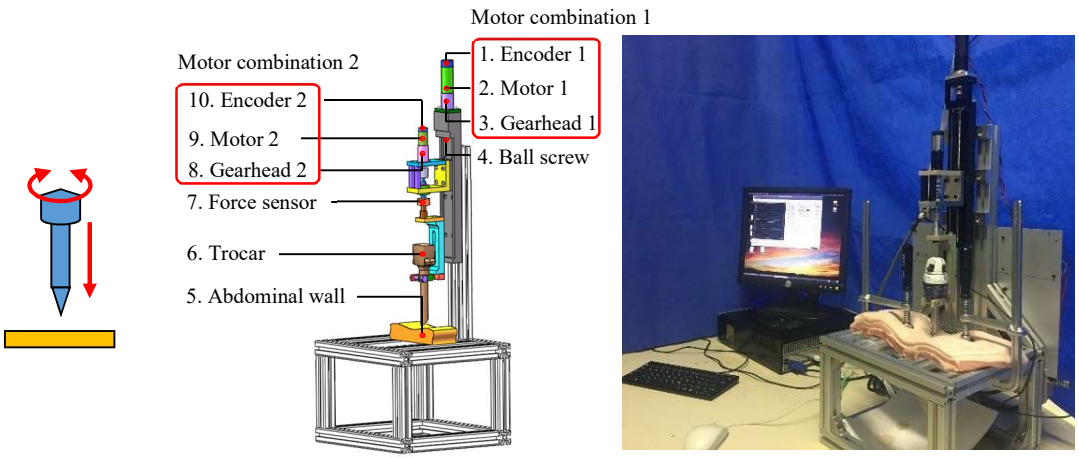

Fig.2-1. Trocar insertion measurement platform

Table 2-I. Components of experimental platform

Component			
No.	Parts	Article	Technical Date
1	Encoder 1	Maxon, Type ML, 225805	Counts per turn: 512
2	Motor 1	Maxon, RE25, 118746	Power: 10 Watt Nominal Speed: 4136 rpm Nominal Torque: 28 mNm
3	Gearhead 1	Maxon, CP26A, 406762	Reduction: 19:1 Max. Continuous Torque: 2.25 Nm
4	Ball screw	Misumi-JP, LX2602C-B1-250	Stroke: 117 mm Lead: 2 mm
5	Abdominal wall	Porcine Abdominal Wall	Thickness: 45-50 mm
6	Trocar	Three types	Diameter: 12 mm
7	Force sensor	Forsentek FL25-10kg	Single-axis Measure Range: -100~100 N Measurement Error: ±0.2%
8	Gearhead 2	Maxon, GP22L, 232773	Reduction: 62:1 Max. Continuous Torque: 0.4 Nm
9	Motor 2	Maxon, A-max22, 110140	Power: 3.5 Watt Nominal Speed: 3720 rpm Nominal Torque: 6.05 mNm
10	Encoder 2	Maxon, Type ML, 201940	Counts per turn: 512
Information			
Insertion speed range		Constantly 0-12 mm/sec	
Frequency of trocar rotation		0-1 Hz	
Period of calculating		1 ms	

information of the measurement platform are listed in Table 2-I.

Measurement range of force sensor is ±100 N and measurement error is 0.2%. Two motors are controlled by a Linux Ubuntu PC, whose period of calculating is 1 millisecond. In addition, in order to trace images in different phases of insertion, a high-definition (1920 * 1080) camera is set to record the video of insertion process.

Fig.2-2. Porcine abdominal wall

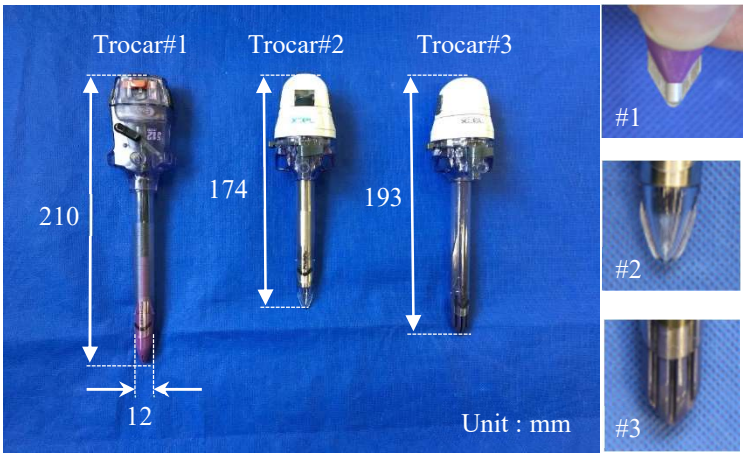

Fig.2-3. Three types of 12 mm trocars

2.1.2 Experiment method

In experiments, the trocar moves vertically downward at a constant speed (0-10 mm/sec), and the rotation follows the equation 2-1.

$$\theta = Asin(2\pi ft) \tag{2-1}$$

Where, θ represents the angle trocar turns, and A ranges 0-π/2, and f ranges 0-1Hz.

In this experiment, porcine abdominal wall is chosen as the material because its structure and mechanical properties are similar to human beings [71-75]. In addition, its thickness (30–50 mm) are close to human beings. It is necessary to emphasize that except experiments of discussing the thickness influence, the porcine abdominal walls

which are used in this research are all 45-50 mm thickness， as shown in Fig.2-2 .

As introduced in chapter 1, overshooting always occur in the primary trocar insertion, three types of trocars, which are the commonest during the primary insertion, are chosen to research the insertion force. As shown in Fig.2-3, the first type is a bladed trocar, whose cutter head is retractile. The second one is a plastic bladed optical trocar, whose obturator is hollow for placing a laparoscopy. And the third one is a bladeless optical trocar, which has no obvious sharp cutter head. Diameters of them are all 12 mm.

As surgeons normally finish the insertion through the abdominal wall in 20-30 sec [76] and the thickness of the abdominal wall is approximately 30-50 mm, in this measurement experiment the trocar is driven at a constant insertion speed of 4.0 mm/s. and when we see the trocar has penetrated out of the abdominal wall, we stop driving. Fig.2-4 shows the process of trocar insertion. Firstly, the trocar does not contact to the abdominal wall. Then it contacts and the abdominal wall deforms. Finally, the trocar tip penetrates out of the abdominal wall.

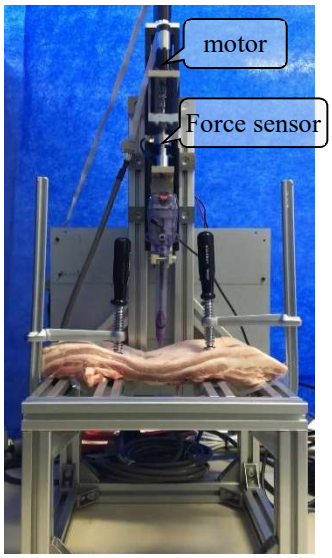

(1) Before contact

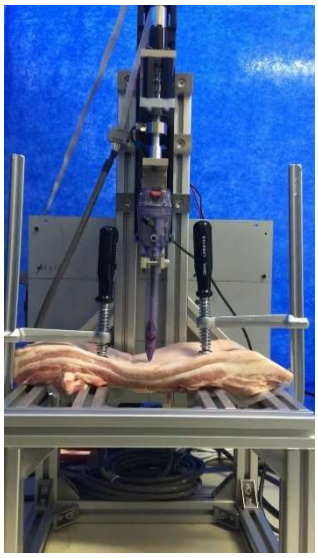

(2) Contact

(3) Slightly deformed

(4) Deform

(5) Cutter head penetrates out

(6) Tip penetrates out

(7) Stopped

Fig.2-4. Process of trocar insertion on the measurement platform

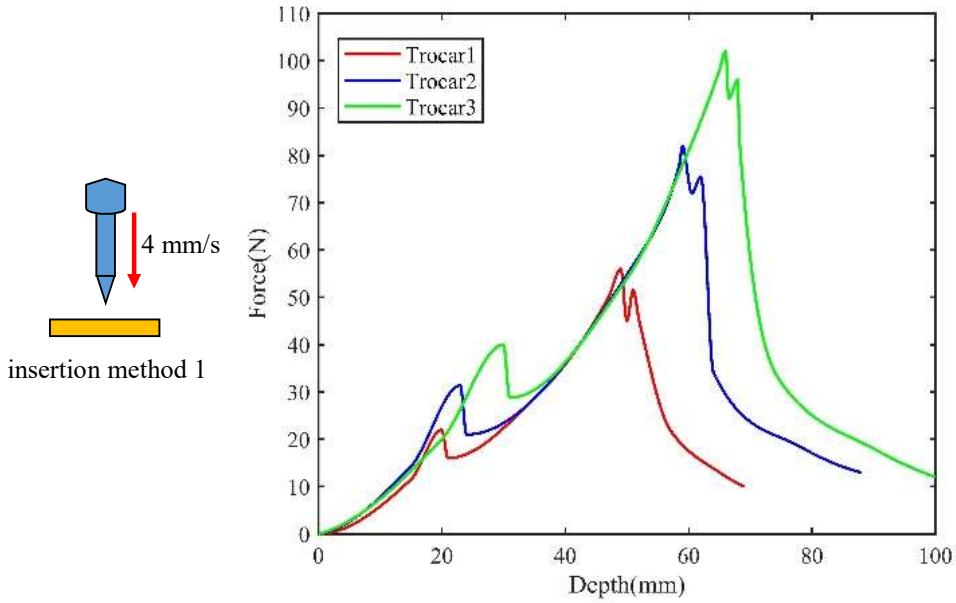

Fig.2-5. Insertion force measurement with the three trocars by method 1

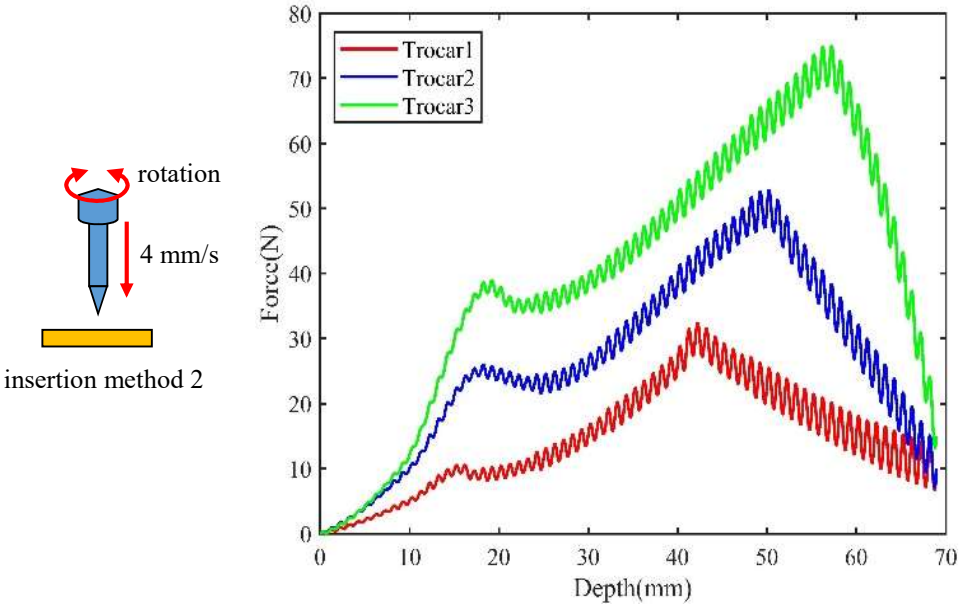

Fig.2-6. Insertion force measurement with the three trocars by method 2

2.1.3 Experimental Results

As shown in Fig.2-5 and Fig. 2-6, two insertion methods are utilized to make comparing experiments. In method 1, the trocar inserts at a constant speed (4 mm/s) without rotating. And in method 2 the trocar inserts downwards constantly at 4 mm/s with rotating. In method 2, the rotation follows the equation 2-1. The amplitude A is

set to π/4 and the frequency *f* is set to 1 Hz. The insertion force curves of each insertion method are shown respectively in Fig 2-5 and Fig 2-6.

The horizontal axis represents the displacement the trocar moves downward since it contacts to the abdominal wall. And the vertical axis represents the vertical force.trocar bears in the whole insertion process. In Fig.2-5 and Fig.2-6, it can be obviously observed as follows:

1) The specific maximum insertion force differs among the three types. The largest insertion force peak of kinds of trocars roughly range from 50 N to 100 N.

2) Comparing the two figures, it can be observed that when using the same trocar, insertion with rotation requires less force than without rotation to finish the insertion. For instance, when insertion trocar#2 without rotation, the largest force is about 84 N. Whereas when insertion with rotation, the largest force is about 50 N.

3) Comparing the two figures, there are obvious force fluctuations when insertion with rotation. The fluctuation ranges about ±3 N.

4) Three types all show that in the same insertion method, the sharper the trocar is, the less insertion force it requires to finish insertion.

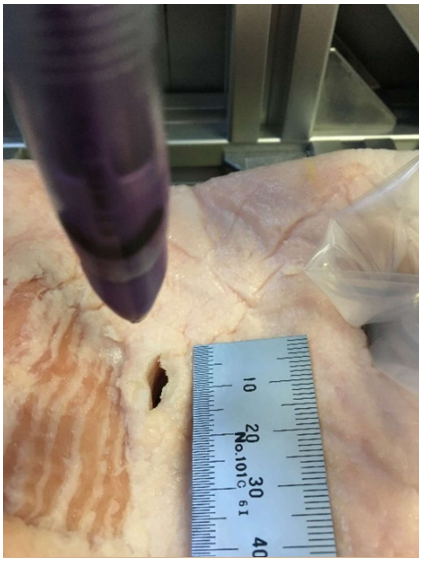

Fig.2-7. The abdominal port after insertion

2.1.4 Moment of penetrate-out

In addition to the above phenomena, in Fig.2-8 it can be obviously learned that three kinds of trocars have a similar force trend: there is an initial increase from zero, and a small peak occurs at approximately 20-30 N. After that peak, the force continues to increase to the maximal force peak and falls down. Then a smaller peak next to the biggest one appears before the force falls to approximately 10 N.

The force curves have the same characteristics as follows:

1) In a whole insertion process, there are three obvious peaks.

2) The second peak is the largest among them.

3) The third peak is nearly next to the second one.

In order to find out the corresponding point in the force curve when the trocar penetrates out of the abdominal wall, in Fig.2-9 we list images corresponding to the feature points in the insertion force curves, which are clearly marked in Fig.2-8.

In Fig.2-9, it can be observed that the trocar had not penetrated out at the moment

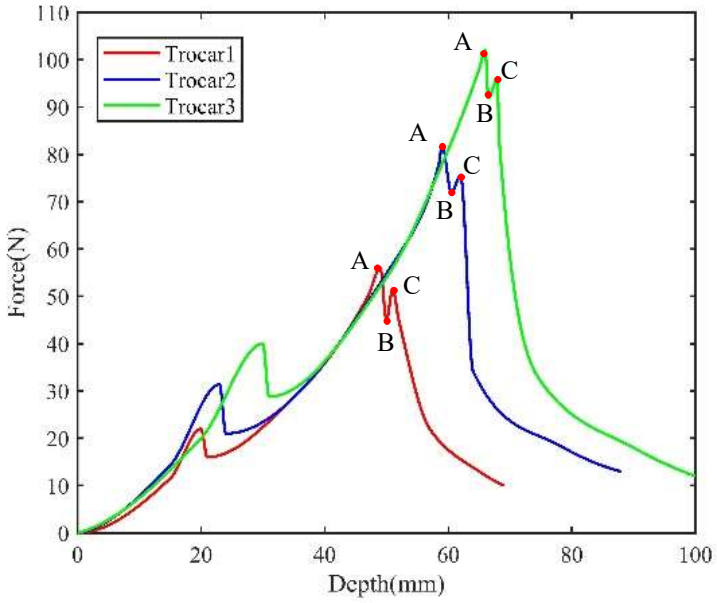

Fig.2-8. Feature points in trocar insertion force curves

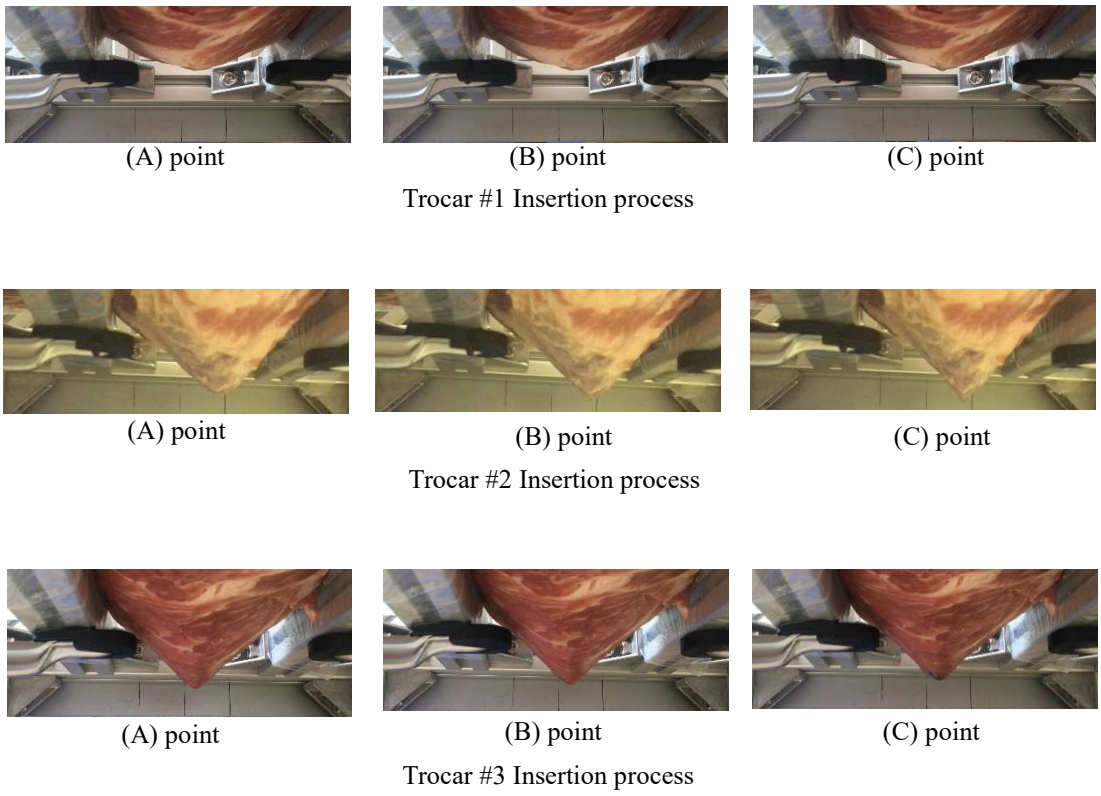

Fig.2-9. Images during insertion with the three trocars

of the biggest force peak as shown in Fig.2-8 (A point), and the indication of penetrate-out can be found at the subsequent smaller peak (C point in Fig.2-8). By corresponding Fig.2-8 to Fig.2-9, this phenomenon can be observed in all experiments no matter which type is used. Thus, we consider that the smaller peak next to the maximum one can be regarded as a force indicator which can remind of penetrate-out. And the computer is able to recognize the abdominal penetrate-out by detecting this smaller force peak.

On the other hand, as shown in Fig.2-6, there is obvious fluctuation when trocar is inserted with rotation. But similar results can be observed, bladed trocar (trocar #1) requires the least force to penetrate out and the blade-less trocar (trocar #3) requires the largest one. And as well the three trocars have the same force trend. However, there is a difference from insertion without rotation. In Fig.2-6, the smaller peak next to the maximal one all cannot be observed.

In front of the phenomena mentioned above, what we should discuss deeply is

that during insertion without rotation, why penetrate-outs all occur at the smaller peak next to the max force peak no matter which trocar type is used, and why during insertion with rotation, the small peaks behind the max one all disappear.

2.2 Mechanism of a force peak's occurrence

In order to explain the questions above, we firstly need to analyze why a force peak occurs.

First of all, a simple physical model, which a long sharp tool inserts through a uniform tissue, must be discussed. Fig.2-10 shows the whole process from the moment, when the tool contacts to the tissue, to the moment, when the tool penetrates out of the tissue. S_b represents bearing stress of the tissue at the point where the needle or trocar contacts. Thus, S_b depends on the deformation and the physical characteristics of the tissue itself. When there is no deformation of tissue, S_b equals to zero. And S_b grows with the increasing of deformation. On the other hand, S_c represents critical failure stress, which is a physical quantity only depending on the physical characteristics of tissue itself. And it determines the stiffness of the tissue.

As shown in Fig.2-10, the whole insertion process is divided into four phases.

A phase: the trocar or veress needle has not contact to the tissue.

B phase: the moment the trocar or veress needle contacts to the tissue.

C phase: the tissue deforms but is not penetrated out.

D phase: the moment tissue is penetrated out.

In A phase, S_b equals to zero because there is no deformation before contact.

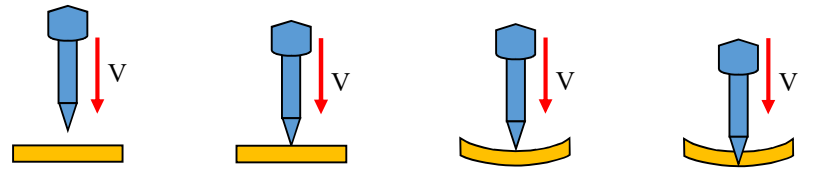

A phase	B phase	C phase	D phase
$0 = S_b < S_c$	$S_b < S_c$	$S_b = S_c$	penetrate out

Fig.2-10. Images during insertion with three trocars

And since the needle or trocar contacts to the tissue (B phase), S_b increases with deformation of the tissue, which can be approximately regarded as an elastic model. From B phase to the C phase, S_b increases with deformation but still remains smaller than S_c. When S_b equals to S_c (C phase), the deformation reaches maximum, then the tissue is destroyed and the needle or trocar penetrates out of the tissue.

And from the viewpoint of insertion force, since the B phase, insertion force increases and reaches a peak in the C phase. Subsequently, the force drops to a certain value that is required to overcome friction between the tissue and the needle. Thus, a force peak occurs in this whole process.

It is necessary to state that the model, introduced above, is ideal. In actual insertion, the insertion force $F_{insertion}$ can be divided to friction, cutting force and internal stiffness, as expressed in equation (2-2).

$$F_{insertion} = F_{friction} + F_{cutting} + F_{stiffness} \quad (2\text{-}2)$$

The cutting force and the friction occurs along the length of the tool inside the tissue and is due to Coulomb friction, tissue adhesion and damping [77, 78]. However, it does not influence on understanding the relationship between the stiffness and force peak.

2.3 Explanation of trocar insertion force curve

The theory of a force peak's occurrence has been introduced in 2.2 section. Based on that, we can explain why the insertion force have a similar trend regardless of trocar types or even insertion methods as following.

In experiments of trocar insertion, the abdominal wall is a none-uniform tissue not like the simple model mentioned before. It has a structure of multilayers, which consists of skin, subcutaneous fat, rectus muscle, and peritoneum from outside to inside [79-81], as shown in Fig.2-11. And of course they have different stiffnesses. Thus, $S_{c(s)}$, $S_{c(f)}$, $S_{c(m)}$ and $S_{c(p)}$ represent the critical failure stresses of skin, fat, muscle and peritoneum, respectively. Accordingly [71], their size relationship can be expressed in inequality (2-3). $S_{c(m)}$ is the largest among them and $S_{c(s)}$ is larger than $S_{c(f)}$. In other words, muscle is the hardest tissue in these four tissues and skin is harder than subcutaneous fat. The test measurement of individual layers can refer to Table 2-II.

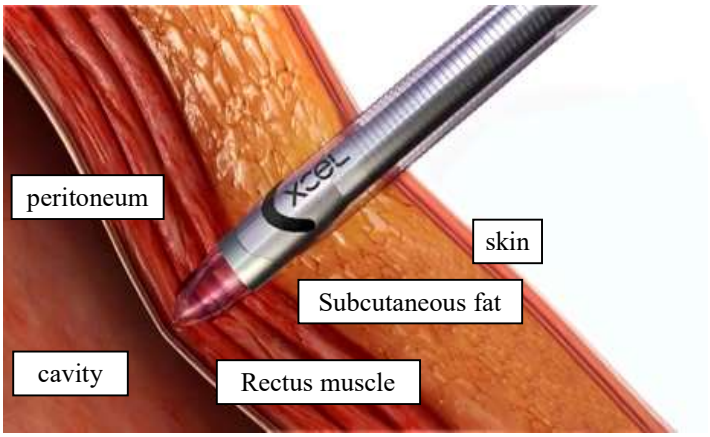

Fig.2-11. Images during insertion with three trocars [81]

Table.2-II. Elastic modulus of individual layers [79-81]

skin	Subcutaneous fat	Rectus muscle	peritoneum
~2.1 MPa	~0.83 MPa	~3.5 MPa	~0.7MPa

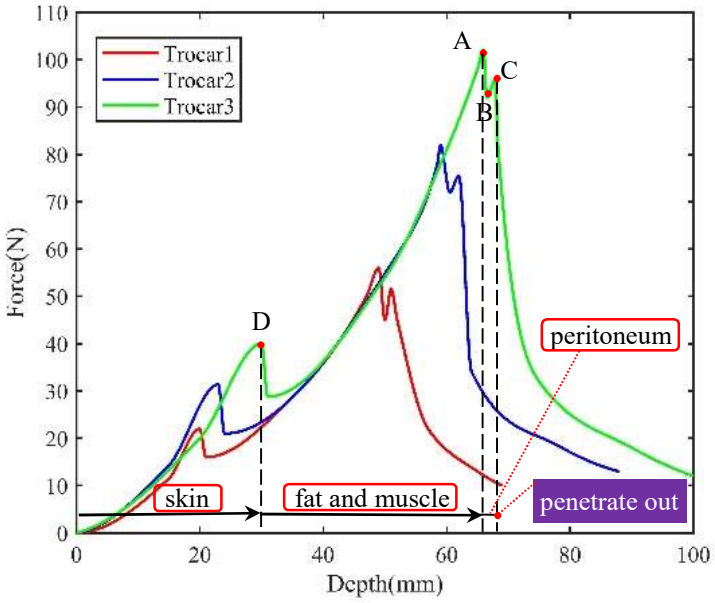

Fig.2-12. Interpretation of insertion force trend

$$S_{c(s)} > S_{c(f)} < S_{c(m)} > S_{c(p)} > 0 \tag{2-3}$$

Therefore, the insertion force trend when insertion without rotation is well agreement with the multilayer structure of the abdominal wall as shown in Fig.2-12.

Taking an instance of the trocar#3 insertion force curve, as $S_{c(m)}$ is the largest, it corresponds to the maximal force peak (A point). When the bearing stress of muscle $S_{b(m)}$ increases to its own critical failure stress $S_{c(m)}$, the insertion force reaches the maximal peak (A point). And at this moment, the trocar penetrates out of the muscle tissue. Subsequently, the trocar comes to contact to the peritoneum, which is softer than muscle tissue, and the force, which trocar is bearing, decreases (A to B). Then, further insertion deforms the peritoneum and correspondingly insertion force increases back (B to C). When the bearing stress of the peritoneum $S_{b(p)}$ increases to its own critical failure stress $S_{c(p)}$, the trocar penetrates out of the peritoneum and the insertion force reaches the smaller peak (C point) next to the maximal one. As peritoneum tissue is the last layer of the abdominal wall, the smaller peak next to the maximum force peak, which is caused by peritoneum penetrate-out, reflects the penetrate-out of the

entire abdominal wall. Since $S_{c(s)}$ is larger than $S_{c(f)}$, a force peak (D point) can be found before the biggest peak in all of the insertion force curves as shown in Fig.2-12. It reflects the penetrate-out of the skin. After that, since $S_{c(f)}$ is smaller than $S_{c(m)}$, no further force peaks could be observed until the trocar penetrates out of the muscle layer.

Besides that, the muscle and peritoneum is adjacent, as a result, the third peak is near next to the biggest one. And because there is fat tissue between skin and muscle, there is certain distance between the first peak and the second one.

In further experiments, to prove the explanation stated above more persuasively, we insert trocars into porcine abdominal wall, whose peritoneum is removed out, and measure its insertion force. As shown in Fig.2-12, insertion force curves of normal abdomens have a smaller peak next to the maximum force peak. Whereas, in Fig.2-13, no such smaller peak can be observed because of the absence of peritoneum. This comparison fully confirms that the smaller peak next to the maximum force peak corresponds to final penetrate-out of the peritoneum.

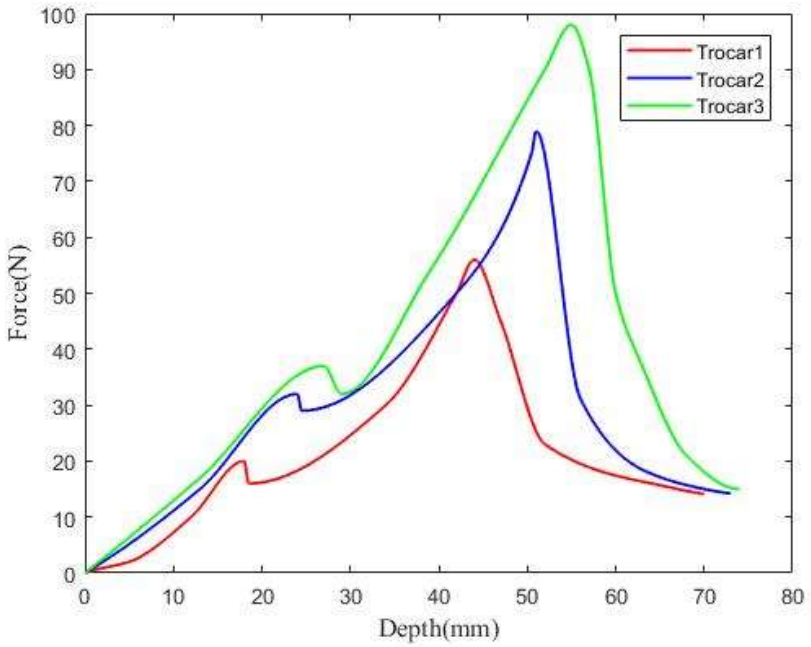

Fig.2-13. Insertion force when insert abdominal wall without peritoneum

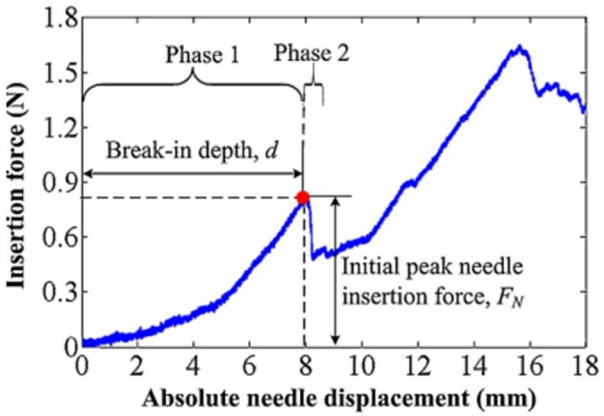

Fig.2-14. Insertion force when a Veress Needle inserts into human abdominal wall [40]

Now, the relationship between trocar insertion force trend and the abdominal multilayers structure has been clarified. However, before we make computers to recognize the penetrate-out by monitoring the insertion force when designing the insertion device, there are still two questions to solve.

1. The insertion force measured above are all using porcine abdominal wall. Does human abdominal wall also follow that trend?

2. In Fig.2-6, when trocar inserts with rotation, the peak behind the biggest peak cannot be observed. Why?

According to the explanation above, the insertion force trend should depend on the abdominal structure. And as known to us, human abdominal structure also follows the multilayers rule [71-75]. And here, we cite experimental results from other research [40] to verify it. Fig.2-14 shows a force measurement when a thin Veress Needle (diameter 2 mm) inserts into human abdomen. It can be obviously seen that it has the same trend as the results we measured using the porcine abdominal wall. It also effectively proves that the insertion force trend is exactly decided by the multilayers structure. And because the abdominal multilayers structure does not vary from factors such as personal individuality, trocar types and insertion speed, etc. This theory can be regarded as a reliable evidence to recognize the abdominal penetrate-out by computers in future research.

However, why does the smaller force peak behind the maximal one cannot be

observed in Fig.2-6? When a trocar inserts with rotation, the rotation causes obvious force fluctuation, which can be seen in Fig.2-6. The force peak, which reflects the penetrate-out of peritoneum comes to difficult to observe among fluctuations. This is a reason. Besides, in Fig.2-5 and Fig.2-6, it can be seen that when conducting by the same kind of trocar, insertion with rotation requires smaller force than that without rotation when it penetrates out of different tissues of abdominal wall. And the peritoneum is the order of only approximately 0.8 mm thickness [82]. Thus, it is easier to be destroyed when insertion with rotation than that without rotation. Two reasons above make the smaller peak next to the maximal one not obvious as much as insertion without rotation. However, peaks corresponding to the skin and muscle tissue penetrate-out can be obviously recognized.

As mentioned above, the thickness of peritoneum is approximately 0.8 mm, but in Fig.2-12 the width of the third peak is about 4-5 mm. This is because when the trocar inserts, the soft peritoneum deforms.

In Fig.2-12, the third peaks of the three force curves approximately have the same width, it seems not reflect the sharpness of different trocars. As shown in Table 2-II, the stiffness of peritoneum is less than 0.7MPa, which is the smallest among the four tissues. And in actual insertion, peritoneum has viscosity. Reasons above cause the width of third force peak cannot reflect the sharpness of different trocars.

2.4 Relationship between insertion force and other factors

Many factors influence the insertion force, such as insertion speed, trocar types, etc. This section describes the relationship between them and figure out the optimal insertion parameters.

2.4.1 Influence of abdominal thickness on insertion force

Firstly, insertions using porcine abdominal wall with different thickness (40, 45, 50, 55 mm) have been conducted. Using the trocar#2 at a constant speed of 4mm/s without rotation, the force measurements are shown in Fig.2-16.

It can be seen that the thicker the abdominal wall is, the force peak corresponding to the same tissue is higher, respectively. It is not difficult to understand. The thicker the abdominal wall, the thicker for each layer.

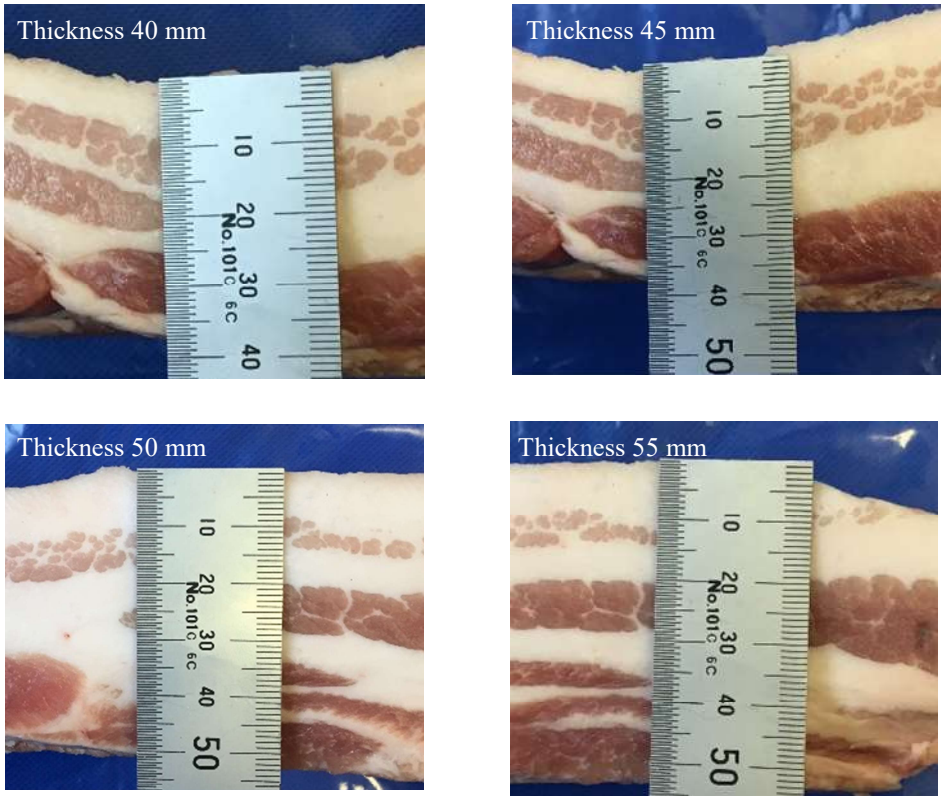

Fig.2-15. Abdominal wall materials in different thickness

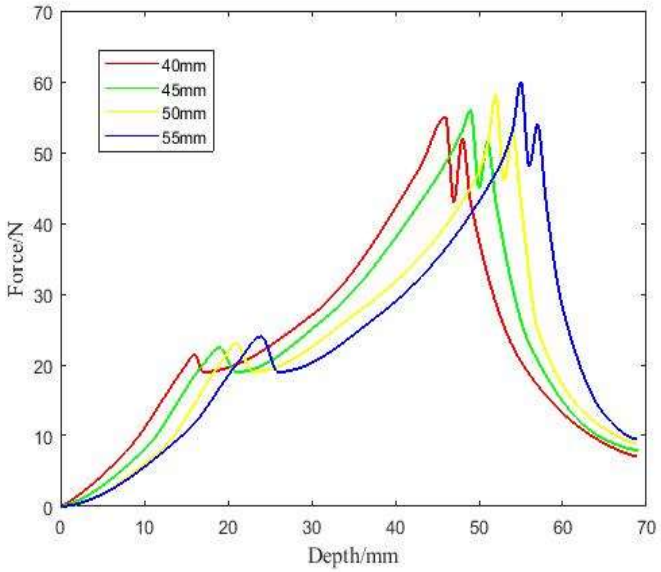

Fig.2-16. Insertion force using different thickness abdominal wall

2.4.2 Influence of insertion speed on insertion force

On the force measurement platform, we insert the trocar#1 (the retractile bladed one) at different constant speeds with and without rotation. Note that when insertion with rotation, the rotation follows the equation 2-1. The amplitude A is set to π/4 and the frequency f is set to 1 Hz.

$$\theta = Asin(2\pi ft) \tag{2-1}$$

And in every speed interval, insertions are repeated five times. Fig.2-17 shows the maximum force value of every experiment.

It can be learned that when the trocar#1 (the retractile bladed one) inserts without rotation at different speeds (2, 4, 6, 8 mm/s), maximal insertion force ranges from 50 to 60 N approximately. And when the trocar#1 inserts with rotation at different speeds, it ranges from 30 to 35 N. The results obtained confirm the conclusions from Fig.2-5 and Fig.2-6 regarding the lower force when rotating trocar. And when the trocar#1 inserts in the same method, the faster the trocar inserts, the less insertion force it requires to penetrate out.

Here we do not explain why the biggest force peak decreases with insertion speed increasing in details. In brief, the increasing insertion speed will decrease the cutting

force in the equation (2-2) mentioned in section 2.2. A research [69] can be cited to explain this phenomenon. Mohsen Mahvash and Pierre E have researched on the mechanics of dynamic needle insertion into a biological material. This research clarified why insertion force decreases with insertion speed increasing and proposed a concept "saturation velocity". It tells that when the insertion speed increases to a certain value, the insertion force will not decrease any more. And this certain insertion speed depends on many factors like specific sharp tool, biotissue, etc. Even though their research used a thin needle to insert the porcine cardiac tissue, the theory is also accessible for trocars insert abdominal wall.

In addition, three types of trocars are used to take the insertion measurement.

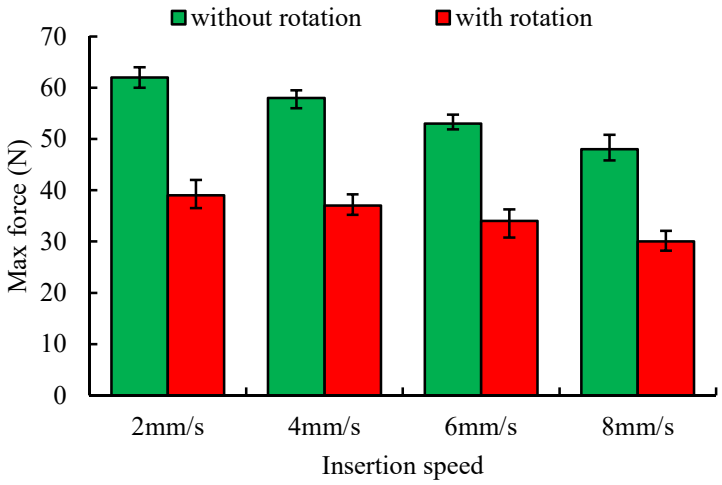

Fig.2-17. The Max force peak of insertion when trocar#1 inserts with different constant speeds

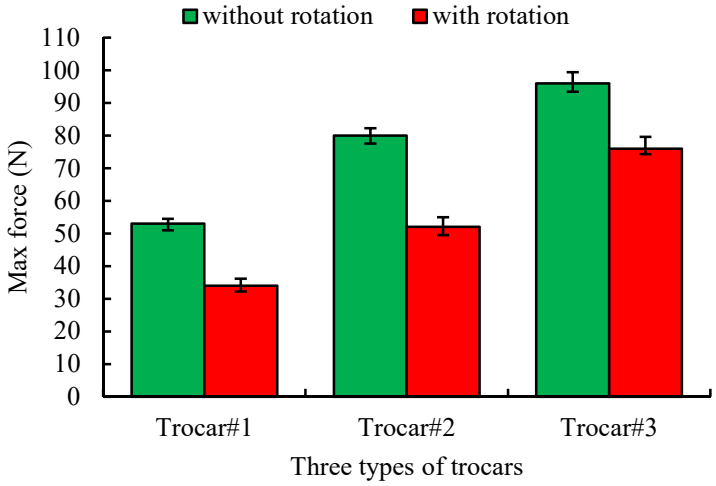

Fig.2-18. The Max force peak of insertion when three types of trocars inserts

Insertion speed is 4 mm/sec, rotation is the same with the experiment above. Fig.2-18 also confirms the conclusions from Fig.2-5 and Fig.2-6 regarding higher force for blunted trocar, which is easy to understand.

2.4.3 Influence of insertion speed on abdominal deformation

Fig.2-19 shows the deformation of the abdominal wall, which are measured when the trocar penetrates out and has stopped. In Fig.2-19, when the trocar#1 inserts without rotation at different speeds (2, 4, 6, 8 mm/s), the deformation approximately ranges from 17 to 26 mm. In contrast, when it inserts with rotation, it ranges from 16 to 20 mm. Since the deformation has positive relation with the maximal force, we can find out similar results to those of the max force.

Fig.2-20 shows the deformation when three types of trocars are used at a constant speed of 4 mm/s. the rotation is the same with the experiments above.

In experiments and discussion above, insertion with rotation, using a sharper trocar at higher speed can decrease the insertion force and the abdominal deformation at a certain level. However, it is not difficult to understand that faster insertion with sharper trocar would cause overshooting and injuries more easily. It stresses the necessity of this development of trocar insertion device, which can ensure safe insertion at high speed.

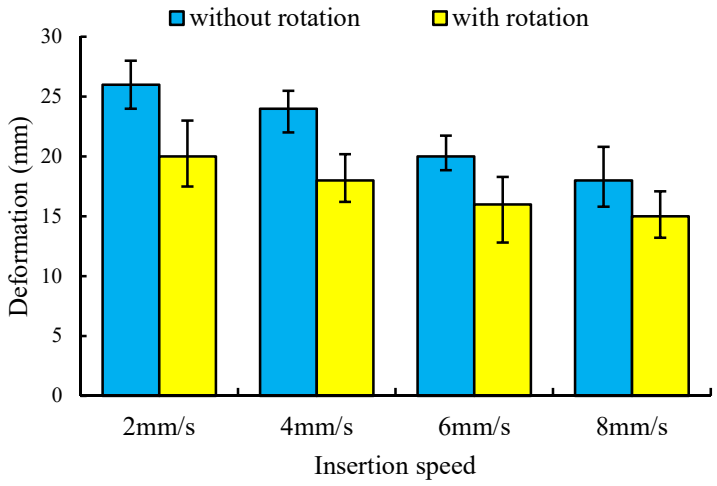

Fig.2-19. Deformation of the abdominal wall when trocar#1 inserts at different constant speed

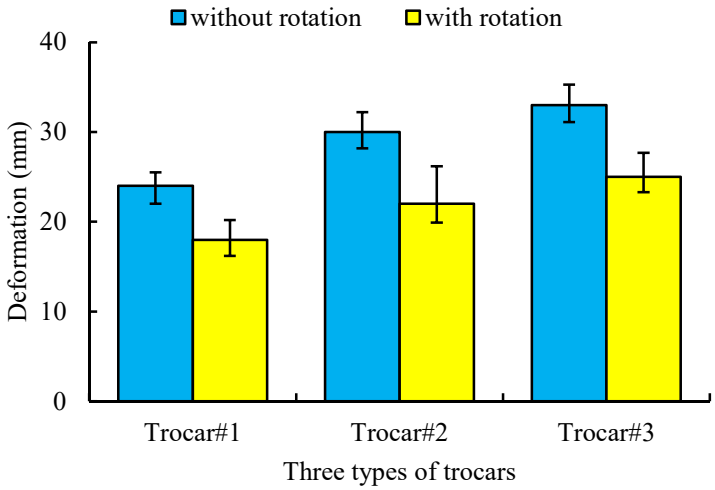

Fig.2-20. Deformation of the abdominal wall when three types of trocars inserts

Given the normal abdominal thickness (30-50 mm) and motors dynamic characteristics, we set the insertion speed at 10 mm/s for the insertion device later.

2.5 Summary

We list the following conclusions from the experiments and interpretations in this chapter:

1. The insertion force with different kinds of trocars and different insertion methods were measured. Although the force varied from different trocars, force curves had a similar trend. By tracing images of every moment, when a trocar inserted without rotation, the moment, when it penetrated out of the abdominal wall, can be located at the smaller peak next to the maximal one of its insertion force curve. However, when a trocar inserted with rotation, the small peak behind the biggest force peak could not be obviously seen because of fluctuation.

2. The insertion force trend was well interpreted with the theory of a force peak's occurrence and the abdominal multilayers structure. Three peaks in the whole process correspond to skin penetrated-out, muscle penetrated-out and peritoneum penetrated-out. The correctness of this interpretation was experimentally verified. It can be regarded as a reliable evidence for recognizing the penetrate-out regardless of individuality, trocars types and insertion speeds.

3. According to experiment results, insertion with rotation, using a sharper trocar at higher speed was able to cause less insertion force and deformation of the abdominal wall at a certain level.

Technologically, the small peak behind the biggest one is the indicator of abdominal penetration out. However, in the actual application process, because the peritoneum is soft and thin, it is difficult to detect the corresponding peak during monitoring insertion force, especially insertion with rotation. Thus, we adopt to detect the second peak (which corresponds to the muscle penetrate-out) to indict abdominal penetration out, which will be introduced in chapter 3 and 4.

Chapter 3. Design of Trocar Insertion Device and Control System

3.1 Trocar insertion device design

3.1.1 Concept of the insertion device

In trocar insertion, two motions, which drive trocar to move forward and rotation, are necessary. This device also consists of these two motions. However, in this device design, which kind of actuators is appropriate? It is a question need to discuss.

As mentioned in chapter 1, the ideal insertion device is desired to be able to stop timely upon the trocar penetrates out of the abdominal wall. When the trocar penetrates out of the abdominal wall, the bearing force decreases rapidly. In order to decrease the negative influence of external force on actuators, the actuator, which drives the trocar insertion, must have fast dynamic responsiveness and low backdrivability. The ball screw obviously has advantages in this aspect because of less friction. As shown in Fig.3-1, one motor drives the insertion forward by a ball screw, and the other one drives the trocar rotating directly.

There is no device till now, which can achieve stable the abdominal wall and drive the insertion at the same time. Usually, other assistant is necessary to lift up the

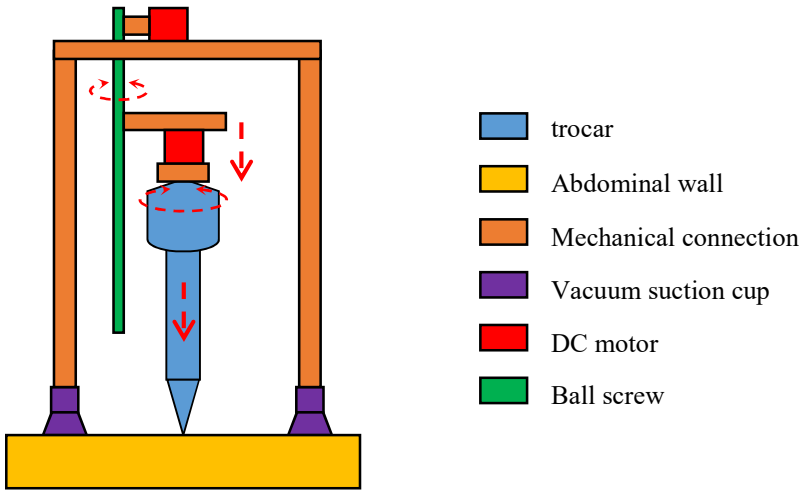

Fig.3-1. The concept of developed device

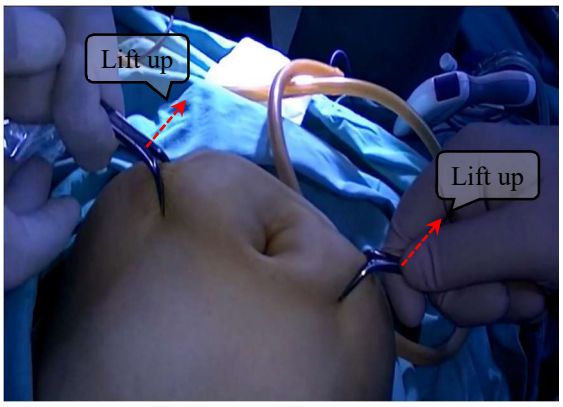

Fig.3-2. Lifting up by assistant surgeons [19,20]

Fig.3-3. Cupping therapy [83]

abdominal wall, as shown in Fig.3-2. In this research, we desire this device can both lift up the abdominal wall and insert trocar. That would access one surgeon to finish the insertion with this device independently.

In order to achieve this function, the cupping method is utilized, as shown in Fig.3-3. Cupping is a common therapy, which is popular in Asia and Europe [83]. It targets area by creating a partial vacuum either by the heating and subsequent cooling of the air in the cup, or via a mechanical pump. The cup is usually left in place for somewhere between five and fifteen minutes. It has been proved that cupping is generally safe when applied by trained professionals on people who are otherwise healthy [84, 85]. There is no harm to the human body in medicine.

In this device, we connect the suction cups to vacuum generator to make sure they can be adhered to the abdominal wall. Fig.3-1 shows the concept of this design.

3.1.2 Design of the device

The prototype model of trocar insertion device is shown in Fig.3-4. It has a pistol-shape and its size is 282 mm * 122 mm * 237 mm, which allows operators to handle easily. The trocar is located along the central axis. The device has two motor combinations, the first one is assembled inside the handle part, and this motor drives the ball screw through belt and belt wheels, to drive the trocar to inserte forward indirectly. The other one is assembled behind the trocar, which can drive the trocar to rotate along the central axis. Because the trocar would bear the insertion force along the central axis, an angular bearing is assembled above the trocar.

As illustrated in chapter 2, the trocar insertion force ranges about 50-100 N, insertion speed ranges about 0-10 mm/sec, the rotation frequency ranges about 0-3 Hz, and the distance from trocar contacts to the abdominal wall to it penetrates out ranges about 100 mm. These are important requirements during design. Based on those requirements, specifications of this device are listed in Table 3-I.

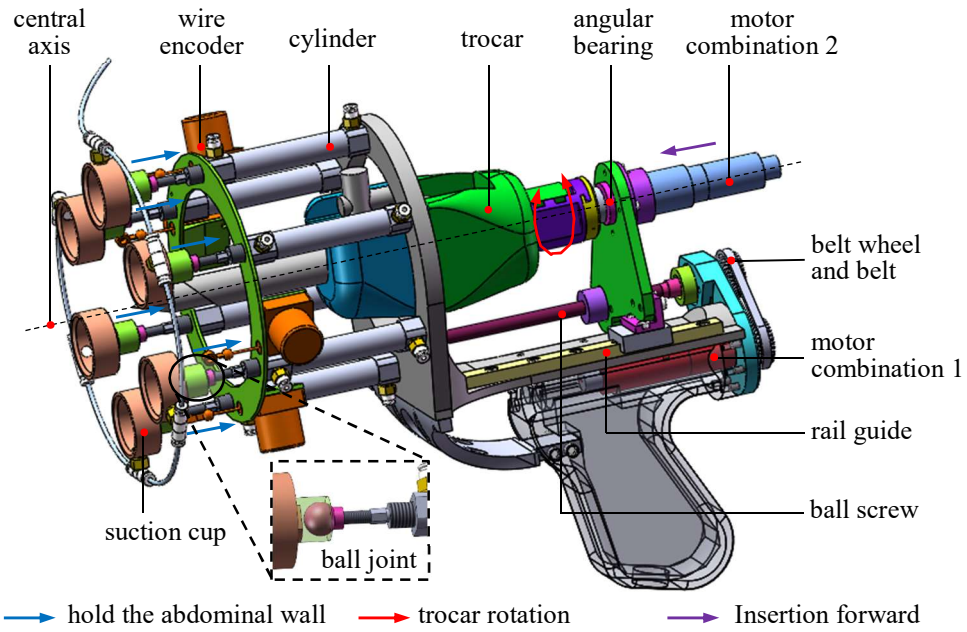

Fig.3-4. Trocar insertion device model

Table 3-I. Specifications of the trocar insertion device

Movable range of insertion	115 mm
Movable range of lifting	30 mm
Max pull force for lifting	6 * 30 N
Adhesive force of suction cups	6 * 62.17 N
Insert speed range	0-12 mm/s
Rotation frequency range	0-3 Hz
Max insertion force	180 N
Area of action	230 mm^2
Size (L * W * H) (mm)	282 * 122 * 237
Weight	1.09 kg
Sampling Frequency of control system	1 kHz

In term of Max pull force for lifting, 30 N represents the max pull force of a pneumatic cylinder. The same interpretation for adhesive force of suction cups.

The components for abdominal lifting up consist of pneumatic cylinders, wire encoders, suction cups and ball joints. As introduced in section 3.1.1, the suction cups are connected to a vacuum generator to adhere to the abdominal wall as the assistant surgeon grip the abdominal wall. Therefore, as shown in Fig.3-4, the suction cups are connected to the air cylinders. The air cylinders pull up the abdominal wall as the assistant surgeon lifts up the abdominal wall. Because the abdominal wall is uneven and easily deforms, the ball joint between air cylinders' rod and suction cups can make the suction cups to fit on abdominal wall better. Near the air cylinders, wire encoders are installed to measure the displacements of the air-cylinders. The role of these encoders will be introduced in details in the later section of cylinder control.

In this way, the device integrates both functions of trocar insertion driving and abdominal lifting up at the same time.

3.1.3 The whole system

The whole system of this trocar insertion device is shown in Fig.3-5. Kinds of actuators are all driven by the same control computer. AD, DA, CNT three kinds of boards are prepared in the computer. The middle parts consist of pressure sensors, servo amplifiers, servo valves unit, a vacuum generator and a pressure regulator.

The air flow path is described by dotted lines. The compressed air flows from the compressor. After passing through the pressure regulator, it has two paths. One path flows into the vacuum generator, the vacuum generator is connected to the six suction cups. The other path flows through servo valves unit to drive the air cylinders.

The electrical signal is described by solid lines. The wire encoders (measuring the cylinders' rod extend) and the rotation encoders in the motor combination (measuring the motor turns) are read by the CNT board. The air pressure of cylinders' chambers are measured by air pressure sensors. And the pressure are read by AD board. After computing, the control signals are sent out by DA board. One is sent to the servo valve unit to control the cylinders, the other one is sent to servo amplifiers to control motors.

Finally, the middle components are stored in a control box, which is 310 mm * 280 mm * 150 mm. the 3D model of the control box and the prototype of the control box are shown in Fig.3-6.

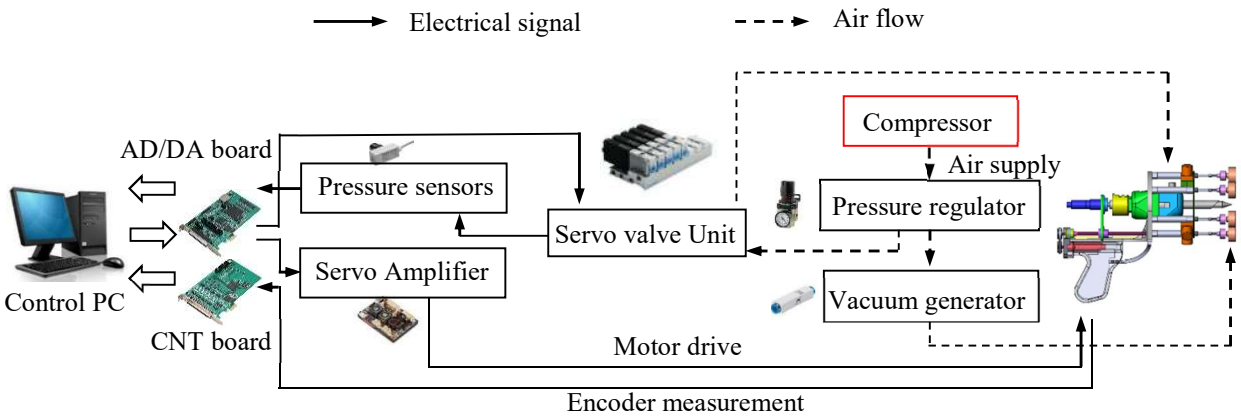

Fig.3-5. The whole trocar insertion device system

The prototype of the whole system is shown in Fig.3-7. It consists of the air compressor, Control PC, the Control box and the trocar insertion device.

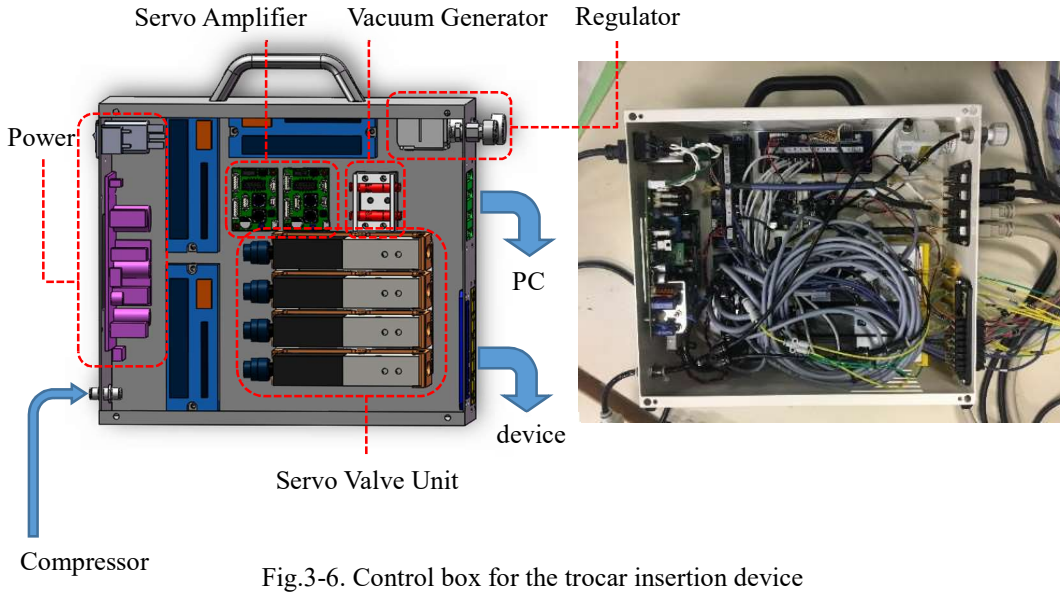

Fig.3-6. Control box for the trocar insertion device

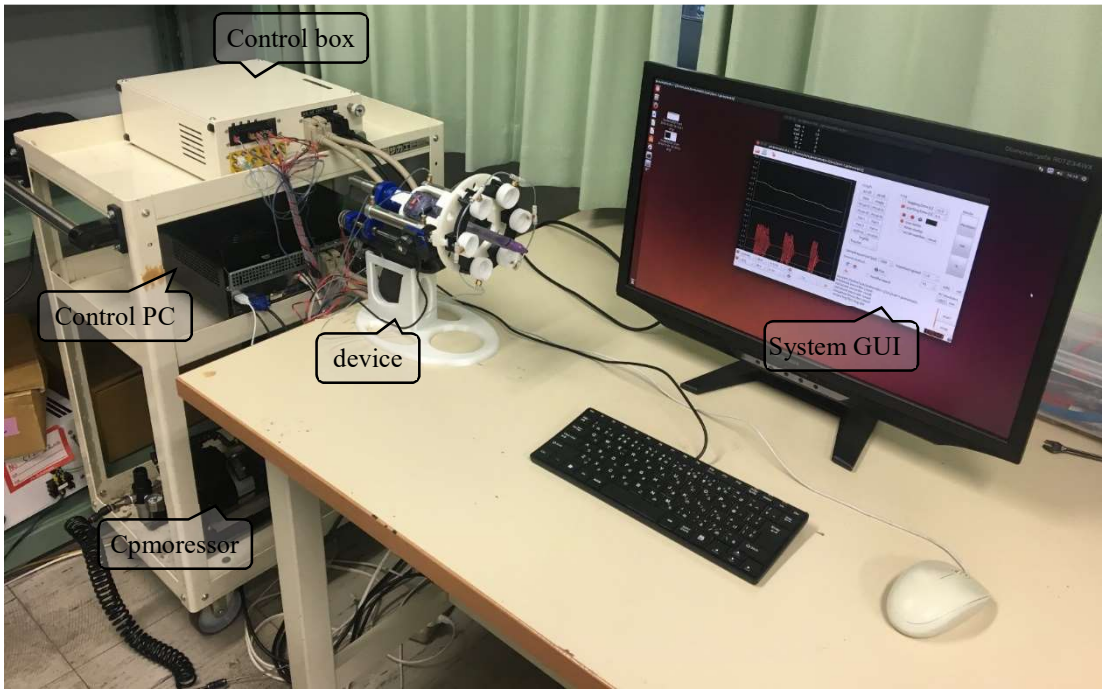

Fig.3-7. Prototype of the whole trocar insertion device system

3.2 Control methods

The whole system has been described in section 3.1. According to the type of actuators, it can be classified to three kinds, the suction cups (adhere the device to the abdominal wall), the air-cylinders (lift up the abdominal wall to make it stable) and the motors (drive the trocar inserting). The control methods of these actuators are described respectively in this section.

3.2.1. Suction Cups

As introduced above, the suction cups are placed in front of the device handle, and connected to a vacuum generator. Because the area covered by device (Fig.3-8 left) is limited and the abdominal wall is uneven, six suction cups are placed uniformly and symmetrically in a circle of 105 mm diameter. If the suction cup's diameter is too small, six suction cups will not be able to bear the insertion force, which is approximately 50-100 N. And increasing the suction cup's number to satisfy the insertion force will result in too many pipes. On the other hand, if to enlarge the suction cup's diameter, mutual interference of suction cups will occur because of the limited circle where suction cups locate. According to the circumstances and limitations, the suction cups' number and diameters need to satisfy following inequalities.

$$100 * K_s < N * \pi \left(\frac{D}{2}\right)^2 * P \tag{3-1}$$

$$2 * \left(\frac{D}{2}\right) * K_s' < 2 * R * \sin\left(\frac{180^\circ}{N}\right) \tag{3-2}$$

Where, K_s represents safety coefficient, which ensures that the resultant is enough to bear the insertion force. N represents the number of suction cups, D represents the diameter of a suction cup, P represents the reaching vacuum of the vacuum generator.

In inequality (3-2), D represents the diameter of a suction cup, K_s' represents safety coefficient, which ensures that mutual interference of suction cups can be avoided. R represents the radius of the circle, where suction cups are placed. N represents the number of suction cups. In this design, K_s and K_s' were set to 1.3 and 1.2 respectively.

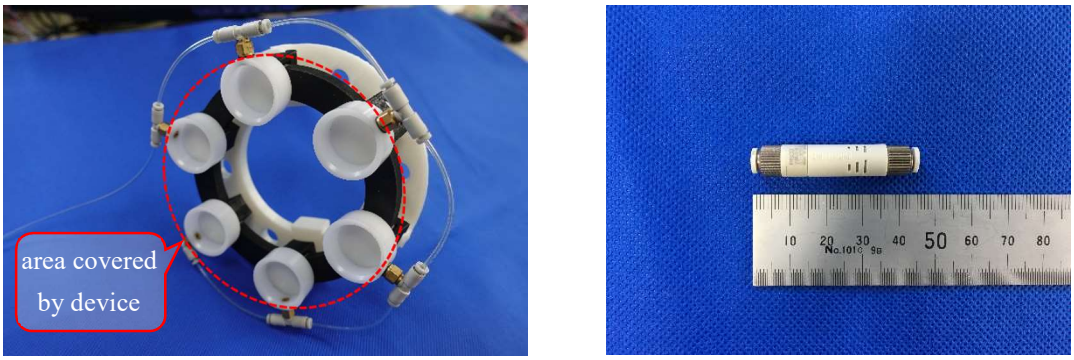

Fig.3-8. Suction cups parts (left) and vacuum generator (right)

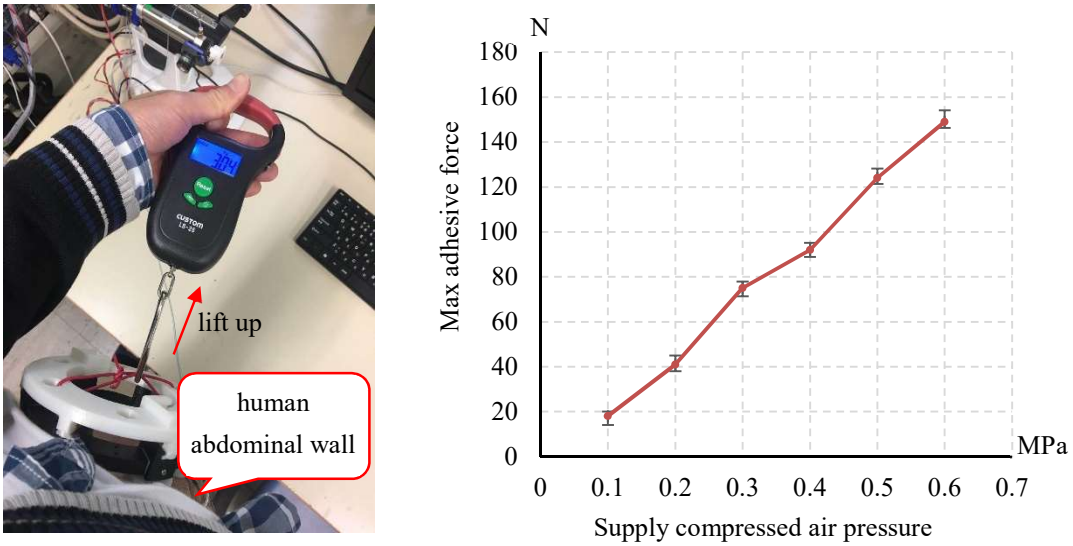

Fig.3-9. Measurement of adhesive force on human abdominal wall

In actual design, specifications of the suction cups and the vacuum generator are shown in Fig. 3-8 and Table 3-II. The diameter of a suction cup is 28 mm. There is chamfer of 1 mm at the edge of the suction cup. It helps to improve sealing. And air supply for the vacuum generator ranges about 0-0.7 MPa. The largest vacuum it can generate is approximately -88 kPa. In the whole system, the compressed air from regulator flows into this vacuum generator.

Table 3-II. Specifications of suction cups and vacuum generator

Diameter of a suction cup	28 mm
Air supply to vacuum generator	0-0.7 MPa
Max ranching vacuum	-88 kPa
Suction Cups Connection type	Series connect

This insertion device has a series connection of the six suction cups. Six suction cups were connected in a line as shown in Fig.3-4. An experiment was conducted to verify the effectiveness of the suction cups. As shown in Fig.3-9, compressed air is supplied by different pressures to the vacuum generator, and the corresponding suction force for human abdominal wall are measured by a hand gauge. In every experiment condition, measurements were repeated five times and the maximum resultant force to adhere to the abdominal wall were measured.

It can be obviously seen that it can achieve a suction resultant approximately 160 N when the air supply reaches 0.6 MPa. This experiment proves that the suction cups with vacuum can adhere to human abdominal wall effectively. And according to the measurement in chapter 2, these six suction cups can ensure to bear the trocar insertion force (about 50-100 N).

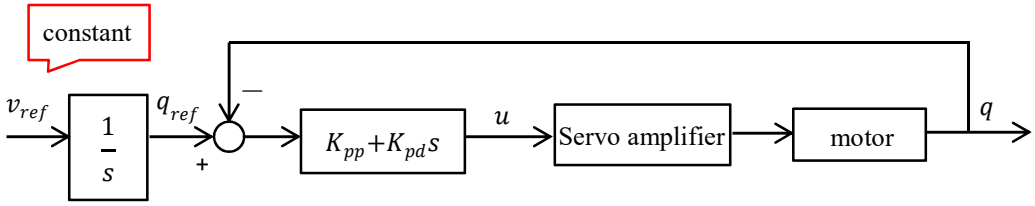

Fig.3-10. Block diagram of the motor for trocar insertion forward

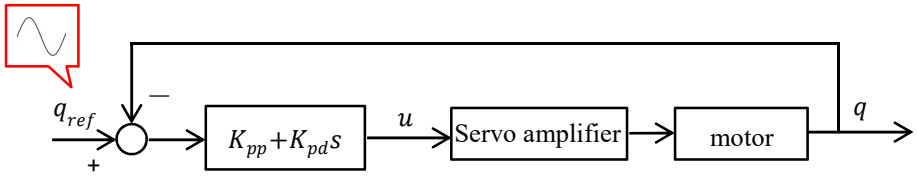

Fig.3-11. Block diagram of the motor for trocar rotation

3.2.2 Motor control

As introduced in section 3.1, the two DC motors drive the trocar to insert forward and to rotate. The two motors are connected to the control PC and servo amplifiers in the same way, as shown in Fig.3-5. The motor for insertion forward is under a velocity PD control and its control block diagram is shown in Fig.3-10.

v_{ref} represents the reference velocity for the insertion forward.

The motor for rotation is under a position PD control and its control block diagram is shown in Fig.3-11.

q_{ref} represents the reference angle for the trocar turns.

The q_{ref} of the motor for rotation can be expressed as following equation (3-3),

$$q_{ref} = Asin(2\pi ft) \tag{3-3}$$

Thus, it can be learned that the rotation of the trocar is following a sine signal under position control. A represents the amplitude, and f represents the frequency of the rotation.

Table 3-III. Gains for two motors control

Insertion forward	K_{pp}	10 V/rad
	K_{pd}	5 V·sec/rad
rotation	K_{pp}	12 V/rad
	K_{pd}	5V·sec/rad

K_{pp} and K_{pd} for the insertion forward and rotation are listed in Table 3-III. The motor can achieve better dynamic response by large K_{pp} and K_{pd}. However, the stability would decrease if these two parameters are too large. Fig.3-12 and 3-13 show the results during trocar rotates ±15deg with different frequencies (1.5 Hz and 3.0 Hz). And Fig.3-14 shows the magnitude-frequency characteristic of the rotation motor. It can be seen that it has good dynamic in 0-3.2 Hz.

The control system accesses the trocar insertion at a speed ranged about 0-12 mm/sec, and rotate at a frequency ranged about 0-3 Hz.

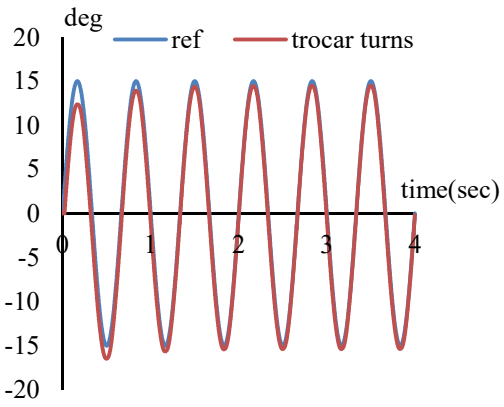

Fig.3-12. Experimental results of trocar rotate control (f = 1.5 Hz)

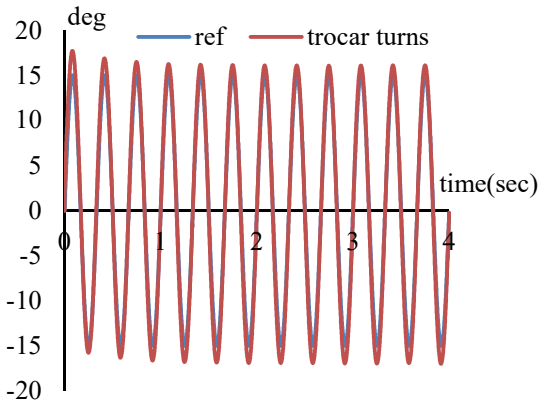

Fig.3-13. Experimental results of trocar rotate control (f = 3.0 Hz)

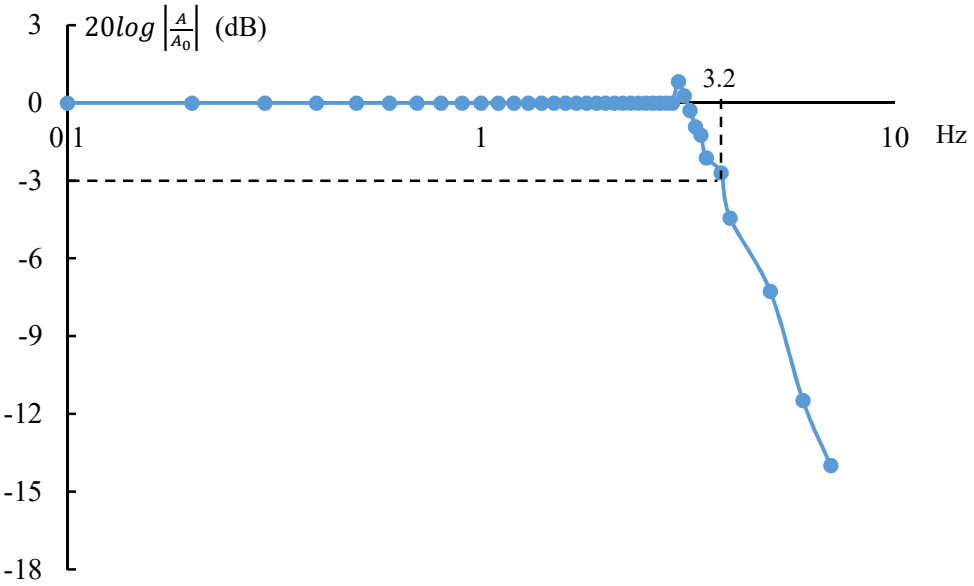

Fig.3-14. the magnitude-frequency characteristic of the rotation motor

3.2.3 Cylinder control

As introduced in section 3.1, cylinders of the device pull up the abdominal wall. It plays a role of assistant surgeons, who lifts up the abdominal wall. In this section, the control method for the cylinder is described.

Six cylinders are placed around the trocar. As shown in Fig.3-15, the six cylinders are divided into four groups. And there is only one air cylinder in the 1st and 4th group respectively. There are two air cylinders in the 2nd and 3rd group respectively. The connection of different groups are also shown in Fig.3-15.

In the 1st or the 4th group, one cylinder is driven by a servo valve. And there are two air pressure sensors to connect to the two chambers of the cylinder to measure the pressure respectively. And there is a wire encoder placed near the cylinder to measure the displacement of the cylinder rod, which can be seen in Fig.3-4.

In the 2nd or the 3rd group, two cylinders are driven by one same servo valve. And two air pressure sensors are placed in the pipe to measure the pressures of the two

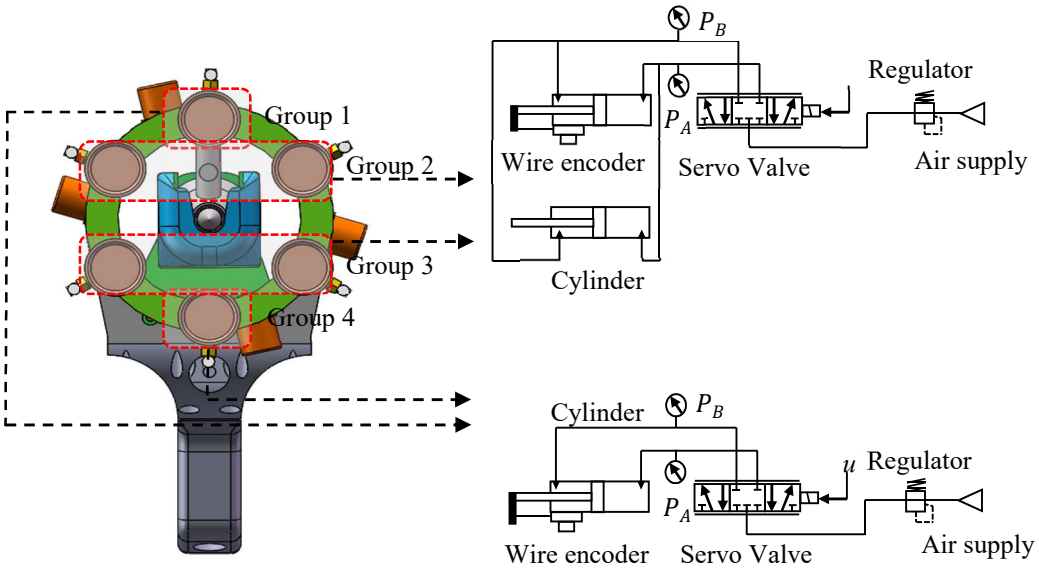

Fig.3-15. Cylinders connection of the trocar insertion device

chambers respectively. There is only one wire encoder to measure the displacement of one cylinder.

In the insertion device system, all the four groups are under an impedance control for position. And what should emphasize is that every group runs its own control independently. Fig.3-16. shows the impedance control block diagram.

q_{ref} represents the reference of the displacement, the cylinder rod moves. q represents the measurement (read by wire encoder) of the displacement, the cylinder rod moves. F_{dr_ref} represents the reference of the air driving force, which is calculated in equation (3-3).

$$F_{dr\_ref} = K_{pp}\left(q_{ref} - q\right) + K_{pd}\frac{d(q_{ref}-q)}{dt} \tag{3-3}$$

And the F_{dr} represents the actual air driving force calculated in equation (3-4).

$$F_{dr} = P_A \times S_A - P_B \times S_B \tag{3-4}$$

This control system has two feedbacks, the inner force feedback and the outer position feedback. K_{pp} and K_{pd} is coefficients for the PD position control of the outer feedback. K_{ap} and K_{ai} is coefficients for the PI force control of the inner feedback. Thus, the stiffness of this system mainly depends on the coefficient K_{pp}. The larger K_{pp} increases, more rigid the system becomes.

In the actual using process, the compressed air firstly only flow into the vacuum generator. Then to adjust the lengths, air cylinders' rods extend, to make sure suction cups were all adhered onto the abdominal wall. After that, the lengths, cylinder rods extend, are all read into the program and the impedance control set these lengths as the

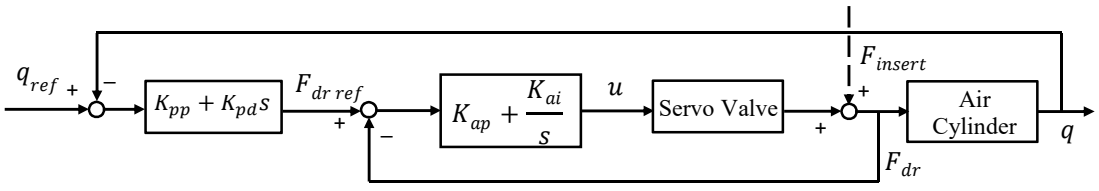

Fig.3-16. Block diagram of the cylinder impedance control

reference q_{ref} for every group. So q_{ref} of groups are all constant values, which are the extended length of cylinders rod in every group. In this control system, the coefficient K_{pp} is set to large value to make the system rigid enough. So that it can hold the abdominal wall stably. And K_{ap} and K_{ai} determines the dynamic response of the force feedback. If they are too large or too small, the air cylinder cannot achieve good stability.

A simple test is done as shown in Fig.3-17. To make sure the impedance control has both fast dynamic response and good stability, gains of the impedance control are listed in Table 3-IV. The cylinder's rod is pulled some times to test whether this impedance control is rigid enough and the gains are appropriate. Experiment results are shown in Fig.3-18- 3.20. In Fig.3-18 it can be learned that the q_{ref} is set to 40 mm, and the rod is pulled five times. Fig.3-19 shows that the cylinders generate F_{dr} to resist the pulling. It can be seen the force feedback have a good dynamic response. Fig.3-20 shows the pressure change in the two chambers. In the figures above, 1 mm displacement of air cylinder rod causes about 11 N F_{dr}. And because trocar insertion ranges about 100 N, which is known in chapter 2. It can be calculated that one air cylinder rod would extend approximately 1.4 mm during trocar insertion. And it is acceptable.

Table 3-IV. Gains of the cylinder impedance control

Outter PD	K_{pp}	9.3 N/mm
	K_{pd}	0.04 N·sec/mm
Inner PI	K_{ap}	0.06 V/N
	K_{ai}	0.13 V/N·sec

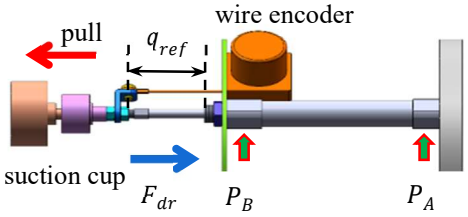

Fig.3-17. Impedance control of this device

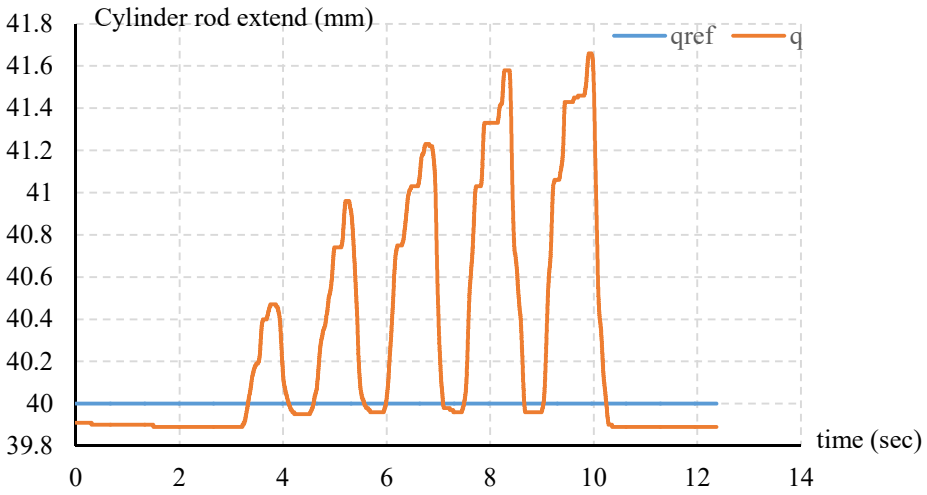

Fig.3-18. Cylinder rod extends length – time when pull a cylinder rod

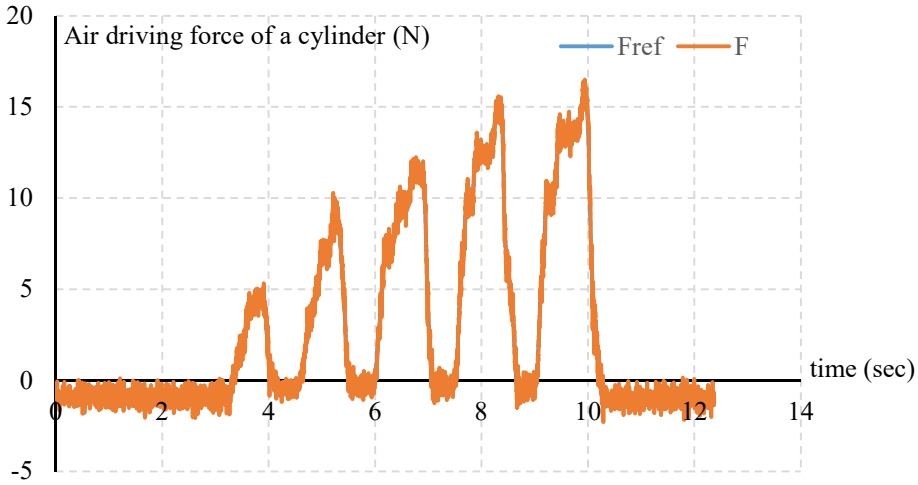

Fig.3-19. Air driving force – time when pull a cylinder rod

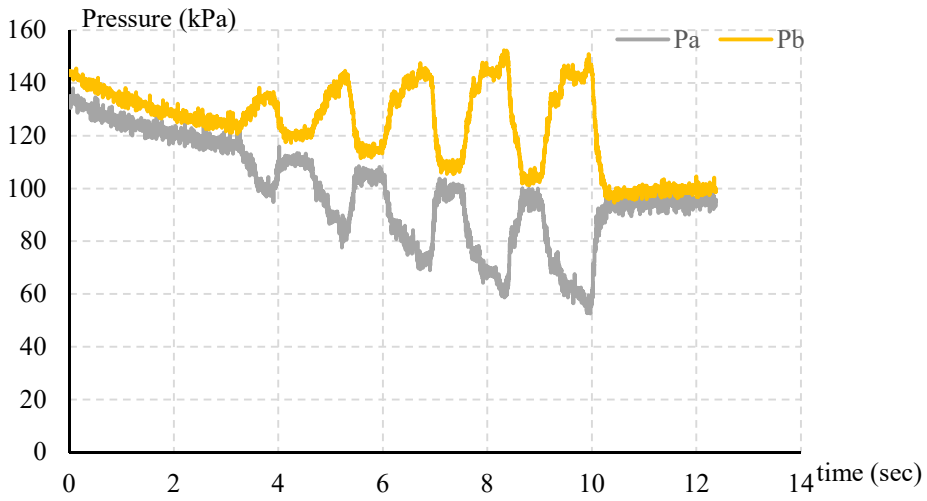

Fig.3-20. Air pressure in two chambers – time when pull a cylinder rod

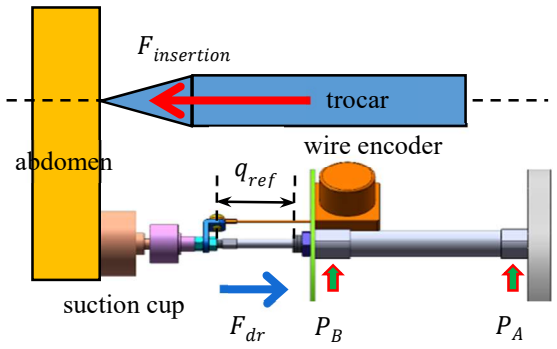

Fig.3-21. Insertion force analysis of the trocar insertion device

Fig.3-21 shows the force analysis of the trocar insertion device. When the trocar inserts forward, the abdominal wall bears an insertion force toward left. And because the suction cups are adhered onto the abdominal wall, the abdominal wall will pull the suction cups to left. However, suction cups moving left will extend the cylinders rod to lead to q_{ref} increasing and the air cylinders are all under a high stiffness impedance control. Thus, the servo valve will adjust the pressures of the two chambers to enlarge F_{dr}. So that the force abdominal wall beard will come to balance. In this way, the high stiffness impedance control for the air cylinders achieves the abdominal wall lifting up to make it stable.

Not only that, it may be noticed that there is no force sensor in the trocar insertion device. In this development, we monitor the force F_{dr_ref} to detect the insertion force change. Reasons of using pneumatic cylinders instead of a force sensor can be concluded as following:

1) The air cylinders play a role of lifting up the abdominal wall. Although by air driving force F_{dr_ref} it's difficult to calculate the insertion force precisely, the air driving force of the cylinders can reflect the change of the insertion force according to the positive relationship as the force feedback in Fig.3-16. And the test experiment about the stiffness of the impedance control and statements about insertion force analysis also prove that monitoring the air driving force is enough to recognize the insertion force change.

2) The trocar driven by this device inserts forward with rotating. If adding a force

sensor along the central axis (Fig.3-4), force fluctuation caused by trocar rotation will be recorded by the force sensor and it has a negative influence on the recognition of force peaks. In the latter experiment we will see the force fluctuation caused by trocar rotation does not appear when measuring the insertion force indirectly by air driving force F_{dr_ref}.

3) According to previous research and measurements in chapter 2, the insertion force approximately ranges from 70 N to 130 N. Force sensors in this measuring range are easy to be damaged by accidents. That increases the cost of maintenance.

3.3 Verification of actuators drive control and insertion force sensing

3.3.1 Experiment condition

Using the designed trocar insertion device, *Exvivo* experiments are conducted. As introduced in chapter 2, porcine abdominal wall has a great much similarity to human beings, so it is chosen as the experimental material. As shown in Fig.3-22, it is cut to a circle (diameter 110 mm). The insertion experiments are repeated several times, the thickness of the porcine abdominal wall selected all ranges about 40-50 mm. and because ambient temperature influences on tissue stress, all insertions are conducted at 24-26℃.

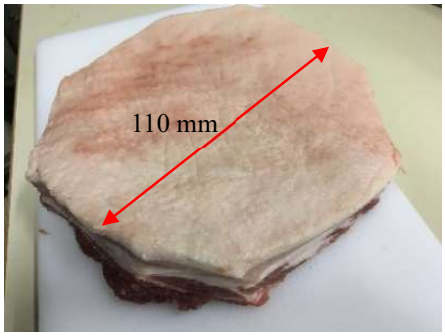

Fig.3-22. Porcine abdominal wall

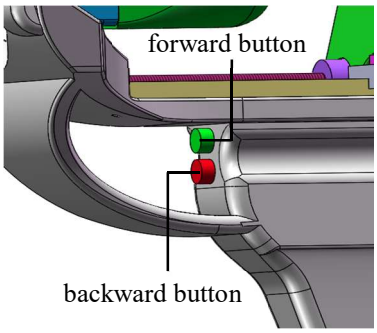

Fig.3-23. Two control buttons

3.3.2 Experimental operation

As shown in Fig.3-23, the device has two buttons in the place of trigger. When the green one is pressed, the device inserts the trocar forward with rotating. When the red one is pressed, the trocar moves backward with rotating. The specific experimental steps are described as follows:

1) set the insertion speed, the amplitude and frequency of rotation on GUI

2) open the switch to supply the compressed air, the regulator is turned at 0.6 MPa.

3) turn on the power switch for power supply

4) adhere the suction cups onto the abdominal wall

5) assemble the trocar on the device

6) start the system on GUI

7) keep pressing the green button until penetration-out is saw

As shown in Fig.3-24, the insertion experiment is conducted using the insertion device. It inserts at a low speed (2.5 mm/sec). The rotation all follows the equation 2-1, the amplitude A is $\pi/2$ and the frequency f is 1Hz.

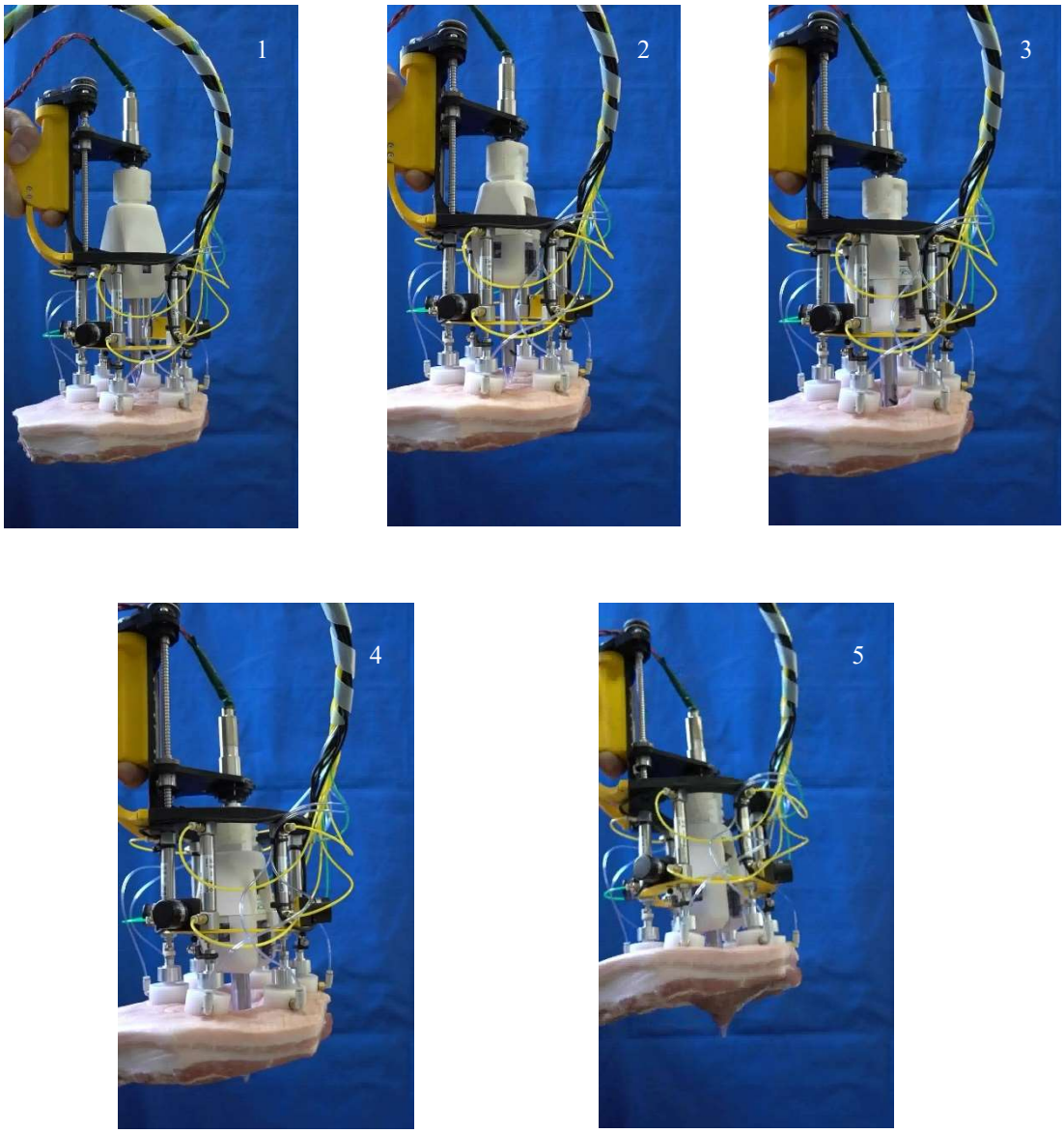

Fig.3-24 Insertion experiment using the trocar insertion device

3.3.3 Experimental results

In Fig.3-25, the horizontal axis represents the displacement the trocar inserts forward since it contacts to the abdominal wall. The vertical axis represents the resultant of six pneumatic cylinders' F_{dr_ref} in the respective impedance control. It can be seen that the two peaks (correspond to skin and muscle) can be recognized easily. As mentioned above, the resultant of the cylinders' F_{dr_ref} does not equal to the insertion force precisely, but it can be seen in the Figs 3-25, the resultants basically reflects the insertion force, both the trend and the approximate magnitude. Fig.3-26 shows the displacement the trocar moves forward and Fig.3-27 shows the rotation angle, the trocar turns.

In these experiments, it proves that the designed device enables one person to finish the insertion by himself or herself. The lifting up by pneumatic cylinders and the insertion driven by DC motors are effective.

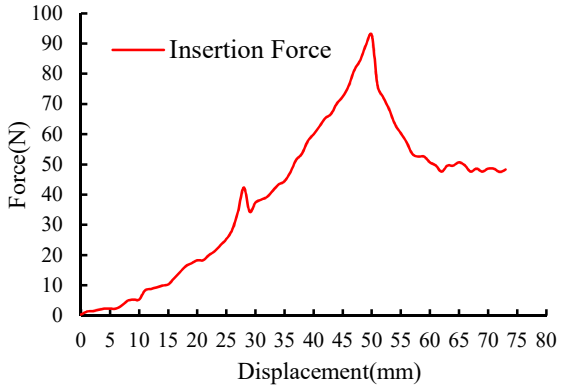

Fig.3-25. Resultant of the force F_{dr_ref} during insertion

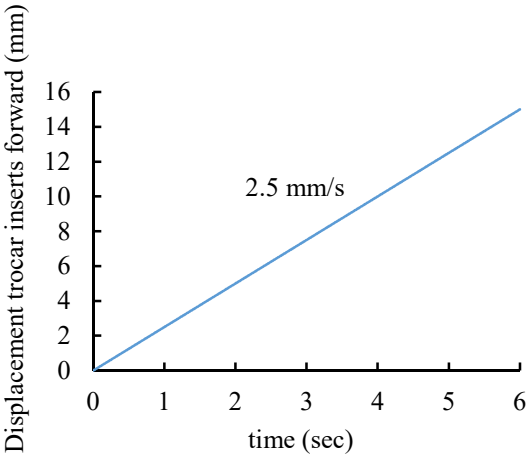

Fig.3-26. Trocar insertion forward displacement

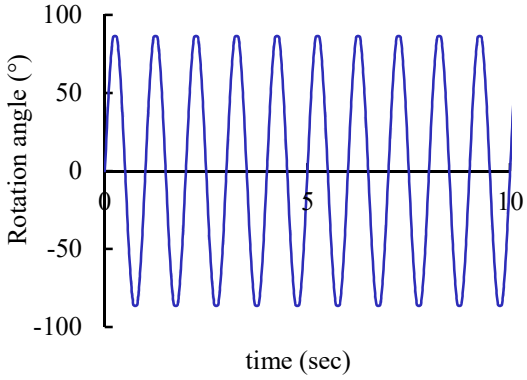

Fig.3-27. Trocar rotates

However, there are still two points need to pay attention.

One point is that the small peak corresponding to the peritoneum penetration-out cannot be seen in this force sensing method.

As mentioned in explanation of its disappearance when trocar insertion with rotation in chapter 2, the peritoneum tissue is so thin and soft that it is easy to destroy. And when the force monitoring method by pneumatic cylinders is used, the cylinders are places around the trocar. Added to the soft abdominal tissue has absorption of force, it is not difficult to understand that the cylinders' $\sum F_{dir\_ref}$ cannot reflect the small peak of peritoneum.

The other one is that the force fluctuations caused by trocar rotation almost cannot be seen in this force sensing method.

In the measurement of trocar insertion with rotation in chapter 2, the force fluctuation caused by rotation can be obviously seen in Fig.2-6. Because in that condition, the force sensor is placed right above the trocar. However, when the pneumatic cylinders are used to monitoring the insertion force, the cylinders are placed around the trocar. The fluctuation would be absorbed during transmission at a certain level.

However, it does not influence the recognition of the second force peak, which corresponds to the penetration-out of muscle tissue. By contraries, it has the effect of denoising at a certain level.

3.4 Improvement of trocar insertion device design

According to statements above, the preliminary design purpose has been achieved. However, considering the actual clinical application, there are still some questions, for example, sterilization, easiness of operation, numbers of pipes and so on. Thus, an improved version is developed.

As shown in Fig.3-28, the improved version has similar mechanical structure to the initial one, but some improvements have been made. Firstly, the six thin air cylinders are replaced by two larger air-cylinders, whose diameter is 16 mm. That can decrease the air cylinder's number and the pipes effectively. In consequence, there is only one wire encoder in this version to measure the air-cylinder-rod displacement.

Besides that, because there are only two air cylinders in this improved version, a soft ring and a hard ring are adopt to connect the handle part and the suction cups part. What most important is that it can satisfy the sterilization for the actual clinical application. As shown in Fig.3-28, the drape can be covered to separate the front parts and the back parts. The front parts (suction cups, soft and hard ring, the trocar and corresponding trocar fixed) can be sterilized. And the handle, which includes of motors and electrical parts can be left unclean.

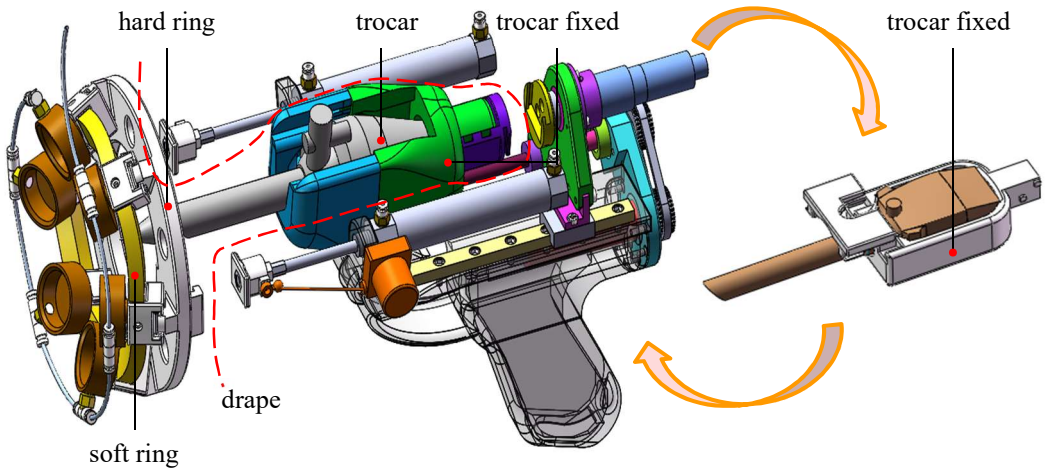

Fig.3-28. Trocar insertion device model of the improved version

Table 3-V. Specifications of the improved version device

Movable range of insertion	115 mm
Movable range of lifting	**60 mm**
Max pull force for lifting	**2 * 120 N**
Adhesive force of suction cups	6 * 62.17 N
Insert speed range	0-12 mm/s
Rotation frequency range	0-3 Hz
Max insertion force	180 N
Area of action	230 mm^2
Size (L * W * H) (mm)	**220 * 123 * 182**
Weight	**0.78 kg**
Sampling Frequency of control system	1 kHz

When the design purpose was proposed in chapter 1, the device need to able to be used for the majority of trocars products in the market. Thus, here a mechanic of trocar fixed is adopted to stable the trocar. And trocars with different shapes can be assembled on this device by changing the trocar fixed, as shown in Fig.3-28.

The design of this combination disassembly and assembly increases the easiness in actual operation. Finally, the specifications of final version device are listed in Table 3-V. The improvements are marked by bold font.

This improved version device has the same control system to the initial one. But as shown in Fig.3-28, there are only two cylinders to lift up the abdominal wall. The connection of them is as the same as the group 2 or 3 shown in Fig.3-15. The two air cylinders are connected to the same one servo valve, and there is only one wire encoder to measure the displacement of the cylinder rod. Thus, comparing with the initial version, it has less pipes and components (air cylinders, wire encoders and joints).

The insertion experiments are also conducted using the improved insertion device, as shown in Fig.3-29. It inserts at a high speed (10 mm/sec). The rotation all follows the equation 2-1, the amplitude A is $\pi/2$ and the frequency f is 1Hz. And the resultant of the two pneumatic cylinders' F_{dr_ref} during insertion is shown in Fig.3-30. The two force peaks corresponding to skin and muscle also can be obviously recognized.

Experiments and measurements above proves that using both two version devices, the force peaks can be well sensed by monitoring the pneumatic cylinder's F_{dr_ref} in impedance control. It is important for the development of the automatic stop algorithm latter.

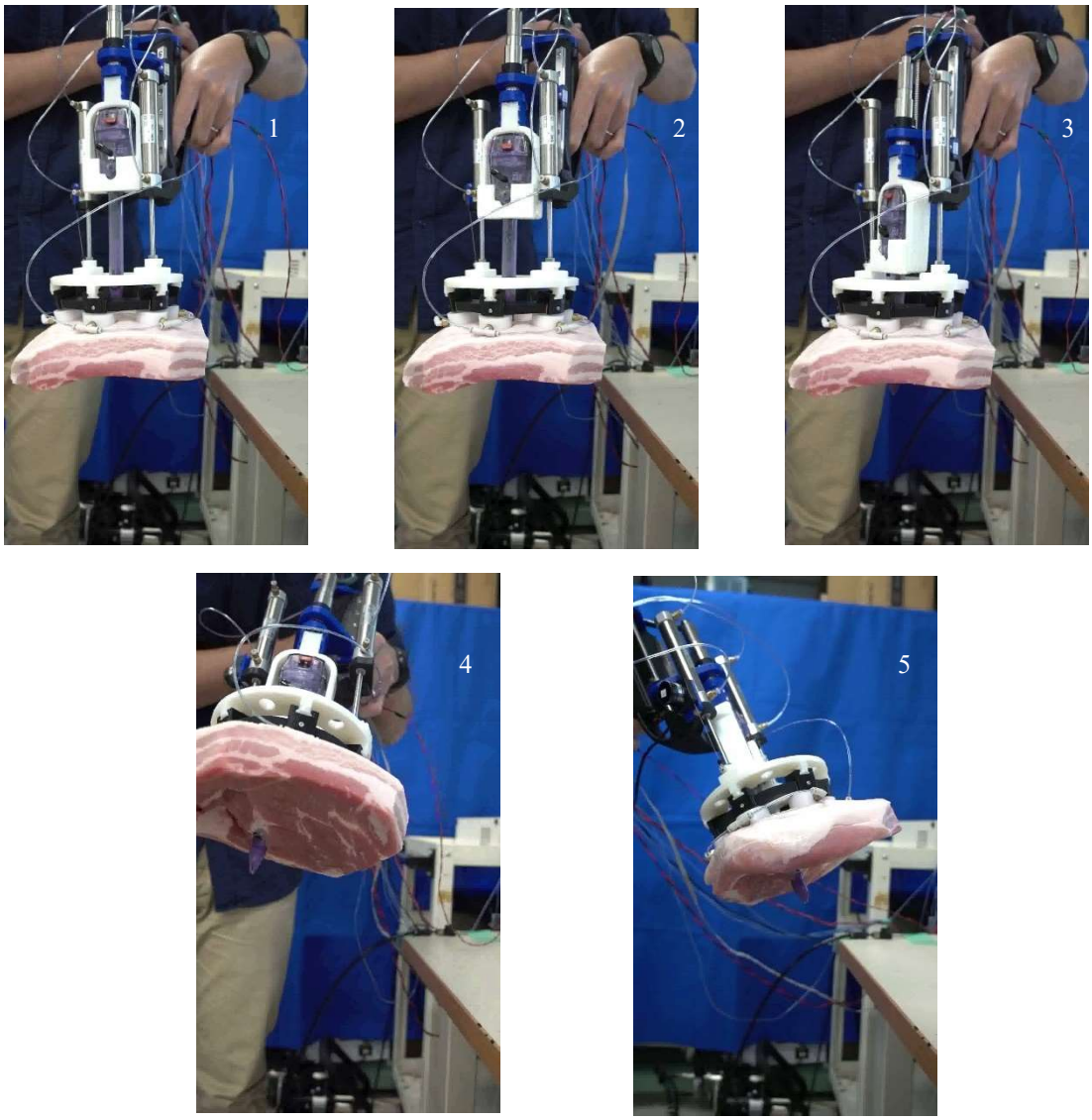

Fig.3-29. Insertion experiment using the improved version device

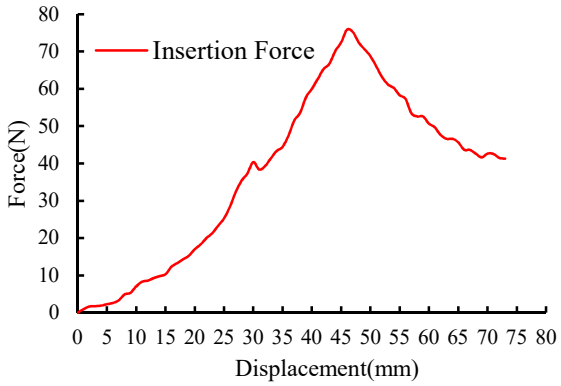

Fig.3-30. Resultant of the air driving force F_{dr_ref} during insertion using the improved version

3.5 Summary

In this chapter, the insertion device is designed. It is a device which integrates both functions of lifting up the abdominal wall and driving a trocar insertion.

Based on the method of cupping, vacuum suction cups are used to adhere the device onto the abdominal wall. Under a high stiffness impedance control, the pneumatic cylinders play a role of lifting up the abdominal wall to make it stable as the assistant surgeon hold up. And two DC motors drive the trocar inserting forward with rotation. Instead of using force sensor, air driving force in cylinder's impedance control is monitored to recognize the force peaks. In addition, the improved version device takes the form of assembly of components (trocar relating parts, device body and suction cup relating parts) to make it possible for adapting to different trocars and sterilization in clinical application. Lastly, *Exvivo* experiments using porcine abdominal wall are conducted. Even though the automatic stop algorithm for safe insertion has not been added up, it has proved that this device can successfully insert a trocar while lifting up the abdominal wall and force monitoring method by pneumatic cylinders can obviously sense the force peaks during insertion.

Chapter 4. Automatic Stop Control Algorithm and Verification of Safe Insertion

4.1 Automatic stop control algorithm

4.1.1 The Control algorithm of the insertion device

At the beginning of this research, it has been proposed that this device must be able to finish safe insertion without human control. In other words, in order to avoid overshooting, it requires to discontinue inserting upon the trocar penetrates out of the abdominal wall. In this section, the automatic stop algorithm is described in details.

There are only two physical buttons in the whole system, which are placed as triggers of the device handle, as shown in Fig.4-1. However, there are some virtual buttons on the GUI panel as shown in Fig.4-2. Gains for every actuator's control are set in this GUI panel.

Fig.4-3 shows the simplified flow chart of the device system. As introduced in chapter 3, the motor for inserting forward is under a velocity control, the motor for rotating is under a position control, and cylinders are under an impedance control. They are independent. In Fig.4-3, firstly, the insertion speed v, the amplitude A and frequency T of the rotation need to be set in GUI dialog box. Then the system starts and waits the pressed button. When the green button is pressed, the system drives the trocar to insert forward and rotate. By counting the time *K(mean)* turns to negative, the contact and the penetration-out are detected. Upon *K(mean)* turns to negative twice or the trocar inserts forward over 80 mm since contact, the system stops inserting.

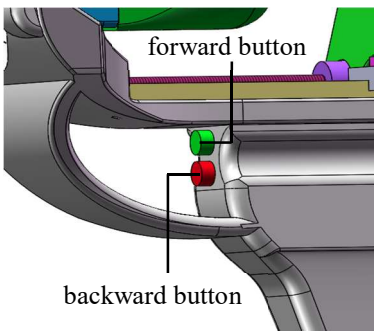

Fig.4-1.Two buttons of the trocar insertion device

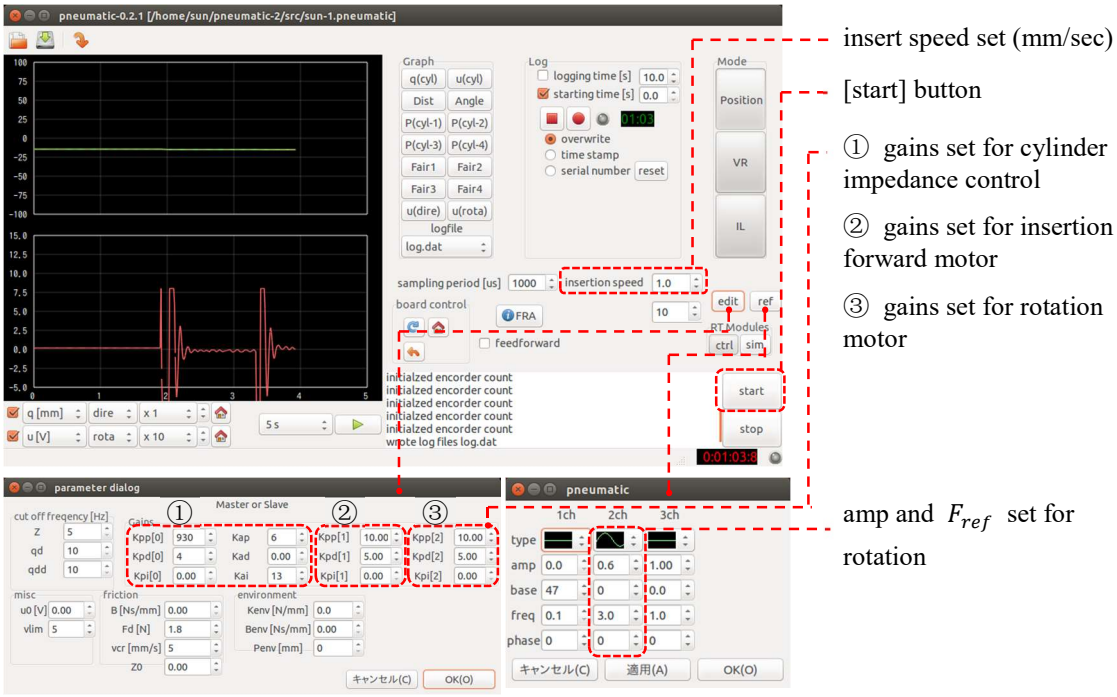

Fig.4-2. GUI panel of the trocar insertion device

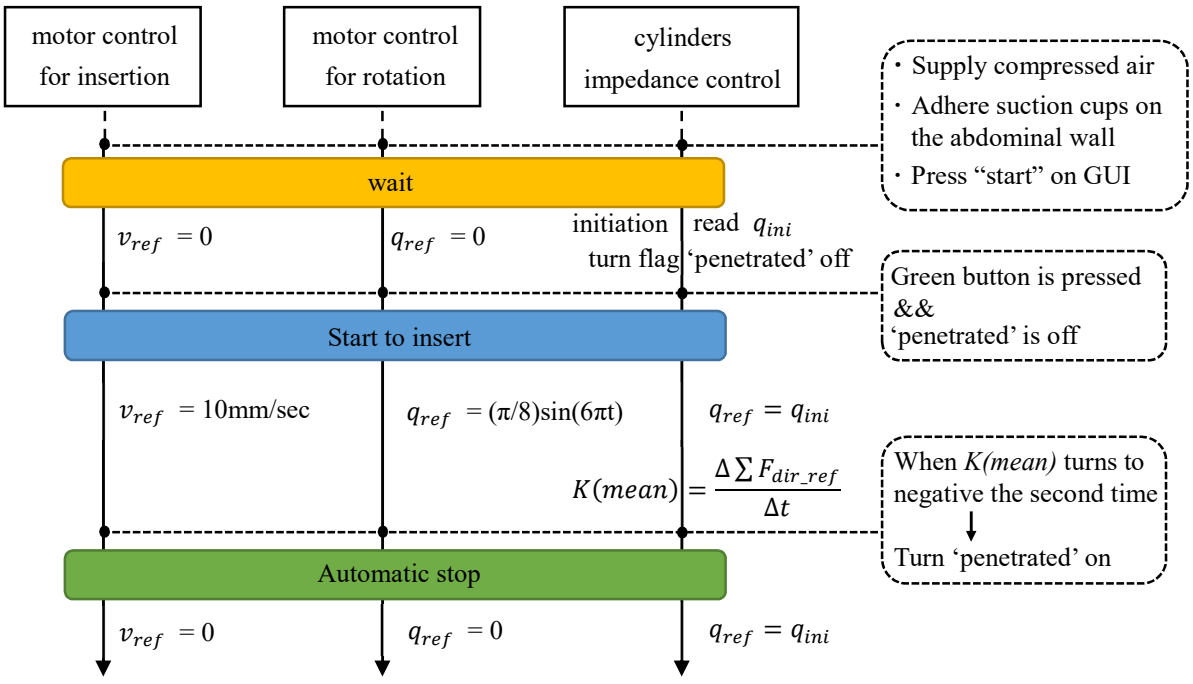

Fig.4-3. Simplified flow chart of the device system

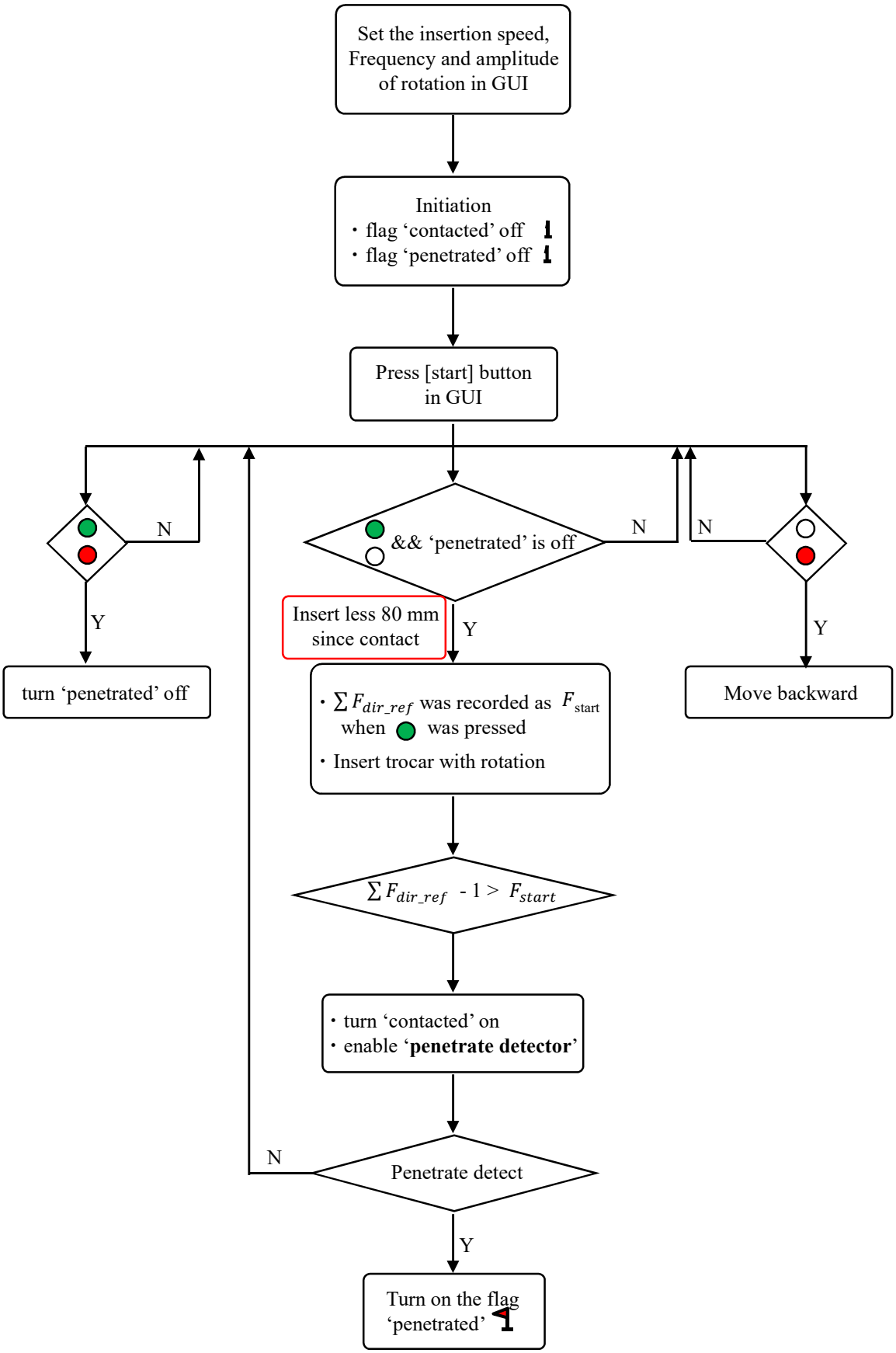

Fig.4-4. The specific flow chart of the trocar insertion device

Fig.4-4 shows the specific flow chart of the device system. In Fig.4-4, it can be seen that two flags (‘contacted’ and ‘penetrated’) ensure the safe insertion. For example, when the penetration out is detected, the flag ‘penetrated’ turns on. It leads to the trocar stops inserting even the green button is pressed.

As shown in Fig.4-4, the logic of the device operation is:

Only green button is pressed: drive the trocar to insert forward and to rotate only if the flag ‘penetrated’ is off.

Only red button is pressed: drive the trocar to move backward.

The two buttons are both pressed: turns the flag “penetrated” off.

The method how to detect the penetration-out is described in section 4.1.2.

4.1.2 Penetration out detector module

In Fig.4-4 as soon as the flag "contacted" is on, the "penetrate detector" module will start to recognize whether the abdominal wall is penetrated out. In this section, it is described how it works.

As shown in Fig.4-5, since the flag "contacted" turns on, the slope of $\sum F_{dir\_ref}$ is calculated at an interval that the trocar inserts forward 5mm. In this 5 mm interval, the average force of $\sum F_{dir\_ref}$ in 1 mm interval is calculated and recorded as $\text{mean}(\sum F_{dir\_ref})$. And based on these five $\text{mean}(\sum F_{dir\_ref})$ in the 5 mm interval and the least squares fitting, the slope of the force in this 5 mm interval is calculated, which is recorded as *K(mean)*. In this way, the slope of the force *K(mean)* is calculated at an interval of 5 mm since the trocar has contacted on the abdominal wall. And When the *K(mean)* turns to negative, it would be counted once. When it turns to negative at the second time, the flag "penetrated" turns on. And According to the experiments and

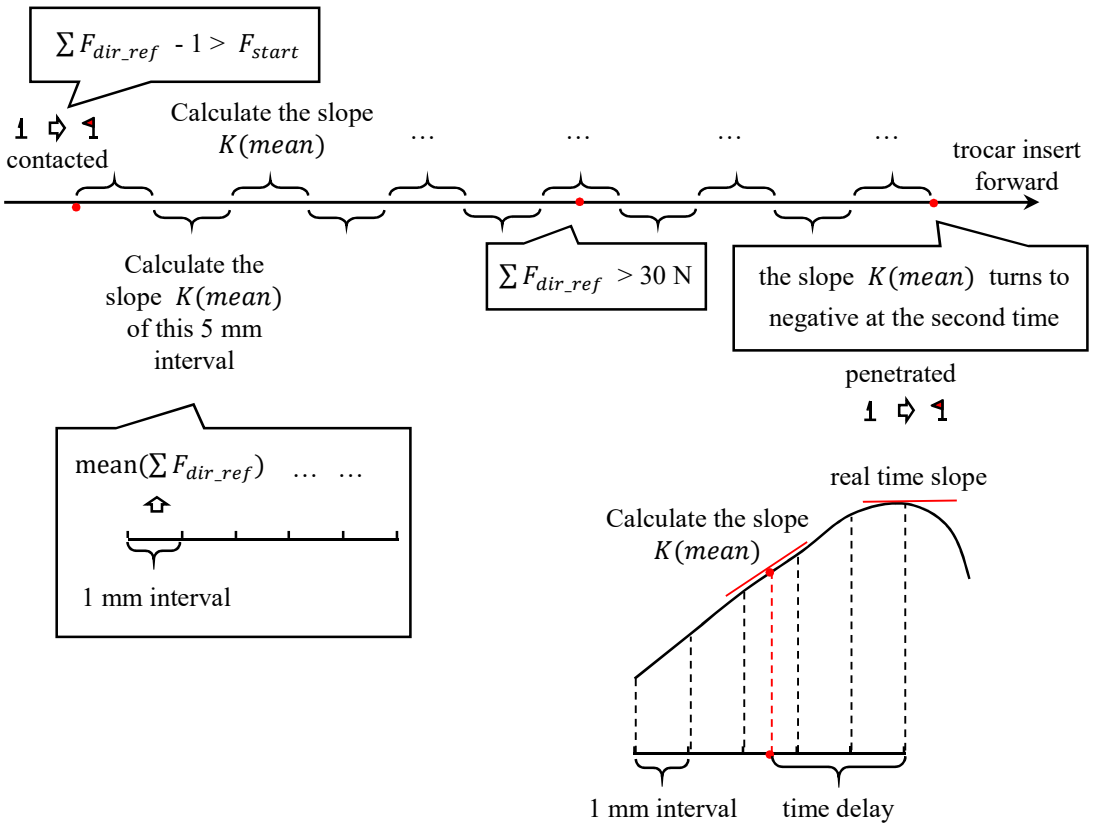

Fig.4-5. "Penetrate detector" module

explanations above, the second force rupture, which corresponds to the muscle tissue penetrate-out, usually occurs when the insertion force ranges about 50 N. So it is added as a judgment condition for the second force rupture, that the resultant of the F_{dr_ref} must be larger than 30 N as shown in Fig.4-5.

The "penetrate detector" module introduced above is based on the trocar insertion trend, which is interpreted in chapter 2. However, there are still something to emphasize before experiments.

1. This program regards the muscle penetrate-out as the whole abdominal penetrate-out.

In chapter 2, the insertion force trend has been well explained, and technically the third force peak corresponds to the whole abdominal penetrate-out. However, it has been described that the third force peak is difficult to recognize caused by trocar rotation, absorption and attenuation of the force while monitoring by pneumatic cylinders. In a word, it is difficult to be used in actual engineering. Thus, in this algorithm, the second peak is adopted to recognize penetrate-out approximately.

2. There is a certain time delay for recognition when the algorithm introduced above is applied.

The time delay is caused by calculation of *K(mean)*. As shown in Fig.4-5, when the actual time has finished the 5 mm insertion, the *K(mean)* calculated approximately equals the real time force slope at the moment of 2.5 mm (assume the force increase can be regarded as linearly). Thus, in this method, there is approximately a time delay, which is about half calculation interval.

Let's discuss it deeply. If we longer the calculation interval, the time delay will become longer, and it influences the insertion safety negatively. On the other hand, if we shorter the calculation interval, there would be more noise or fluctuations to influence the recognition of the second peak negatively.

It has proved in chapters before, that insertion at a higher speed can decrease the insertion force at a certain level. In the experiments later, the insertion speed is set to

10 mm/sec. As introduced above, the calculation interval is set to 5 mm and the period of the system is 1ms. Thus, there are 100 samples in 1 mm interval to calculate the $\mathrm{mean}(\sum F_{dir\_ref})$. And the time delay may cause approximately 2.5 mm overshooting since the muscle penetrate-out is recognized. The question about the safety of this 2.5 mm overshooting would be discussed in details later.

3. A limit insertion distance (80 mm since contact) is added up in the program.

This is a medical device and requires to ensure 100% safety. Therefore, a limit insertion distance is added up in the program. When it inserts forward over 80 mm since the flag “contacted” is turned on, it stops insertion compulsively no matter whether the flag “penetrated” is turned on or not. “80 mm” is an approximate estimate based on the experimental data of clinical anatomy. Its reasonableness will be described in section 4.2.2.

4.2 Verification of safe insertion by *Exvivo* experiment

4.2.1 Exvivo experiments

Using the improved version device, the insertion speed is set to 10 mm/s constantly, the rotation follows the equation (2-1). In order to verify the effectiveness of this automatic stop algorithm, the comparative experiments were conducted. Fig.4-6 and 4-7 show images of comparative experiments. The automatic stop algorithm is not added in Fig.4-6 experiment, it controls the trocar insertion by simply pressing or releasing the button. And the automatic stop algorithm is added in Fig.4-7 experiment, operators always keep pressing the green button regardless of the situation whether the abdominal wall has been penetrated out or not.

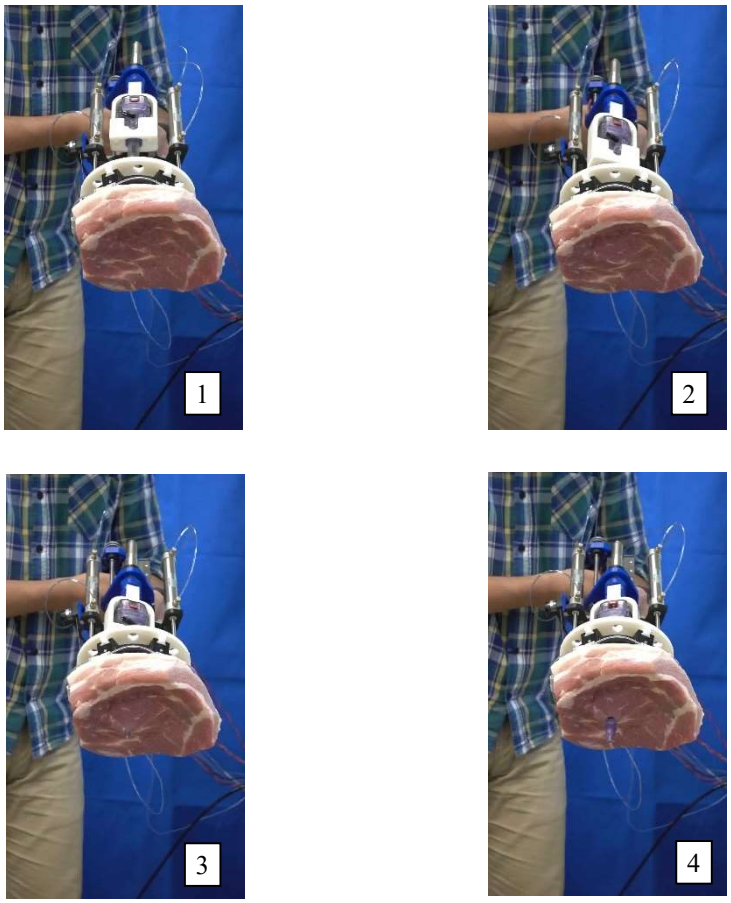

appearance when the trocar stopped

Fig.4-6. Trocar insertion using this device without adding auto-stop algorithm

Comparing the No.4 pictures of the two experiment, it can be learned that in Fig.4-6 when the trocar is stopped, it has overshot. In contrast, Fig.4-7 achieves safe insertion. As soon as the trocar tip has exposed, the system stops the insertion timely.

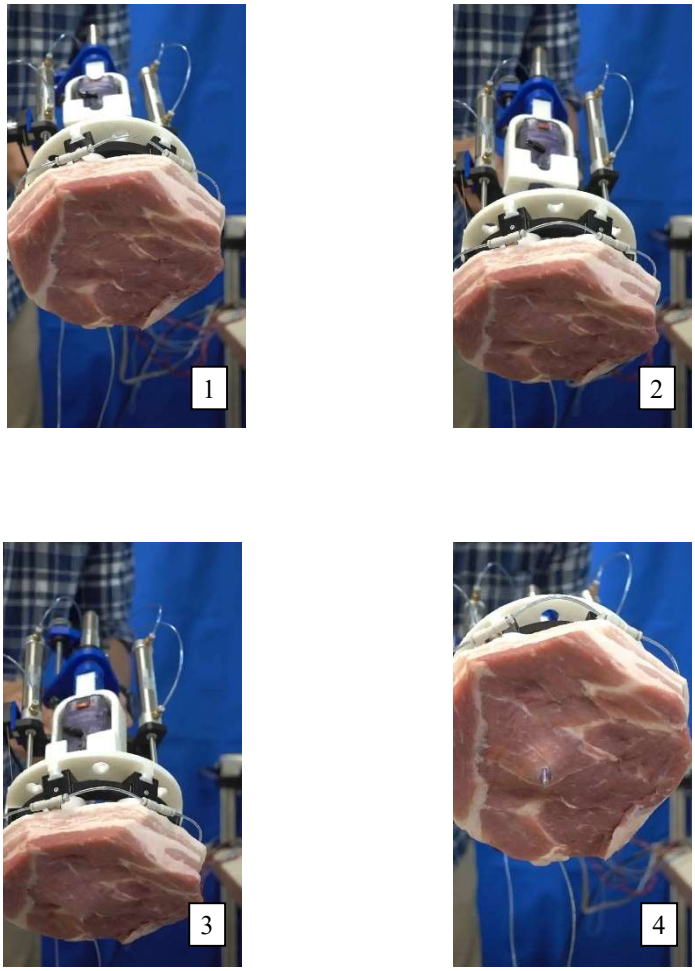

appearance when the trocar stopped

Fig.4-7. Trocar insertion by this device with adding auto-stop algorithm

4.2.2 Reliability and safety of this device

Fig.4-8 shows measurements of the two experiments above. When insertion without automatic stop algorithm, the force $\sum F_{dir\_ref}$ decreases rapidly after the second peak occurs, because the trocar continues inserting even though the second peak occurs. In contrast, when insertion with automatic stop algorithm, the insertion force retains at a certain force after the second peak. Because the trocar has stopped.

Fig.4-9 shows experimental data of a pneumatic cylinder during insertion with automatic stop algorithm. The first from up shows the force $\sum F_{dir\_ref}$ and displacement the trocar inserts forward since contact. The second shows the slope of the $\sum F_{dir\_ref}$. The third shows the air pressure of the two chambers and the fourth one shows the extended displacement of the cylinder's rod, which is measured by the wire encoder.

The rods extend approximately less than 1 mm during insertion. It fully proves that the impedance system of the pneumatic cylinders is rigid enough. In addition, the force peaks also reflect on the air pressure of the two chambers and the displacement of the rods.

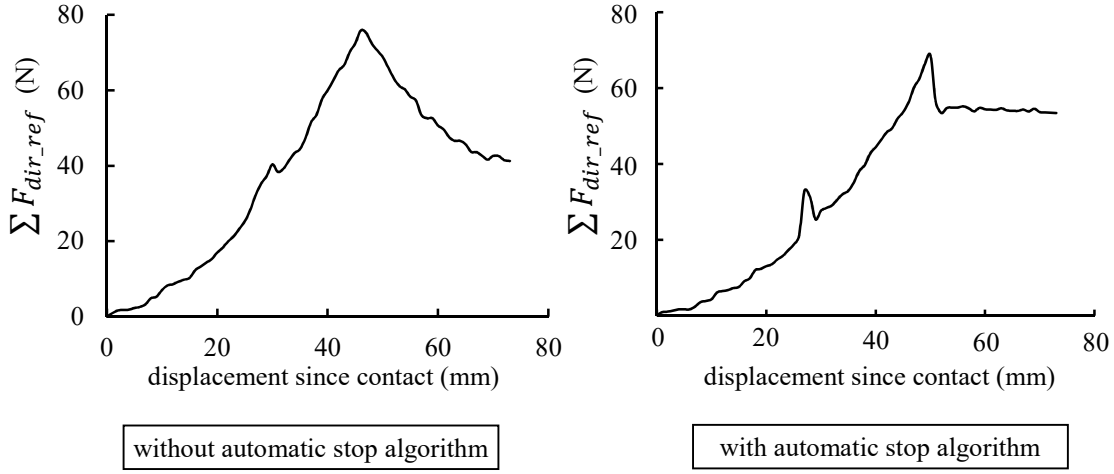

Fig.4-8. $\sum F_{dir\_ref}$ when insert trocar by the improved version device

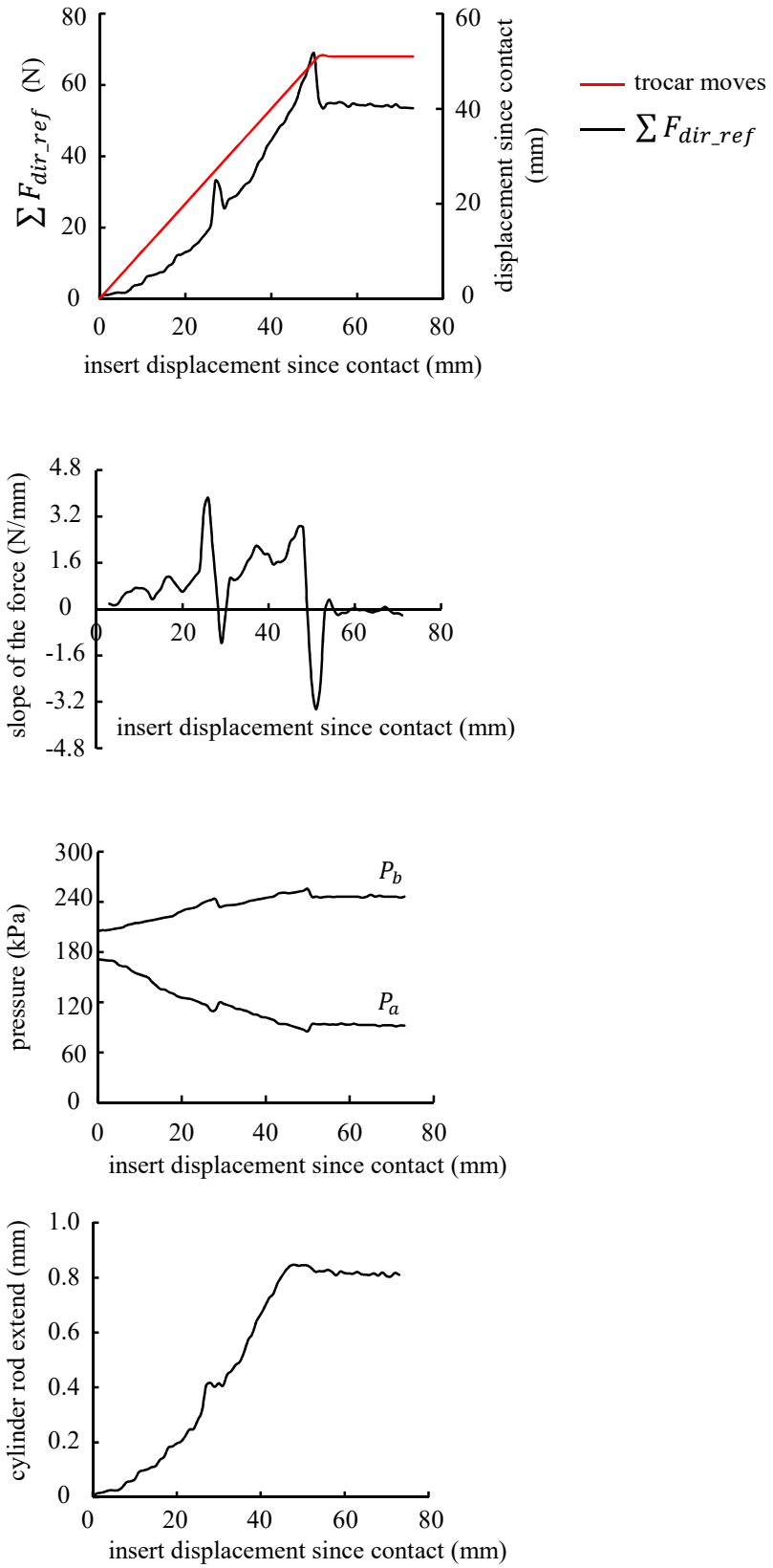

Fig.4-9. Experiment result of a cylinder's impedance control when insertion with automatic stop algorithm

Before discussing the safety of this device, two physical definitions must be introduced.

As shown in Fig.4-10, when the insertion is stopped, the length from the trocar tip to the abdominal bottom is called as exposure length. Accordingly, the exposure length is an important index to evaluate the safety of insertion operation. If the exposure length is too long, it raises the risk of injuries.

And the other one is the space between the abdominal bottom to the organs inside abdomen. We call it allowable length. Some researches [86-88] have reported about this. For instance, the distance between abdominal bottom and retroperitoneal vessel varies from individuality. As shown in Fig.4-11, the distance of patients who is non-obese (BMI ~20 kg/m^2) is 6 ± 3 cm. the overweight (BMI 25-30 kg/m^2) is 10 ± 2 cm and the obese (BMI 30~ kg/m^2) is 13 ± 4 cm.

As is shown in Fig.4-12, another research also measured the distance from the abdominal wall to the anterior surface of organs inside abdomen in the cases of patients with BMI 20 kg/m^2 in different lifting condition. It can be learned that the allowance distance ranges about 9-13 cm. This is also why we set the limit insertion distance in the automatic stop algorithm to 80 mm. And in clinical application, it is necessary to adjust this limit insertion distance according to patient's situation.

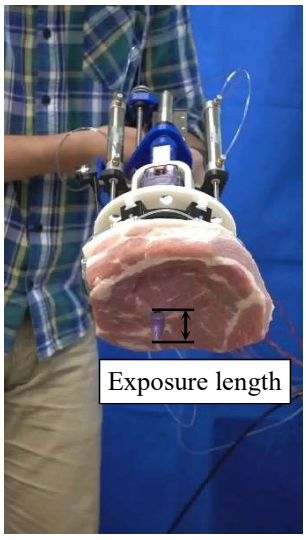

Fig.4-10. Exposure length

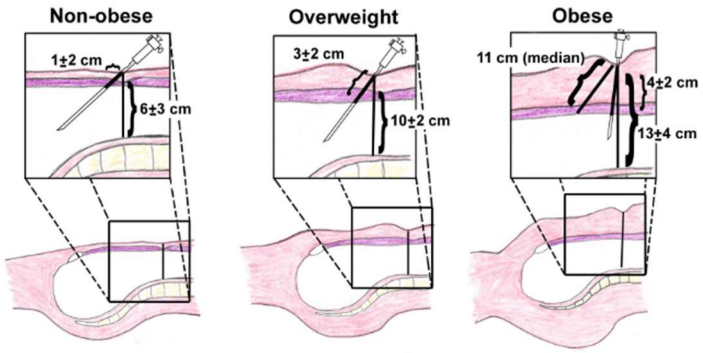

Fig.4-11. Abdominal spaces of different obesities [86]

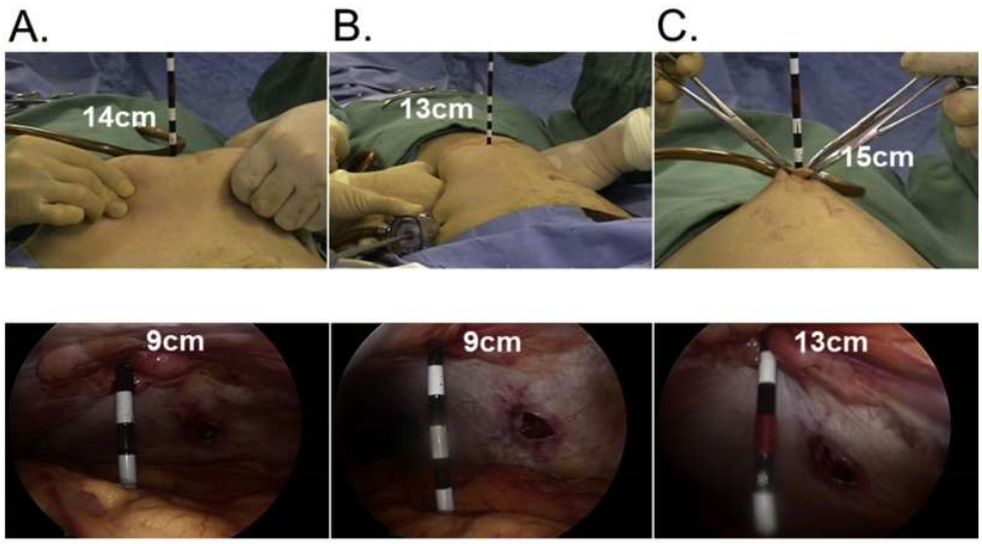

Fig.4-12. Allowance distance in different lift up distance in case of BMI 20 kg/m^2 [87]

After understanding the information above, insertion experiments with this device are repeated eight times to verify the automatic stop algorithm. And the exposure length of every experiment is recorded and shown in Fig.4-13. In addition, the exposure lengths when trocar insertion by experienced surgeons in clinic operation are reported in other research [9]. We Compare them to verify the safety of using this trocar insertion device.

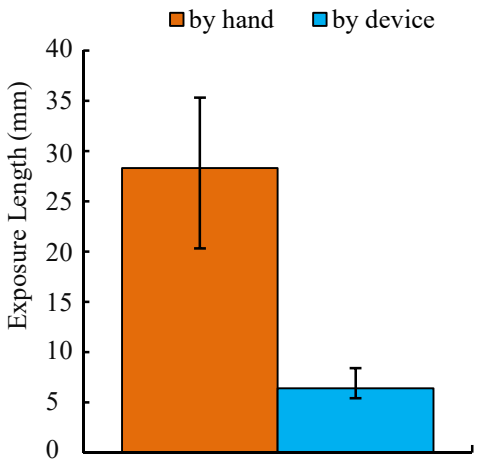

Fig.4-13. Exposure length comparison of using device and insertion by experienced surgeons

It can be seen when insertion by experienced surgeons, the exposure length ranges about 20 – 40 mm. this is less than the distance between abdominal wall to the anterior surface of organs inside abdomen, which is introduced before. In contrast, when insertion by this device, the exposure length can be shorted furtherly, which is less than 10 mm. In addition, using this device, the exposure length can be controlled with less variance and it does not require any experience for operators.

Based on experiments and statements above, it proves that insertion with this device has safer and easier performance than traditional human operation.

4.2.3 Convenience of this device

The safety of using this device has been discussed above. In this section, the operation spent time length of insertion using this device and insertion by human beings are compared. The spent time length of trocar insertion by human operation are measured based on the videos of operations on the Youtube, and in *Exvivo* experiments the spent time length using this trocar insertion device are measured.

As shown in Fig. 4-14, it spent 70-200 sec to finish the insertion by human being. And according to the experiment statistics, operators with less experience would spend longer to finish. In contrast, it only spent 30−40 sec to finish the insertion with this device according to the measurement of the Exvivo experiments. In addition, the advantage of this device did not only reflect this aspect.

In traditional human being insertion, when the initial trocar has finished, pneumoperitoneum must be done before other trocar insertions are operated. It will spend 5-10 min. However, using this device can take other insertions when pneumoperitoneum is doing. It avoids waiting, which greatly improves the efficiency of the surgery.

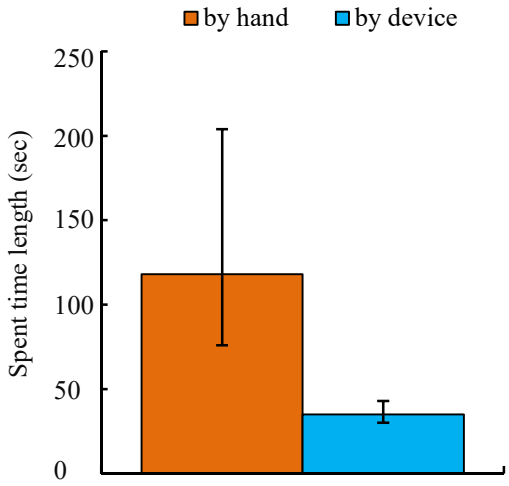

Fig.4-14. Operation spent time length comparison of using device and human being operation

4.2.4 Revalidation of factors influence insertion force

Insertion with the improved version device in different parameters set (different insertion speed, different rotation frequencies and different insertion methods) also have been conducted.

Fig.4-15 shows the influence of insertion speed on the insertion force. As introduced above, this device can drive the trocar inserting forward at a constant speed (0-12 mm/s). Here, insertion experiments at different constant forward speeds are conducted. Note that at the same insertion speed, experiments are repeated five times, and the trocar rotation all follows the equation (4-1).

$$\theta = (\pi/8)sin(6\pi t) \tag{4-1}$$

In Fig.4-15, the vertical axis represents the maximum force of one cylinder arrives in the whole process of insertion. It can be learned in the same rotation, faster insertion speed can decrease the insertion force. That is in accordance with the results in chapter 2.

On the other hand, insertion with different rotation frequencies are also conducted. Similar to the experiments above, the maximum force of the pneumatic cylinder are

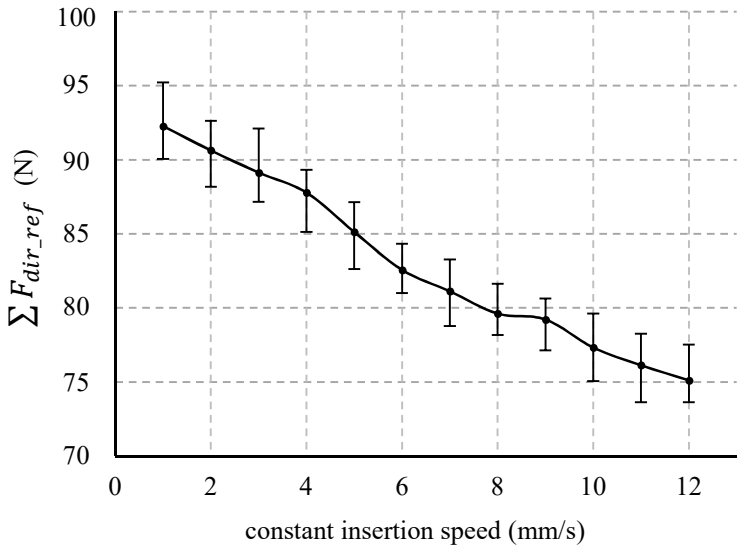

Fig.4-15. $\sum F_{dir\_ref}$ – insertion speed using the improved version device

measured at an interval of 0.3 growth frequencies. Note that at the same rotation frequency, experiments are repeated five times, and the constant insertion speed and amplitude of rotation A were all 10 mm/sec and π/8. As shown in Fig.4-16. It can be seen that insertion with fast rotation requires less insertion force.

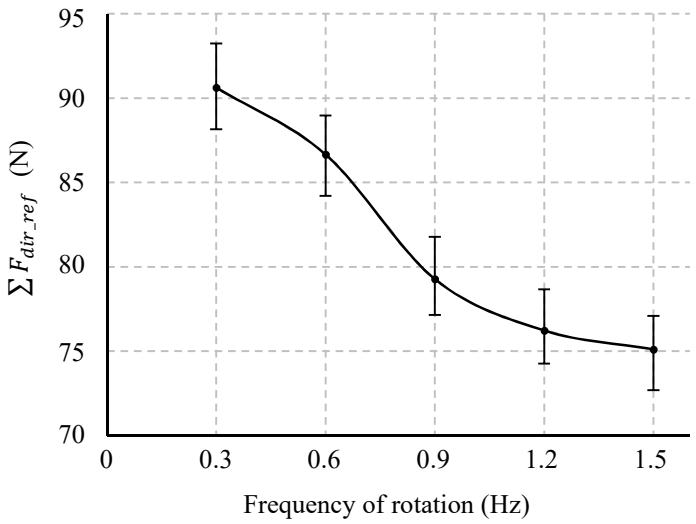

Fig.4-16. $\sum F_{dir\_ref}$ – rotation frequency using the improved version device

4.3 Summary

In this chapter, the *Exvivo* experiments using the improved device were conducted. The safety and the convenience of using this device were described. The details are following:

Firstly, based on the insertion force trend interpreted in chapter 2, the algorithm for automatic stop is proposed and installed in the trocar insertion device. Using this algorithm, the trocar achieved the timely stopped to avoid overshooting in *Exvivo* experiment. Comparing with the statistics of human insertion, this device can shorter the exposure length and time length the insertion operation spent. What's more, this device exempted operators from technical requirements or experience.

Chapter 5. Conclusion

5.1 Summery

In this research a novel trocar insertion device for laparoscopic surgery is developed. This device integrates functions of lifting abdominal wall and trocar insertion, which enables one surgeon to operate by himself or herself. In addition, this device recognizes the penetration-out by monitoring the insertion force. It enables a person even without experience to achieve safe trocar insertion.

In the first chapter, the fact is introduced that majority of surgical injuries caused by overshooting occur during the initial trocar insertion in laparoscopic surgery. Under this background, some researches have been carried out to improve the design of trocar products, and other researchers focus on developing a trocar insertion training system. However, there are still defects in aspects of easy operation, safety and automation. Therefore, developing an easy-operated trocar insertion device, which is safe and can be used by people even without any experience, has been established as the purpose of this research

In the second chapter, insertion force of different trocars have been measured using a porcine abdominal wall. The magnitude of insertion force differs from many factors, such as types of trocars, insertion speed and insertion method, but all experiments have similar force trend, that there are three peaks obviously in the whole process of insertion and the second peak is the largest one. Based on abdominal multilayers structure and the theory of the force peak's occurrence, it is clarified that the insertion force trend reflects the abdominal multilayers structure. Technically the small peak next to the largest one responds to the penetration-out of the abdominal wall. In engineering, the largest force peak (the second one) is regarded as a reminder to help computers recognize penetration-out. Besides that, the influence of factors (insertion speed, insertion method, trocar types) on the insertion force are discussed in this chapter. It proves that insertion with a sharper trocar, at a higher insertion speed, and with rotation can decrease the insert force at a certain level.

In the third chapter, based on the measurement of insertion force, an easy-handheld device is designed. Its actuators consist of vacuum suction cups, pneumatic cylinders and DC motors. With the method of cupping, vacuum suction cups are used to adhere the device onto the abdominal wall. Under a high rigidity impedance control, the pneumatic cylinders play a role of lifting up the abdominal wall to make it stable as the assistant surgeon hold up. And two DC motors drive the trocar inserting forward with rotation. Instead of using force sensor, air driving force in cylinder's impedance control is monitored to recognize force peaks. In addition, the improved device takes the form of assembly of components (trocar relating parts, device body and suction cup relating parts) to make it possible for adapting to different trocars and sterilization in clinical application. Lastly, *Exvivo* experiments using porcine abdominal wall are conducted. Even though the automatic stop algorithm for safe insertion has not been added up, it has proved that this device can successfully insert a trocar while lifting up the abdominal wall and force monitoring method by pneumatic cylinders can obviously sense the force peaks during insertion.

In the fourth chapter, based on the insertion force characteristics introduced in chapter 2 and the trocar insertion device designed in chapter 3, an automatic stop algorithm has been programed for this device system. When the force monitor of pneumatic cylinders under high rigidity impedance control detect the second force peak during insertion, the device discontinues the insertion automatically and immediately. It access a novice to achieve safe insertion by just press a button. *Exvivo* experiments using the porcine abdominal wall are conducted to verify its effectiveness. The results show insertion by this device can discontinue insertion immediately upon the trocar penetrated out of the abdominal wall. After the trocar stops, the exposure length trocar penetrates out is approximately 5-10 mm, which is considerably shorter than the average length (~90 mm) of human beings between bottom layer of the abdominal wall and organs or arteries.

Three innovations of this research can be concluded as following:

1. The relationship between trocar insertion force trend and abdominal multilayers structure is explained.

2. A novel trocar insertion device has been developed. Using components like suction cup, pneumatic cylinders, DC motors, it integrated two functions of lifting up the abdominal wall and inserting trocars.

3. Without using force sensors, this device recognizes the penetration-out by monitoring the air driving force of the pneumatic cylinders indirectly.

5.2 Future work

5.2.1 Adaptable to patients with abdominal adhesions

Abdominal adhesions are bands of fibrous tissue that can form between abdominal tissues and organs, as shown in Fig.5-1. Normally, internal tissues and organs have slippery surfaces, preventing them from sticking together as the body moves. However, abdominal adhesions cause tissues and organs in the abdominal cavity to stick together. [89]

Abdominal adhesions are a common complication of surgery, occurring in up to 93% of people who undergo abdominal or pelvic surgery. Abdominal adhesions also occur in about 10% of people who have never had surgery. [90] When insert a trocar into a patient who has abdominal adhesions, it is almost impossible to avoid overshooting unless using optical trocar, as shown in Fig.5-2.

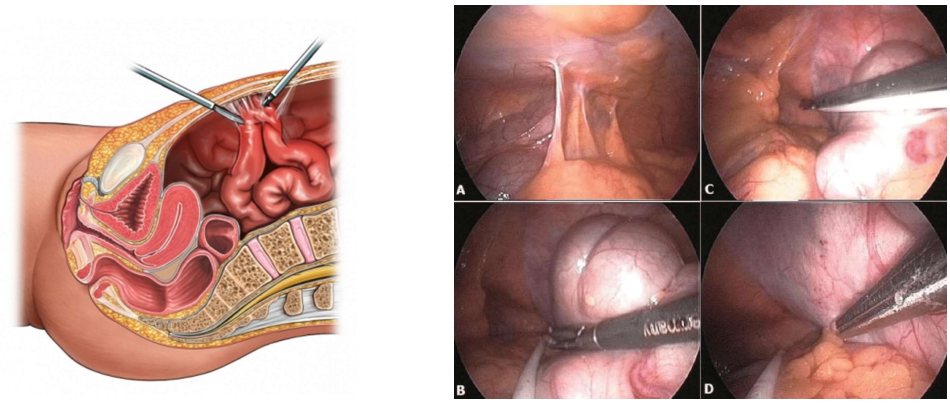

Fig.5-1. Abdominal adhesions [91, 92]

Fig.5-2. Trocar insertion for a patient who has abdominal adhesions [93]

However, using this device may achieve safe insertion for this condition. It requires further research and experimental verifications.

5.2.2 Verification by *Invivo* experiment

The Experiments introduced before are all *Exvivo* and the material is all porcine. In future, experiments that insert a trocar into human being using this device is necessary. In those experiments, the automatic stop algorithm must be verification and may require some debugs. And the effectiveness of adhesion of suction cup for patients of different ages, races, gentles need to be verification. And because of pneumoperitoneum, the influence of the resistance on air-cylinders force sensing also need to be tested.

5.2.3 Improvement of device safety

Although in *Exvivo* experiment above it has proved that the automatic stop algorithm can achieve immediate stop, it still requires multiple guarantees in the control algorithm. In future research, the automatic stop algorithm is appreciated to improve and perfect.

Appendix

In chapter 2, the theory of force peak occurrence was explained by stiffness. Here we cite a research on the mechanics of dynamic needle insertion into a biological material as a supplementary material.

Force-displacement characteristics

Fig.5-3 displays typical force-displacement responses during the insertion and removal of a rigid trocar (three-sided tip) into a pig heart. The process of each needle insertion can be divided into several events [59], which are as follows:

1) Loading deformation (from 0 to 1): This is a deformation event that starts at 0 mm and continues until a deformation (i.e., a deformation depth at the tip of the needle) at which the needle force reaches its maximum.
2) Rupture (from 1 to 2): This is a rupture event when a crack suddenly propagates into the tissue right after the force reaches it maximum.
3) Cutting (from 2 to 3): This is a cutting event that starts after rupture such that the crack propagates in the body in a controlled fashion in response to needle displacement.
4) Unloading deformation (from 3 to 4): This is a second deformation event that starts when the needle is stopped and continues as the needle is removed.

When a trocar or needle inserts into a uniform tissue, fracture model of the rupture

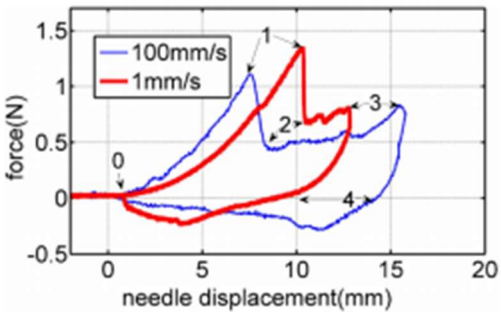

Fig.5-3. Force versus displacement curves for needle insertion into and removal from a pig heart at two velocities: 1 and 100 mm/s [69]

has been proposed in terms of energy, as follow:

$$J \geq R \tag{5-1}$$

Where, J represents the nonlinear energy release rate and R represents the fracture toughness of the tissue. Inequality (5-1) means that during a rupture event, a crack can extend unstably upon the energy release rate exceeds the fracture toughness. It is a necessary and sufficient condition of rupture occurrence.

The qualitative expression of the nonlinear energy release rate can be given by

$$J \propto K_c(\frac{F}{A})^m \tag{5-2}$$

Where, K_c is the crack energy-intensification factor, F is the insertion force, A is the size of the contact area and m depends on the nonlinearity of the material. By inequality (5-1), the crack will extend if $J = R$. Substituting this value into (5-2) and rearranging yields the insertion force necessary to initiate rupture as

$$F \propto \sqrt[m]{\frac{R}{K_c}}A \tag{5-3}$$

This equation can be used to explain the sudden decrease in trocar force during rupture. The decrease is generally due to a reduction in fracture toughness as the trocar passes from a tissue layer with fracture toughness R_1 to another layer with reduced fracture toughness R_2.

Based on the theory above, we can explain the whole process of insertion through abdominal wall. The abdominal wall mainly consists lays of skin, subcutaneous fat, muscle and peritoneum as is shown in Fig.2-11. And the fracture toughness of them meets the following relationship,

$$R_{skin} > R_{fat} < R_{muscle} > R_{peritoneum} > 0 \tag{5-4}$$

Thus, the three peaks occur at the moments when trocar penetrated out of skin to contact to fat, trocar penetrated out of the muscle and penetrated out of the peritoneum.

Operation steps when insertion with the trocar insertion device are described as following:

<Set insertion speed and rotation parameters>

Firstly, the insertion speed *v*, the amplitude *A* and frequency *T* of the rotation need to be set in GUI dialog box.

<Initiation>

Then, in the program there are two flags, which are named by "contacted" and "penetrated". Before "start" at GUI, the program will run the initiation, where the two flags are turned off and the distances cylinders' rod has extended are recorded as q_{ref} in respective impedance control.

<GUI start>

After that, the "start" bottom in GUI panel was pressed and the program starts running. Since the program starts running, it waited until any physical button was pressed

<Press buttons>

As is shown in Fig.4-2, the program have three switches. When the green button and the red one were pressed at the same time, the flag "penetrated" will be turned off. When only the red button was pressed, the trocar will move backward at the speed set before. Only when the green button was pressed and the flag "penetrated" is false, the trocar moves forward at the speed set before. At the same time, the total of all F_{dr_ref} of pneumatic cylinders $\sum F_{dir\_ref}$ was calculated and stored by the name of F_{start}.

<Contact judgment>

Along with trocar inserts forward, the resultant of the F_{dr_ref} of the pneumatic cylinders increases, when it increases to one larger than F_{start}, the flag "contacted" turns on and the judgment module for penetration-out turns to enable.

<Penetrated judgment>

As the “penetrated detector” module is enabled, every period since now will be judged by this module. As soon as the penetration-out is detected by this module, the flag “penetrated” will turn on. Consequently, it will jump out of this branch.

After that, the trocar will not discontinue inserting forward even the green button is pressed. Because the flag “penetrated” has turned on. It can be regarded as a lock to avoid overshooting. It can be unlocked by pressing both buttons at the same time. After that, trocar can continue inserting forward by pressing the green button. The specifics of the “penetration detector” module will be introduced in section 4.1.2.

Reference

[1] Wikipedia : Laparoscopiy. URL: https://en.wikipedia.org/wiki/Laparoscopy
[2] Laparoscopic surgery- Knowledge for medical students and physicians. URL: https://www. amboss.com/us/knowledge/Laparoscopic surgery
[3] 話題：腹腔鏡手術はこんなに危険だった. URL: https://matome.naver.jp/odai/2142941253494063901/2142941444595869403
[4] What is Laparoscopy? URL: https://www.everydayhealth.com/laparoscopy/guide/
[5] Toshio Bandoh, Norio Shiraishi, et al.Endoscopic surgery in Japan: The 12th national survey (2012-2013) by the Japan Society for Endoscopic Surgery. *Asian Journal of Endoscopic Surgery.* Vol.10, Issue 4, Nov.2017 pp: 345-353.
[6] ENDOPATH XCEL Trocars, ETHICON Company. URL: https://www.ethicon.com/na/products/access/trocars/endopath-xcel-trocars
[7] N Mahajan and N Gaikwad, "Direct Trocar Insertion: A Safe Laparoscopic Access," *The Internet Journal of Gynecology and Obstetrics*. 2006 Volume 8 Number 2.
[8] Kii Fios First Entry. Applied Medical. URL: https://www.appliedmedical.com/Products/Kii/Fios
[9] Carlo C, Nikolai Begg, et al, "Safety Profile of Trocar and Insufflation Needle Access System in Laparoscopic Surgery," *Journal of the American College of Surgeons*. Volume 209, Issue 2, Aug. 2009, pp: 222-232.
[10] Blunt Tip Trocars. Medtronic. URL: https://www.medtronic.com/covidien/en-us/products/trocars-access/blunt-tip-trocars.html
[11] ConMed Blunt Tip Surgical Trocar. MFIMedical. URL: https://mfimedical.com/products/conmed-blunt-tip-surgical-trocar
[12] Incorrect Trocar Insertion – Medical Illustration, Human Anatomy Drawing. URL: https://motionlit.medicalillustration.com/generateexhibit.php?ID=12706&ExhibitKeywordsRaw=&TL=&A=
[13] Kunal Chowdhary, Gurinder Kaur, et al. "Laparoscopic Cholecystectomy: Challenges faced by beginners our perspective," *Arch Surg Clin Res*. 2018; 2:018-024
[14] S Krishinakumar and P Tambe, "Entry Complications in Laparoscopic Surgery," *Journal of Gynecological Endoscopy and Surgery,* v.1(1); Jan-Jun 2009, pp: 4-11.
[15] Harrison GR (1989) the epidural space. Anaesthesia 44: 361-362 (lett)
[16] Erik K. Bassett, Alexander H. Slocum, et al, "Design of a mechanical clutch-based needle-insertion device," *Proceedings of the National Academy of Sciences of the United*

Sates of America, vol.106. No.14, April 2009. pp: 5540-5545
[17] Schafer M, Lauper M, et al, "Trocar and Veress needle injuries during laparoscopy," *Surg Endosc*. 2001 Mar; 15(3): 275-280
[18] www.fda.gov/cdrh/medicaldevicesafety/stamp/trocar.html, accessed February 28, 2009
[19] Safe Entry in Laparoscopy. Presentation by Yasser Orief M.D. URL: https://slideplayer.com/slide/9323740/
[20] Sarbjeet Singh and Delie Rhezhii, "Laparoscopic Surgery: Results of a Modified Open Technique of Umbilical Port Insertion," *World Journal of Laparoscopic Surgery*. September-December 2015; 8(3): 72-74
[21] 須賀真美、小山瑠梨子、等。当院の腹腔鏡下手術における第一穿刺の改良と成績。日産婦内視鏡学会第 29 巻第 1 号 224-227 ページ
[22] Andrew IB. Laparoscopic access and instrument ergonomics. URL: http://www.aagl.org/content/PDF/P1BrillB.pdf
[23] Anaam Majeed Hasson, "Risk of Pneumoperitoneum in Obese: Old Myths and New Realities," *World Journal of Laparoscopic Surgery*. May – August 2011; 4(2): 97-102
[24] Peter H, Richard R, et al, "Insertion Forces and Risk of Complications during Cricothyroid Cannulation," *The Journal of Emergency Medicine*. Vol 10, pp417-426, 1992.
[25] Kurt Semm and Isolde Semm, "Safe insertion of trocars and the Veress Needle using standard equipment and 11 security steps," *Gynaecological Endoscopy* 1999 Vol.8, 339-347
[26] Vedio named "Trocar insertion by Angelica Garcia. Cleveland Clinic Florida." URL: https://www.youtube.com/watch?v=mdDb1U5rJAE
[27] J.A. Brown, et al. "Optical-access visual obturator trocar entry into desufflated abdomen during laparoscopic: assessment after 96 cases," *J Endourol.* 2005 Sep; 19(7): 853-5
[28] Daniel Glozman and Moshe Shoham, "Image – Guided Robotic Flexible Needle Steering," *IEEE Transactions on Robotics*, VOL.23, No.3, June 2007. pp: 459-467
[29] S. P. DiMaio and S. E. Salcudean, "Needle steering and model-based trajectory planning," in *Proc. Medical Image Comput. Comput. –Assisted Intervention*, Montreal, QC, Canada, 2003, vol. LNCS2878, pp.33-40.
[30] M. O'Leary, C. Simone, T. Washio, K. Yoshinaka, and A. Okamura, "Robotic needle insertion: Effects of friction and needle geometry," in *Proc. IEEE Int. Conf. Robot. Autom.*, 2003, pp. 1774-1780.
[31] R. Ebrahimi, S. Okzawa, R.Rohling, and S. Salcdean, "Hand-held steerable needle device", in *Proc. Med. Image Comput. Comput. –Assisted Intervention*, pp.223-230.
[32] R. Alterovitz and K. Goldberg, "Planning for steerable bevel-tip needle insertion through 2D soft tissue with obstacles," in *Proc. IEEE Int. Conf. Robot. Autom.*, Barcelona,

Spain, Apr. 2005, pp. 1652-1657.
[33] N. Simaan, D. Glozman, and M. Shoham, “Design considerations of new six degrees-of-freedom parallel robots,” in *Proc. IEEE Int. Conf. Robot. Autom.*, 1998, vol. 2, pp.1327-1333.
[34] W. Park, J. S. Kim, Y. Z. Cowan, A. M. Okamura, and G. S. Chirikjian, “Diffusion-based motion planning for a nonholonomic flexible needle model,” in Proc. IEEE Int. Conf. Robot. Autom., Barcelona, Spain, Apr. 2005, pp.4611-4616.
[35] S. P. DiMaio and S. E. Salcudean, “Interactive simulation of needle insertion models.” IEEE Trans. Biomed. Eng., vol. 52, no. 7, pp. 1167–1179. Jul. 2005.
[36] K. B. Shimoga and P. K. Khosla, “Visual and force feedback to aid neurosurgical probe insertion,” in 16th Int. Conf. IEEE Engineering in Medicine and Biology Society, vol. 2, 1994, pp. 1051-1052.
[37] S. P. DiMaio and S. E. Salcudean, “Needle insertion modeling and simulation,” IEEE Trans. Robote. Autom. (Special Issue on Medical Robotics), vol. 19, No. 5, pp. 864-875, Oct, 2003
[38] Joho Yun, Hyeon Woo Kim, Hyoung-lhl Kim and Jong-Hyun Lee, “Electrical impedance spectroscopy on a needle for safer Veress needle insertion during laparoscopic surgery”, Sensors and Actuators B: Chemical, Vol. 250, Oct, 2017, pp. 453-460
[39] Erik K. Bassett, Alexander H. Slocum, et al. “Design of a mechanical clutch-based needle-insertion device,” Proceedings of the National Academy of Sciences of the United Sates of America, vol.106. No.14, April 2009. pp: 5540-5545
[40] Yancheng Wang, Roland K.Chen, Bruce L. Tai, Patrick W. McLaughlin, “Optimal needle design for minimal insertion force and bevel length,” Medical Engineering & Physics, 36(2014) 1093-1100.
[41] Kuhnapfel U, Cakmak HK, Maas H, “Endoscopic surgery training using virtual reality and deformable tissue simulation,” Computers Graphics 2000; 24-5: 671-682.
[42] Tarnay CM, Glass KB, Munro MG, “Entry force and intra-abdominal pressure associated with six laparoscopic trocar-cannula systems: a randomized comparison,” Amer Coll Obstet Gynecol 1999; 94:83-88;
[43] Shafer DM, Khajanchee Y, Wong BSJ, Swanstrom LL, “Comparison of five different abdominal access trocar systems: analysis of insertion force, removal force, and defect size,” Surgical Innovation2006; 13:183-189.
[44] Kesavadas T, Srimathveeravalli G, Arulesan V, “Parametric modeling and simulation of trocar insertion,” Medicine Meets Virtual Reality 2006; 14: 252-254.
[45] Arulesan V, Srimathveeravalli G, Kesavadas T, Nagathan P, Baier RE, “Data acquisition

and development of a trocar insertion simulator using synthetic tissue models," Medicine Meets Virtual Reality 2007; 15: 25-27.
[46] Okrainec A, Farcas M, Henao O, Choy I, Green J, Fotoohi M, Leslie R, Wight D, Karam P, Gonzalez N and Apkarian J, "Development of a Virtual Reality Haptic Veress Needle Insertion Simulator for Surgical Skills Training," Stud Health Technol Inform, 142, pp. 233-238, 2009.
[47] Duriez C, Guebert C, Marchal M, Cotin S and Grisoni L, "Interactive Simulation of Flexible Needle Insertions Based on Constraint Models," Medical Image Computing and Computer – Assisted Intervention-MiCCAI 2009, 5762, pp. 291-299, 2009
[48] Kesavadas T, Scrimathveeravalli G and Arulesan V, "Parametric modeling and simulation of trocar insertion procedure," Studies in Health Technology Inform, pp. 119-252-254, 2005.
[49] Watanabe T, Fujiwara M, Kodera Y, Sakaguchi M, Hidaka H, Fujimoto H and Nakao A, "Measurement of Inserting Motion of Bladeless Trocar at Real Surgery for Development of a Virtual Training System for Initial Trocar Placement in Laparoscopic Surgery," Hepatogastroenterology, 58(107-108), pp. 854-858, May-June 2011.
[50] Brummer V, Carnahan H, Okrainec A and Dubrowski A, "Trocar Insertion: The Neglected Task of VR simulation," Medicine Meets Virtual Reality 16, 2008.
[51] Narayanan M, Zhou X, Grimella S, Waz W, Mendel F and Krovi V, "Data Driven Development of Haptic Models for Needle Biopsy Phantoms," ASME 2012 5th Annual Dynamic Systems and Control Conference joint with the JSME 2012 11th Motion and Vibration Conference, 2012.
[52] Hambli R, Chamekh A and Salah H, "Real-time deformation of structure using finite element and neural networks in virtual reality applications," Journal Finite Elements in Analysis and Design, 42(11), pp 985-991 July 2006.
[53] Chentanez N, Alterovitz R, Ritchie D, Cho J, Hauser K, Goldberg K, Shewchuk J and O'Brien J, "Interactive Simulation of Surgical Needle Insertion and Steering," ACM Transactions on Graphics (Proc. SIGGRAPH), 28(3), pp. 88:1-88:10, August 2009.
[54] Ogden R, "Large deformation isotropic elastic – on the correlation of theory and experiment for incompressible rubberlike solids," Proc. R. Soc. Lond. A, 326(1567), pp. 565-584, February 1972.
[55] M. Sakaguchi, Akari Hayashi, H. Fujimoto, M. Fujiwara, K. Misawa, A. Nakao, "Development of virtual trocar insertion training system for endoscopic surgery," International journal of computer assisted radiology and surgery, VOL.1, Issue.7, 2016, pp. 159-161.

[56] 藤原 道隆, 坂口 正道, 日高 広貴, 渡邉 卓哉, 小寺 泰弘, 中尾 昭公, 藤本 英雄。腹腔鏡下手術トロッカー挿入法に関するバーチャルリアリティ・シミュレーション訓練システム。VR 医学、9 巻(2011) 1 号

[57] Ashirwad Chowriappa, Raul Wirxz, Yong Won Seo, Aditya Reddy, Tushar Kesavadas, Peter Scott, Khurshid Guru and Thenkurussi Kesavadas, “A Predictive Model for Haptic Assistance in Robot Assisted Trocar Insertion,” IEEE World Haptics Conference 2013, pp.121-126.

[58] Yong An Seo, Ashirwad Chowriappa, Anand Abraham and T. Kesavadas, “Methodology for Haptic Modeling of Trocar Insertion Procedure,” ASME 2013, International Mechanical Engineering Congress & Exposition Congress.

[59] M. Mahvash and V. Hayward, “Haptic rendering of cutting, a fracture mechanics approach,” *Haptics-e, Electron. J. Haptics Res.*, vol. 2, no. 3, pp. 1-12, Nov. 2001.

[60] M. Heverly, P.Dupont and J. Triedman, “Trajectory optimization for dynamic needle insertion,” in *Proc. IEEE Int. Conf. Robot.*, Bacelona, Spain, 2005, pp. 1658-1663.

[61] R. J. Webster III, J. Memisevic and A. M. Okamura, “Design considerations for robotic needle steering,” in *Proc. IEEE Int. Conf. Robot. Autom.*, 2005, pp. 3599-3605.

[62] S. P. DiMaio and S. E. Salcudean, “Interactive simulation of needle insertion models.” *IEEE Trans. Biomed. Eng.*, vol. 52, no. 7, pp. 1167–1179. Jul. 2005.

[63] H.-W. Nienhuy and F. A. van der Stappen, “A computational technique for interactive needle insertion in 3rd nonlinear material,” in *Proc. IEEE Int. Conf. Robot. Autom.*, 2004, pp. 2061-2067.

[64] P. Brett, T. Parker, A. Harrison, T. Thomas and A. Carr, “Simulation of resistance forces acting on surgical needles,” *Proc. Inst. Mech. Eng.*, vol.201, pp 335-347, 1997.

[65] J. Hing, A. Brooks and J. Desai, “A biplanar fluoroscopic approach for the measurement, modeling, and simulation of needle and soft-tissue interaction,” *Med. Image Anal.*, Vol. 11, No.1, pp. 62-78, 2007.

[66] T. Azar and V. Hayward, “Estimation of the fracture toughness of soft tissue from needle insertion,” in *Proc, 4th Int, Symp. Biome. Simul* (ISBMS 2008). Lecture Notes in Computer Science, F. Bello and E. Edwards, Eds., vol. 5104, Berlin, Germany: Springer-Verlag, 2008, pp. 166-175.

[67] J. R. Rice and G. F. Rosengren, “Plane strain deformation near a crack tip in a power law hardening material,” *J. Mech. Phys. Solids*, vol. 16, pp. 13-31, 1968.

[68] A. G. Atkins, X.Xu and G. Jeronimidis, “Cutting, by pressing and slicing, of thin floppy slices of materials illustrated by experiments on cheddar cheese and salami,” *J. Mater. Sci.*, vol. 39, No. 8, pp. 2761-2766, 2004.

[69] Mohsen Mahvash and Pierre E. Dupont, “Mechanics of Dynamic Needle Insertion into a Biological Material,” *IEEE transactions on biomedical engineering*, vol. 57, No. 4, 2010.pp. 934-943.

[70] A. M. Okamura, C. Simone, and M. D. O’Leary, “Force modeling for needle insertion into soft tissue,” *IEEE Trans. Biomed. Eng.*, vol. 51, No, 10, pp. 1707-1716, Oct.2004.

[71] Corey R. Deeken and Spencer P. Lake, “Mechanical properties of the abdominal wall and biomaterials utilized for hernia repair,” *Journal of the Mechanical Behavior of Biomedical Materials*, 74(2017) 411-427

[72] Podwojewski Florence, Ottenio Melanie, Beillas Philippe, Guerin Gaetan, Turquier Frederic, “Mechanical response of animal walls in vitro: Evaluation of the influence of a hernia defect and a repair with a mesh implanted intraperitoneally,” Journal of Biomechanics, 46, 5, Elsevier, pp. 882-889.

[73] C.R. Deeken, L. Melman, E.D. Jenkins, S.C. Greco, M.M. Frisella, B.D. Matthews, “Histologic and biomechanical evaluation of crosslinked and non-crosslinked biologic meshes in a porcine model of ventral incisional hernia repair,” *J. Am. Coll. Surg.* (212) (2011), pp. 880-888

[74] B. Hernandez, E. Pena, G. Pascual, et al. “Mechanical and histological characterization of the abdominal muscle. A previous step to modelling hernia surgery,” *J. Mech. Behav. Biomed. Mater.*, 4 (3) (2011), pp. 392-404

[75] B. Hernandez-Gascon, A. Mena, E. Pena, G. Pascual, J.M. Bellon, B. Calvo, “Understanding the passive mechanical behavior of the human abdominal wall,” *Ann. Biomed. Eng.*, 41 (2) (2013), pp. 433-444

[76] Mami Suga, Ruriko Oyama et al., “The optical trocar insertion technique using Kocher Clamps in laparoscopic surgery” Japanese Journal of Gynecologic and Obstetric Endoscopy 29(2013) pp. 224-227.

[77] C. Richard, M. R. Cutkosky, K. MacLean, "Friction identification for haptic display", *Proc. Amer. Soc. Mechanical Engineers Dynamic Systems and Control Division*, vol. 67, pp. 327-334, 1999.

[78] B. Armstrong-Helouvry, P. Dupont, C. Canudas De Wit, "Survey of models analysis tools and compensation methods for the control of machines with friction", *Automatica*, vol. 30, pp. 1083-1138, July 1994.

[79] The anterolateral abdominal wall. URL: https://teachmeanatomy.info/abdomen/muscles/abdominal-wall/

[80] O’ Rahilly, Muller, Carpenter and Swenson, basic human anatomy, Chapter 25: Abdominal walls. URL:

https://www.dartmouth.edu/~humananatomy/part_5/chapter_25.html
[81] ENDOPATH XCEL Trocars, ETHICON Company. URL: https://www.ethicon.com/na/products/access/trocars/endopath-xcel-trocars
[82] Y.- S. Lin et al., "A computer-aided method for automatic localization and thickness measurement of peritoneum in ultrasound images" *the 33rd Annu. Int. Conf. IEEE EMBS*, Boston, MA, USA, 2001, pp. 8005–8008.
[83] Cupping therapy, Wikipedia. URL: https://en.wikipedia.org/wiki/Cupping_therapy
[84] Cupping therapy, Healthline. URL: https://www.healthline.com/health/cupping-therapy
[85] Cupping therapy. Maple Clinic. URL: http://themapleclinic.com/articles/
[86] William W Hurd, Tommaso Falcone and Howard T Sharp, "Gynecologic Laparoscopy Treatment & Management", Medscape >> Drugs & Diseases >> Clinical Procedures. URL: https://emedicine.medscape.com/article/265201-treatment
[87] Aiko Sakamoto, Iwaho Kikuchi, Hiroto Shimanuki, Kaoru Tejima, Juichiro Saito, Kano Sakai, Jun Kumakiri, Mari Kitade and Satoru Takeda "Initial closed trocar entry for laparoscopic surgery: Technique, umbilical cosmesis, and patient satisfaction," *Gynecology and Minimally Invasive Therapy*. 6(2017) 167-172.
[88] Jamie Stanhiser, MD, Linnea Goodman, MD, Enrique Soto, MD, Ibraheem AI-Aref, MD, Jenny Wu, MD, Anar Gojayev, MD, Benjamin Nutter, MS and Tomaso Falcone, MD, "Supraumbilical primary trocar insertion for laparoscopic access: the relationship between points of entry and retroperitoneal vital vasculature by imaging," American Journal of Obstetrics & Gynecology, 2015; 213:506. e1-5.
[89] Abdominal adhesions. UCSF, General Surgery, Department of Surgery. URL: https://general.surgery.ucsf.edu/conditions--procedures/abdominal-adhesions.aspx
[90] Adhesions, General and After Surgery. WebMD. URL: https://www.webmd.com/a-to-z-guides/adhesion-general-post-surgery#1
[91] Diane W. Shannon, "Lysis of adhesions," *Western New York Urology Associates*. URL: https://www.wnyurology.com/content.aspx?chunkiid=100928
[92] Or Cohen-inbar, Michael M Krausz, Menashe Zaaaroor and Ahmad Mahajna, "Laparoscopic Implantation of Distal Peritoneal Ventriculoperitoneal Shunt Catheter: A Comparative Study," *Journal of Neurological Surgery. Part A: Central European Neurosurgery*. 75(5) June 2014.
[93] Smart Imagebase, Scientific & Medical ART. URL: https://ebsco.smartimagebase.com/search?q=++++++++++++++++++++trocars+into+the+properitoneal+space.+++++++B.+The+peritoneum+is+pulled+down+off+the+abdominal+wall+laterally+and+super

Thanks

Time flies. I still remember the scene when I walked into the suzukakedai campus for the first time. In this three years and half, there are so many people helped me. And I have learned a lot both in study and life. Firstly, I want to thank my families for their love to me. It is them who support me to finish my study. And my advisor, Asso Prof. Tadano, he is an outstanding engineer and academic, who gave me precious guidance and advices in research and help me to finish the doctoral program. And I also want to thank Prof. Kagawa and Prof. Cai for their helping and recommending me to study in Japan.

In Tadano lab, Zhou sann has much experience in Japanese life and helped me a lot in both study and life. Saito sann is a very interesting people, and we have good three years life. Imu sann is a foreign student from Korea, we shared some different cultures and interesting things of different countries. The graduated doctoral student Yoshigi sann is also a great people who helped me a lot when I first came to Japan. And Dr. Kawakura often told me some unknown news about Japan and world, which let me know a different world.

The master students of Tadano Lab are excellent people. Shiode sann, Koyama sann, Chen sann, Ogawa san, Numai sann, Ono sann, Mizutani sann, Funami sann, Takayama sann, Kimura sann, Shiozaki sann, Takeishi sann, et al.

I feel fortunate to have this great three years in Japan. And also look forward to the challenging future.

2019.1.21

Tokyo Tech